

**Catalytic application of carbon nanotubes obtained from solid waste for
oxidative desulfurization of a simulated fuel with a green solvent**

Maria Clara Carneiro Batista

Thesis report submitted to
Escola Superior de Tecnologia e Gestão
Instituto Politécnico de Bragança
Master Degree in
Chemical Engineering

Supervisors:

Prof. Dr. Helder Teixeira Gomes
Prof. Dra. Raquel Vieira Mambrini

Bragança
June 2023

**Catalytic application of carbon nanotubes obtained from solid waste for
oxidative desulfurization of a simulated fuel with a green solvent**

Maria Clara Carneiro Batista

Thesis report submitted to **Escola Superior de Tecnologia e Gestão of
Instituto Politécnico de Bragança** to obtain the master's degree in **chemical
engineering** in the ambit of the double diploma with the **Centro Federal de
Educação Tecnológica de Minas Gerais - Campus Nova Suíça**

Supervisors:

Prof. Dr. Helder Teixeira Gomes

Prof. Dra. Raquel Vieira Mambrini

Bragança

June 2023

*“O valor das coisas
não está no tempo em que elas duram,
mas na intensidade com que acontecem.
Por isso existem momentos inesquecíveis,
coisas inexplicáveis
e pessoas incomparáveis.”*

Fernando Pessoa

ACKNOWLEDGMENTS

First, I would like to thank to God for guiding me along this journey and for giving me the courage and strength needed for this experience. I am deeply thankful to my family for their support in pursuing this dream, right from the start. To my mother and father, I express my sincerest gratitude for always believing in me and being there for me, even with an ocean apart. I am immensely grateful to my grandparents and godparents for having taught me the true essence of what matters most in life. I express my deepest gratitude to Bruno and Mi, the incredible family I am lucky to have, for supporting me and for taking care of the most important people in my life. To my sister, I thank for being the source of my sincerest laughs and my greatest inspiration.

I would like to express my sincere gratitude to my advisors, Dr. Helder T. Gomes from the Instituto Politécnico de Bragança (IPB), for welcoming me into his research group and providing all the support to carry out this work. To Dra. Raquel V. Mambrini, from Centro Federal de Educação Tecnológica de Minas Gerais (CEFET-MG), I am immensely thankful for accepting the invitation to contribute to this project and for all the substantial contributions to its development. All my gratitude to my professors at CEFET-MG and IPB, who contributed to my personal and professional growth.

I thank all my colleagues in my research group for their support and also for the enjoyable moments we shared throughout this experience. In particular, I extend my immense gratitude to MSc. Fernanda Roman, who has been an exceptional mentor and teacher to me from the very beginning. I am deeply thankful for your patience and dedication throughout these months. Your guidance and expertise have enriched my understanding both inside and outside the lab. I hold great admiration for you, and you will always remain an exemplary figure in my life.

To my friends, I am immensely grateful to Ju Murta, who received me so well in Bragança and helped me so much from the beginning. To the best friends I could have had: Ana Flávia, Carol, Márcio, who supported me so much in this experience and never left my side! To my greatest meeting of soul and heart, Mari, thank you for living this experience with me from beginning to end. Last but not least, I thank CEFET-MG for providing me with this wonderful experience. To the double degree program and to IPB for having received me so well and provided me with the necessary structure for the development of this work. To CIMO for the opportunity and knowledge acquired.

This work was financially supported by PLASTIC_TO_FUEL&MAT (POCI-010145-FEDER-031439) by Foundation for Science and Technology (FCT, Portugal), and through national funds FCT/MCTES (PIDDAC) to CIMO (UIDB/00690/2020 and UIDP/00690/2020) and SusTEC (LA/P/0007/2020).



ABSTRACT

This study focuses the development and evaluation of various carbon nanotubes (CNTs) for biphasic oxidative processes involving the degradation of dibenzothiophene (DBT) in isooctane, a model contaminant in fuel, simulating contaminated fossil fuels, by Oxidative Dessulfurization (ODS). Hydrogen peroxide was used as oxidation source in these processes, and water as extractive phase. The CNTs were synthesized via chemical vapor deposition (CVD) using different polymers as carbon resource, leading to CNT-MIX (from a mixture of polyolefins), CNT-PS (from pure polystyrene), and CNT-MIX-PS (from polyolefins/polystyrene). Nickel ferrite (NiFe_2O_4) supported on alumina was used as metallic catalyst in the CVD process. The synthesized materials underwent treatment with sulfuric acid and nitric acid, and characterized by Fourier Transformed Infra-Red (FTIR) spectroscopy, metal and ash content analysis, acidity/basicity determination, N_2 adsorption-desorption isotherms, and contact angle measurements. The most promising material, CNT-MIX, was further characterized using Raman spectroscopy and Thermogravimetric analysis (TG). The characterizations revealed the presence of metallic residues of Fe and Ni in the nanotubes, besides the incorporation of acidic and basic sites on the surface of the materials. The contact angle measurements revealed variations in hydrophobicity/hydrophilicity among the synthesized materials and specific surface areas (S_{BET}) ranging from 73 to 98 $\text{m}^2 \text{g}^{-1}$.

The DBT removal tests were conducted over a reaction time of 8 hours, and the results demonstrated satisfactory performance, with the best material (CNT-MIX) achieving 77% removal of DBT by ODS. Additionally, the materials were tested in adsorption systems in the oil phase and aqueous medium, with no significant adsorption being observed in either case.

Further tests were conducted using CNT-MIX to enhance the results and align the experimental conditions with those reported in the literature. Acetonitrile was employed as extractive phase, and the impact of formic acid on these systems was evaluated. By using acetonitrile as extractive phase and a combination of H_2O_2 and formic acid as oxidizing agents, complete removal of DBT (100%) was achieved within 8 hours. The findings of this work highlight the effectiveness of these materials as catalysts, adsorbents, and potentially as phase transfer catalysts for facilitating biphasic oxidative reactions.

Keywords: oxidative desulfurization, DBT, biphasic oxidation, carbon nanomaterials, hydrogen peroxide.

RESUMO

Este trabalho concentra-se no desenvolvimento e avaliação de diferentes nanotubos de carbono (CNTs) para processos oxidativos bifásicos que envolvem a degradação de um contaminante modelo, dibenzotiofeno (DBT) em isooctano, que simula um combustível fóssil contaminado a partir da técnica de dessulfurização oxidativa. O peróxido de hidrogênio é utilizado como oxidante nesses processos, e a água é utilizada como fase extrativa. Os CNTs são sintetizados por meio da deposição química de vapor (CVD) utilizando diferentes polímeros, obtendo CNT-MIX (a partir de mistura de poliolefinas), CNT-PS (a partir de poliestireno) e CNT-MIX-PS (a partir de poliolefinas/poliestireno). Utilizou-se NiFe_2O_4 , suportado em alumina, como catalisador metálico no processo de CVD. Os materiais sintetizados são tratados com ácido sulfúrico e ácido nítrico, e sua caracterização é realizada por meio de espectroscopia de infravermelho por transformada de Fourier (FTIR), análise de teor de metais e cinzas, determinação de acidez/basicidade, isotermas de adsorção e dessorção de N_2 e medição do ângulo de contato. O material mais promissor, CNT-MIX, é posteriormente caracterizado por espectroscopia Raman e análise termogravimétrica (TG). As caracterizações revelam a presença de resíduos metálicos de Fe e Ni nos nanotubos, bem como a incorporação de sítios ácidos e básicos na superfície dos materiais. As medidas do ângulo de contato mostram variações na hidrofobicidade/hidrofilicidade entre os materiais, sendo que a área superficial específica (S_{BET}) dos materiais variou de 73 a 98 m^2/g .

Os testes são conduzidos por um período de reação de 8 horas, e os resultados demonstram um desempenho satisfatório, com o melhor material (CNT-MIX) alcançando uma remoção de DBT de 77% na ODS. Além disso, os materiais são testados em sistemas de adsorção, tanto na fase oleosa quanto em meio aquoso. No entanto, não são observadas adsorções significativas em nenhum dos casos.

Para melhorar os resultados e alinhar as condições experimentais aos estudos relatados na literatura, são realizados outros testes utilizando CNT-MIX. Acetonitrila é utilizada como fase extrativa, e o efeito do ácido fórmico nesses sistemas é avaliado. Ao utilizar acetonitrila como fase extrativa e uma combinação de H_2O_2 e HCOOH como agentes oxidantes, é alcançada uma remoção completa de DBT em 8 horas. As descobertas deste estudo evidenciam a eficácia desses materiais como catalisadores, adsorventes e potencialmente como catalisadores de transferência de fase para facilitar reações oxidativas bifásicas.

Palavras-chave: dessulfurização oxidativa, DBT, oxidação bifásica, nanomateriais de carbono, peróxido de hidrogênio.

TABLE OF CONTENTS

LIST OF FIGURES	vi
LIST OF ACRONYMS	ix
1. INTRODUCTION	1
1.1. MOTIVATION	1
1.2. OBJECTIVES	4
1.2.1. GENERAL OBJECTIVES	4
1.2.2. SPECIFIC OBJECTIVES	4
1.3. REPORT OUTLINE	4
2. STATE OF THE ART	5
2.1. FOSSIL FUELS	5
2.1.1. LEGISLATION CONCERNING SULFUR COMPOUNDS IN FUELS	7
2.1.2. AN OVERVIEW OF THE REFINING PROCESS	8
2.2. TECHNIQUES TO REDUCE THE CONTENT OF SULPHUR COMPOUNDS	10
2.3. OXIDATIVE DESULFURIZATION (ODS)	11
2.3.1. OXIDATION PROCESS	12
2.3.2. SEPARATION PROCESS: EXTRACTION OR ADSORPTION	14
2.3.3. CATALYSIS IN ODS	15
2.4. PRODUCTION OF CNTs	18
2.5. WASTE PLASTICS AS LOW-COST FEEDSTOCKS FOR CNT GROWTH	20
3. MATERIALS AND METHODS	24
3.1. REACTANTS AND EQUIPMENT	24
3.1.1. REACTANTS	24
3.1.2. EQUIPMENT	24
3.2. PRODUCTION OF MATERIALS	25
3.2.1. NICKEL FERRITE	25
3.2.2. CNTs	26
3.3. MATERIALS CHARACTERIZATIONS	27
3.3.1. FOURIER TRANSFORM INFRARED SPECTROSCOPY (FTIR)	27
3.3.2. ACIDIC CHARACTERIZATION	27
3.3.3. SURFACE AND PORE ANALYZER	28
3.3.4. CONTACT ANGLE	28
3.3.5. METAL AND ASH CONTENT	29
3.4. ANALYTICAL METHODS	29
3.4.1. UV-VIS SPECTROPHOTOMETRY	29
3.4.2. GAS CHROMATOGRAPHY WITH A FLAME IONIZATION DETECTOR (GC-FID)	31
3.4.3. HIGH PERFORMANCE LIQUID CHROMATOGRAPHY (HPLC)	31
3.5. ADSORPTION OF DBT	33
3.5.1. IN OILY PHASE	33

3.5.2.	BIPHASIC MEDIUM	33
3.6.	OXIDATIVE DESULFURIZATION OF DBT	33
3.7.	NON CATALYTIC TRIALS	34
4.	RESULTS AND DISCUSSION	35
4.1.	SYNTHESIS OF MATERIALS.....	35
4.2.	CHARACTERIZATION OF THE MATERIALS	37
4.2.1.	FOURIER TRANSFORM INFRARED SPECTROSCOPY (FTIR)	37
4.2.2.	ACIDIC CHARACTERIZATION.....	38
4.2.3.	METAL AND ASH CONTENT	40
4.2.4.	SURFACE AND PORE ANALYSIS	42
4.2.5.	CONTACT ANGLE	45
4.3.	EXPERIMENTAL REACTIONS.....	47
4.3.1.	ADSORPTION OF DBT.....	47
4.3.2.	OXIDATIVE DESULFURIZATION OF DBT	49
4.3.3.	CNT-MIX: ADDITIONAL CHARACTERIZATIONS.....	53
4.3.4.	OXIDATIVE DESULFURIZATION OF DBT: ADDITIONAL EXPERIMENTS WITH CNT-MIX	55
5.	CONCLUSIONS AND FUTURE WORK.....	61
5.1.	CONCLUSIONS	61
5.2.	FUTURE WORK.....	61
6.	REFERENCES	63

LIST OF FIGURES

Figure 1 - World energy consumption by categories measured in terawatt-hours. Adapted from Our World in data [1].....	1
Figure 2 - Basic composition of crude oil. Adapted from Stauffer, E. et al, 2008 [3]	5
Figure 3 - Types of sulfur pollutants found in petroleum: 1 – Sulfide (ethyl phenyl sulfide); 2 – Disulfide (methyl phenyl disulfide); 3 – Mercaptan (phenylmethanethiol); 4 – Thiophene; 5 – Thiophene Derivative (Benzothiophene).....	6
Figure 4 - Molecular Formula of DBT [28]	7
Figure 5 - Limits for sulfur compounds in gasoline (a) and diesel (b) around the world, in ppm. Adapted from Roman, F.F., et al., (2021) [31] and “StratasAdvisors”	8
Figure 6 - Distillation of the crude oil in a refinery. Adapted from CME group [32].....	9
Figure 7 - Papers published on ODS and HDS over the years until December/2022. Source: Web of Science with the keywords “oxidative desulfurization” and “hydrodesulfurization”; search date of February 09 th , 2023	12
Figure 8 - Oxidation of DBT in ODS. Adapted from Houda, S. et al., (2018) [26].....	14
Figure 9 - Examples of different types of carbon-based nanostructures. Collected from Khan., M.E. (2021) [14].....	16
Figure 10 - Schematic representation of single walled carbon nanotube (SWCNT) and multiwalled carbon nanotube (MWCNT). Collected from Ribeiro, B. et al., (2016) [69]	17
Figure 11 - Cumulative global production of plastics (polymers and fibers) until 2019. Adapted from Our World in Data [88]	21
Figure 12 - Distribution of European plastic demand by resin type in 2019. Adapted from: Plastics Europe Market Research Group [17]	23
Figure 13 - Appearance of a CNT synthesized by polymers (CNT-PS)	27
Figure 14 - Classification of isotherms and loop hysteresis according to IUPAC. Adapted from ALOthman, Z. A. (2012) [101]	28
Figure 15 - Calibration curves for (A) Fe determination and (B) Ni determination.....	29
Figure 16 - Calibration curve for H ₂ O ₂ determination.....	30
Figure 17 - Calibration curve for DBT determination	30
Figure 18 - Calibration curve for DBT determination by GC-FID	31
Figure 19 - Calibration curve for the determination of DBT concentration in the extractant phase by HPLC.....	32
Figure 20 - Calibration curve for the determination of DBT _{SO2} concentration in the extractant phase by HPLC	32
Figure 21 - Setup for the experimental trials	34
Figure 22 - Carbon onversion yields in the CVD process	35
Figure 23 - Mass loss after each acidic wash.....	36

Figure 24 - FTIR Spectra of the prepared materials	37
Figure 25 - pHpzc curves for the materials.....	39
Figure 26 - Metal content in the ashes (A) and in the CNTs (B)	41
Figure 27 - Ash content of the materials.....	41
Figure 28 - Adsorption isotherms of N ₂ at 77 K of the A) CNT-PS, B) CNT-MIX, C) CNT-MIX-PS, D) CNT-MIX-800 and E) Nickel Ferrite.....	43
Figure 29 - Adsorption of DBT on the CNTs over time (80 °C, C _{CNT} = 2.5 g L ⁻¹ , C _{DBT} = 500 mg L ⁻¹ in isooctane). The lines are only intended to guide the eyes.	47
Figure 30 - Adsorption of DBT on the CNTs under a biphasic system (80 °C, C _{CNT} = 2.5 g L ⁻¹ , C _{DBT} = 500 mg L ⁻¹ in isooctane). The lines are only intended to guide the eyes...	48
Figure 31 - Decomposition of hydrogen peroxide in the biphasic oxidation runs (80 °C, pH ₀ = 3.0, C _{DBT} = 500 mg L ⁻¹ in isooctane, C _{CNT} = 2.5 g L ⁻¹ , C _{H₂O₂} = 11 g L ⁻¹). The lines are only intended to guide the eyes.	49
Figure 32 - Removal of DBT in oxidative desulfurization using H ₂ O ₂ (80 °C, C _{CNT} = 2.5 g L ⁻¹ , C _{DBT} = 500 mg L ⁻¹ in isooctane; C _{O_{H₂O₂}} =11 g L ⁻¹). The lines are only intended to guide the eyes.....	51
Figure 33 -TG and DTG profiles for CNT-MIX.....	53
Figure 34 - Raman spectra for CNT-MIX.....	54
Figure 35 - Removal of DBT in ODS using different systems (Run A: Extractant: ultrapure water; Oxidizing Agents: H ₂ O ₂ and HCOOH; Run B: Extractant: acetonitrile; Oxidizing Agent: H ₂ O ₂ ; Run C: Extractant: acetonitrile; Oxidizing agent: H ₂ O ₂ and HCOOH; CNT MIX: Extractant: Water (pH=3); Oxidizing Agent: H ₂ O ₂). The lines are only intended to guide the eyes.	56
Figure 36 - Presence of DBT in acetonitrile (Run B: ACN with H ₂ O ₂ ; Run C: ACN with H ₂ O ₂ and HCOOH; 80 °C, C _{CNT} = 2.5 g L ⁻¹ , C _{DBT} = 500 mg L ⁻¹ in isooctane; C _{H₂O₂} = 11 g L ⁻¹ , C _{HCOOH} = 22 g L ⁻¹). The lines are only intended to guide the eyes.	57
Figure 37 - Presence of DBT _{SO₂} in acetonitrile (Run B: ACN with H ₂ O ₂ ; Run C: ACN with H ₂ O ₂ and HCOOH; 80 °C, C _{CNT} = 2.5 g L ⁻¹ , C _{DBT} = 500 mg L ⁻¹ in isooctane; C _{H₂O₂} = 11 g L ⁻¹ , C _{HCOOH} = 22 g L ⁻¹). The lines are only intended to guide the eyes.	59
Figure 38 - Reaction intermediate identified by the same retention time in HPLC (80 °C, C _{CNT} = 2.5 g L ⁻¹ , C _{DBT} = 500 mg L ⁻¹ in isooctane, C _{H₂O₂} = 11 g L ⁻¹ , C _{HCOOH} = 22 g L ⁻¹). The lines are only intended to guide the eyes.	60

LIST OF TABLES

Table 1- Most important oxidizing agents and their respective oxidation potentials.....	12
Table 2- Most frequently used oxidizing agents in ODS	13
Table 3- Examples of works using CNTs in ODS	18
Table 4- Works on the production of CNTs using different types of plastic as carbon source.....	22
Table 5- Conditions and reagents used in the additional set of experiments with CNT-MIX	34
Table 6- Results of the acidic characterization	39
Table 7- Textural properties of the prepared materials.....	44
Table 8- Results for the contact angle measurements of the materials	45

LIST OF ACRONYMS

4,6-DMDBT	4,6-dimethyldibenzothiophene
ABS	Acrylonitrile Butadiene Styrene
ACN	Acetonitrile
ADS	Adsorptive desulfurization
BDS	Biodesulfurization
BioC	Biocatalysts
BT	Benzothiophene
CNTs	Carbon nanotubes
COFs	Covalent organic frameworks
CVD	Chemical vapor deposition
DBT	Dibenzothiophene
DBT _{SO2}	Dibenzothiophene sulfone
EDS	Extractive desulfurization
EPS	Expanded Polystyrene
ETP	Engineered Thermoplastics
FCC	Fluid catalytic cracking
FFL	Fenton and Fenton-like
FTIR	Fourier transform infrared spectroscopy
GC-FID	Gas Chromatography with Flame Ionization Detection
HDN	Hydrodenitrogenation
HDPE	High-density polyethylene
HDS	Hydrodesulfurization
HPLC	High-performance liquid chromatography
ILs	Ionic liquids
K _{ow}	Partition coefficient (octanol-water)
LDPE	Low-density polyethylene
MC	Metal complexes
MF	Metal free
MO	Metal oxides
MOFS	Metal-organic frameworks
NC	Non catalytic
ODS	Oxidative desulfurization
PA	Polyamide

PAFs	Porous aromatic frameworks
PAH	Polycyclic aromatic hydrocarbon
PC	Polycarbonate
PEMRG	Plastics europe market research group
PET	Polyethylene terephthalate
PM	Particulate matter
PMMA	Poly(methyl methacrylate)
POMs	Polyoxometalates
PP	Polypropylene
PS	Polystyrene
PSW	Plastic solid waste
PTFE	Polytetrafluoroethylene
PUR	Polyurethane
PVA	Polyvinyl alcohol
PVC	Polyvinyl chlorine
RP	Relative polarity
S_{BET}	Specific surface area
TBHP	Tert-butyl hydroperoxide
TS	Titanosilicates

1. INTRODUCTION

1.1. MOTIVATION

Nowadays, the use of fossil fuels is of great concern, as energy consumption has been steadily increasing since the Industrial Revolution. Despite the progress in renewable energy generation, data from the Statistical Review of World Energy 2022 show that oil consumption increased by 5.3 million barrels per day in 2021 [1]. Currently, fossil fuels still represent one of the largest energy sources in the world, with petroleum being the most consumed, as shown in Figure 1.

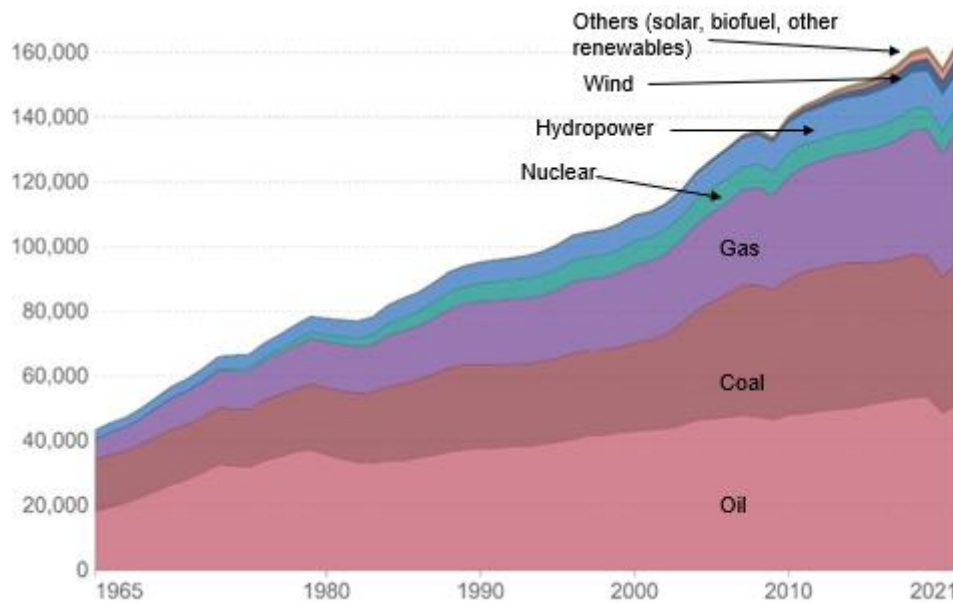


Figure 1 - World energy consumption by categories measured in terawatt-hours. Adapted from Our World in data [1]

A petroleum mixture comprises various hydrocarbons with different structures and chemical properties [2]. In addition, it also contains molecules with sulfur, nitrogen and vanadium atoms. Even though the composition of crude oil varies depending on the location, the basic composition of crude oil differs little from one source to another [3]. Among the main impurities of petroleum, sulfur-containing compounds stand out, with an average content in crude oil between 0.06 and 8% [2].

One of the most important consequences of burning this type of fuel is the release of toxic compounds into the atmosphere, such as nitrogenous and sulfurous gases, which pose a severe threat to the environment. Sulfur-containing gases such as SO_2 and SO_3 can harm the environment by forming acid rain and the oxides that contribute to the formation of particulate matter (PM) [4].

These factors have significant impacts on human health and the environment. Acid rain destroys more fragile ecosystems, and aluminum leaches from the soil. In addition, recent studies have demonstrated the link between the inhalation of particulate matter, the incidence of various diseases, and the intensification of heart and respiratory problems [5].

Due to their high concentrations and undesirable properties, sulfur compounds are removed from the oil by industrial processes at the oil refinery. An oil refinery is a collection of factories that separate the oil into valuable fractions, and this activity requires several steps, such as separation and conversion. The most common process used to treat this material is hydrotreating, which promotes the removal of compounds containing nitrogen and sulfur [4,6].

Hydrotreating is a catalytic process that adds hydrogen at specific pressure and temperature conditions. The desulfurization process, also known as hydrodesulfurization (HDS), is one of the existing types of hydrotreatment in the refinery [2,6]. In this process, the carbon-sulfur bond is broken, and H₂S is formed, reducing the viscosity of the material and promoting the removal of the pollutant [7].

Although the HDS process is still widely used in refineries, it has limitations [8]. The main problem is the composition of the petroleum still present in nature: it is becoming denser and richer in sulfur compounds, with a lower hydrogen/carbon ratio and high levels of contaminants [2]. The catalysts used in the HDS process do not efficiently remove the denser sulfur compounds, such as organosulfur compounds with high steric hindrance. At the same time, legislation is becoming stricter in terms of limits for releasing this type of pollutant into the atmosphere, forcing oil industries to research new alternatives for removing this type of compound [9].

One of the alternatives currently under investigation to remove sulfur compounds from petroleum is oxidative desulfurization (ODS). During the ODS process, refractory sulfur compounds are oxidized to sulfoxides and sulfones, ultimately extracted through polar extraction, adsorption, distillation or decomposition[10]. Desulfurization using ODS is considered a promising technology since it can be operated at mild temperatures (<100 °C), under atmospheric pressure, and does not require the use of hydrogen [11]. Therefore, the ODS method is considered promising, as it allows changing the polarity of the molecules, which facilitates the separation of the fuel.

Since it is a method that combines oxidation and separation steps, it is necessary to use an oxidant. Various oxidizing agents have been used in the ODS process, including

hydrogen peroxide (H_2O_2), oxygen (O_2), cumyl hydroperoxide and tert-butyl hydroperoxide (TBHP). Because H_2O_2 is environmentally friendly and commercially available, it is the most preferred oxidizing agent [10,12]. However, hydrogen peroxide use promotes the formation of a two-phase system. For this reason, it is necessary to use a catalyst that provides the decomposition of hydrogen peroxide and enhances contact between the phases [4].

One type of material whose catalytic properties have been extensively studied is carbon nanotubes (CNTs). Due to their excellent structural, physical, electrical and mechanical properties, CNTs have stimulated the development of new technologies [13]. In heterogeneous catalysis, carbon materials have many advantages, such as chemical stability, lower corrosiveness, the possibility of high yield in the synthesis, lower price, and easiness in tuning their properties, among others. In addition, its chemical properties, such as hydrophobicity/hydrophilicity, provide good contact with the substance to be treated [2,14].

Among the various processes used to obtain CNTs, chemical vapor deposition (CVD) is exciting since it is economically and industrially viable. In this process, CNTs are generated from catalyst particles by thermal decomposition of carbon-containing gases. Various hydrocarbon compounds can be used as carbon source, being one of the main advantages of the process [2,13].

Plastic solid waste can be reused in this process as a type of carbon source, contributing to a circular economy [4]. Solid waste management remains one of the most neglected areas of urban development, as plastics have become an integral part of our lives due to their many properties. Approximately 60% of plastic ever produced is estimated to be discarded in the environment without proper treatment, which will persist for centuries with slow degradation [15,16]. According to the Plastics Europe Market Research Group (PEMRG), global production of plastics has exceeded 350 million tons since 2020. The European continent is responsible for about 15% of this value [17].

It is, therefore, evident that treatment alternatives are urgently needed for plastic solid waste. One of the possibilities is the reuse as a carbon source in the production of CNT's, adding value to a waste that would otherwise be disposed in the environment. CNTs can be used as catalysts in the ODS process described above.

1.2. OBJECTIVES

1.2.1. GENERAL OBJECTIVES

Study the application of Carbon Nanotubes (CNTs) produced from plastic solid waste (PSW) to use them to remove sulfur compounds, by ODS, from fuels.

1.2.2. SPECIFIC OBJECTIVES

- Synthesize nickel-ferrite materials (NiFe_2O_4) by coprecipitation to use it as catalytic support in the preparation of CNTs by CVD.
- Produce CNTs by CVD with different carbon sources (Polystyrene, Polypropylene, Low-Density Polyethylene, High-Density Polyethylene)
- Study the adsorption of DBT using the prepared CNTs at different conditions in both organic and biphasic mediums.
- Investigate the catalytic activity of the CNTs in the decomposition of hydrogen peroxide in the presence of DBT.
- Evaluate the removal of DBT by Adsorptive Desulfurization (ADS) and Extractive desulfurization (EDS) for comparison purposes.

1.3. REPORT OUTLINE

This master's thesis is organized into five chapters, each serving a specific purpose in addressing the topic of sulfur-containing compounds removal in fuels. The present chapter provides an introduction, explaining the motivation behind studying this subject and outlining the main objectives to be achieved.

Chapter 2 focuses on general aspects of fossil fuels, common treatments employed for fuel oil desulfurization, and the two-phase oxidative desulfurization (ODS) process using hydrogen peroxide. Additionally, it discusses the application of carbon nanotubes (CNTs) as catalysts in ODS and the production of CNTs from waste plastics.

In chapter 3 are described the chemicals, materials, equipment and experimental methodology used throughout the study.

Chapter 4 presents and discusses the experimental results obtained, analyzing their significance and implications.

Finally, in Chapter 5, the main conclusions of this thesis are summarized. Additionally, suggestions for future research are provided to further enhance and expand upon the findings and investigations presented within this thesis.

2. STATE OF THE ART

2.1. FOSSIL FUELS

Despite the continuous development of renewable energy sources, fossil fuels, such as liquid petroleum, coal and natural gas, remain the predominant source of energy worldwide, mainly in the transport sectors [1,18]. About 85% of all fuels are currently produced from crude oil, which is a complex mixture of hydrocarbons and organic compounds with heteroatoms. Although its composition varies depending on its origin, the basic composition is described in Figure 2 [18].

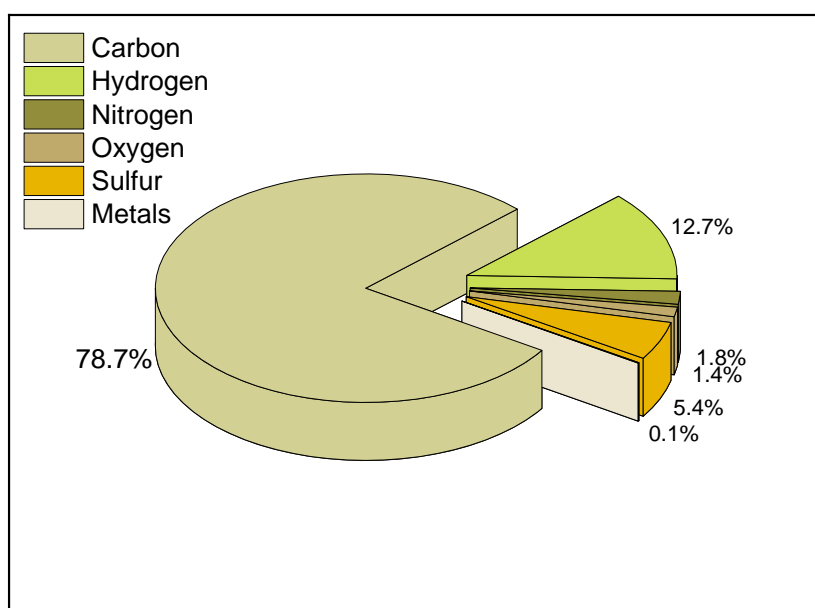


Figure 2 - Basic composition of crude oil. Adapted from Stauffer, E. et al, 2008 [3]

In the face of increasing energy demand and diminishing reserves of fossil fuels, there has been an increase in the use of low-quality fossil fuel sources. Such crude oils contain a higher proportion of sulfur-containing compounds, which are difficult to remove using standard refinery processes [2,19]. As a result, the emission of pollutant gases such as SO_x increases significantly, harming the environment and the refining process itself, as these pollutants contaminate the catalysts in downstream processes and reduce the profit of the production [19,20].

Sulfur compounds found in fuels are usually H_2S , mercaptans, sulfides, disulfides, thiophene and its derivatives [11]. Some examples of these compounds can be seen in Figure 3. The most common class of refractory compounds is thiophenes due to their high stability [20].

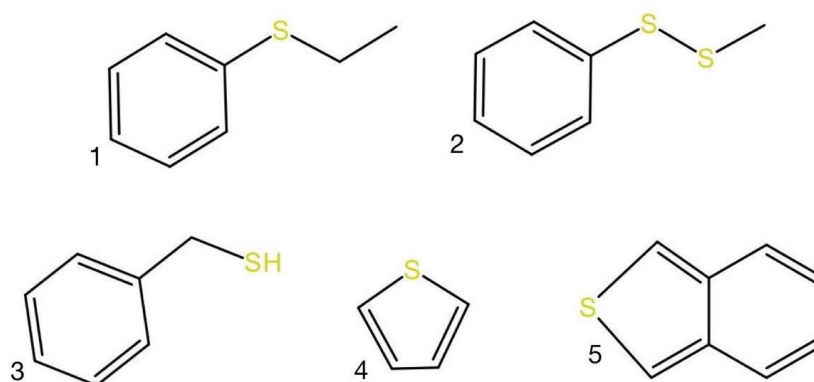


Figure 3 - Types of sulfur pollutants found in petroleum: 1 – Sulfide (ethyl phenyl sulfide); 2 – Disulfide (methyl phenyl disulfide); 3 – Mercaptan (phenylmethanethiol); 4 – Thiophene; 5 – Thiophene Derivative (Benzothiophene)

The word 'thiophene' is derived from the Greek words 'theion' and 'phaino,' which mean "sulfur" and "shine," respectively. Thiophenes are a class of heterocyclic aromatic compounds whose basic structure consists of a five-membered ring with one sulfur and four carbon atoms [21]. Derivatives of thiophenes are formed by the bonding of carbon atoms between neighboring aromatic rings and have alternating single and double bonds between carbon atoms along the chain [22]. Generally, they are classified according to the number of thiophene rings in the structure, such as Bithiophene (two rings), Terthiophene (three rings), and Quinquethiophene (five rings) [22].

Among the main thiophene-type contaminants in fuels are benzothiophene (BT), dibenzothiophene (DBT), and 4,6-dimethyldibenzothiophene (4,6-DMDBT), which are difficult to remove by catalytic hydrodesulfurization (HDS) [23]. In such molecules, the lone pair of electrons of the sulfur atom is in conjunction with the π -electrons of the aromatic ring, resulting in a decrease in the electron density and the reactivity of the compounds [24]. To remove these pollutants, the oil fraction to be treated must be considered, as well as the chemical kinetics of the individual components.

Among the compounds derived from thiophene, dibenzothiophene attracts research attention due to its low reactivity, high boiling point, and high amount in crude oil [25,26]. Dibenzothiophene is a sulfur-containing polycyclic aromatic hydrocarbon (PAH) derivative consisting of 3 fused rings with keratolytic activity. It is a colorless solid with a molecular weight of $184.26 \text{ g mol}^{-1}$ and a boiling point of $332.5 \text{ }^\circ\text{C}$. It is highly soluble in ethanol, benzene, chloroform and methanol and sparingly soluble in water (1.47 mg L^{-1} at $25 \text{ }^\circ\text{C}$) [27,28]. In its pictograms, it is classified as "acutely toxic", "irritant" and "dangerous for the environment". Figure 4 shows the molecular formula of this sulfur-containing component.

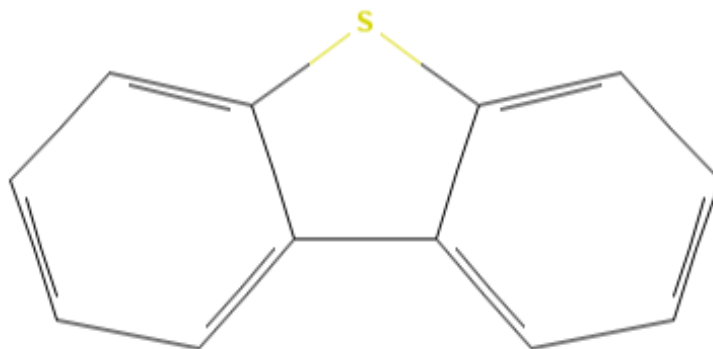


Figure 4 - Molecular Formula of DBT [28]

2.1.1. LEGISLATION CONCERNING SULFUR COMPOUNDS IN FUELS

Globally, the maximum sulfur content for transportation fuels (gasoline and diesel) has decreased in recent years. At the beginning of the 21st century, the sulfur content in fuels in the U.S., Japan and Western Europe was already limited to 0.05 wt.%, or 500 parts per million by weight (ppmw) [29]. Nowadays, the legislation of the European Union and the United States determines much lower values for the permissible sulfur content in fuels (diesel and gasoline). For diesel, EU and U.S. allow only 10 ppm, while for gasoline, the limits are 10 and 15, respectively [30]. Figure 5 shows the current limits for sulfur compounds in gasoline and diesel, according to the legislation for some countries around the world, in ppm.

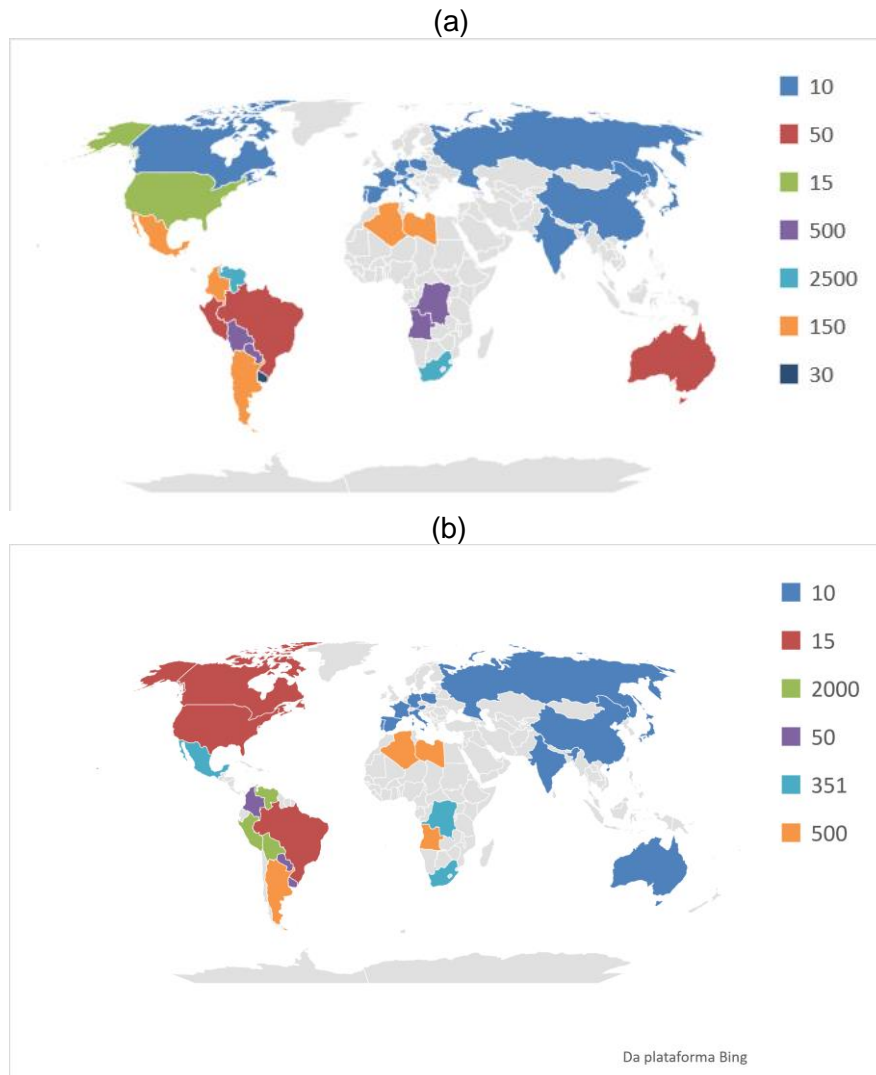


Figure 5 - Limits for sulfur compounds in gasoline (a) and diesel (b) around the world, in ppm. Adapted from Roman, F.F., et al., (2021) [31] and "StratasAdvisors"

To meet the regulated sulfur levels, and other characteristics, petroleum fuels must be treated [31]. The industrial process that converts crude oil into fuel and treats its contaminants is called refining.

2.1.2. AN OVERVIEW OF THE REFINING PROCESS

Separation, conversion and treatment are the three main steps in the refining process. The first step is distillation, which has the function of dividing the raw material into fractions by the difference in their boiling points. The lighter fractions, which will be found at the top, are separated from the heavier fractions, which will be found at the bottom [6], as shown in Figure 6.

Each type of sulfur compound is mainly contained in a certain fraction generated by the distillation process. Mercaptan, sulfite, disulfide and thiophene groups are found in the

boiling range of gasoline. Thiophenes and derivatives are mainly found in heavy distillates, from which diesel and aviation kerosene are produced [31].

Following distillation, heavy fuels can be processed to obtain higher-value products [32]. Due to the increased demand for distilled products like gasoline, refineries have an incentive to convert heavy liquids into lighter ones using processes such as cracking and alkylation. One of the most important is Fluid Catalytic Cracking (FCC).

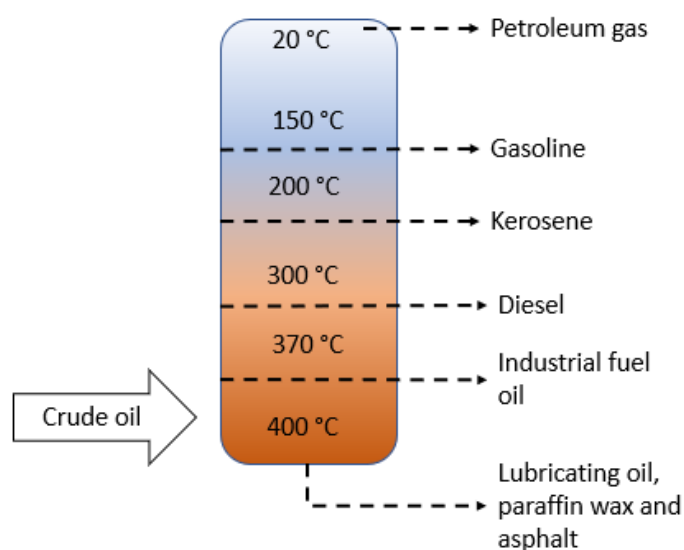


Figure 6 - Distillation of the crude oil in a refinery. Adapted from CME group [32]

FCC converts less useful fractions into lighter products, using heat and pressure to promote the break of heavy elements. In this process, there are two main reaction zones. At the entrance of the reactor, there is a fluidized bed of catalyst particles in contact with the gas oil feed and injected steam. Once the hot catalyst particles contact the feed gas oil in the riser, the gas oil vapors and catalyst particles start to crack, and as they move upward in the reactor, the cracking process begins [33]. After this reaction, the coked catalyst is separated from the cracked products, stripped of residual oil by steam, and then regenerated by burning the coke in a regenerator at 650–760 °C and 2 bar [34]. Cracking, hydrogen transfer, isomerization and coking are some of the reactions that occur during an FCC process [4].

The last stage of refinement is treatment. The process of removing heteroatom impurities such as N, O and S compounds from fuels is called hydrotreating [35]. Hydrotreating involves adding hydrogen to the system in the presence of catalysts to break the bonds between carbon and unwanted heteroatoms [2]. Two types of hydrotreating widely used in refineries are hydrodesulfurization (HDS) and hydrodenitrogenation (HDN), which aim

to remove sulfur and nitrogen compounds, respectively. The two techniques occur simultaneously, producing H₂S and NH₃ as by-products [4,31].

Since S is the predominant impurity in crude oil, the HDS process draws attention to research. Currently, it is the most efficient and widely used desulfurization method used in refineries. It takes place in a single reactor, with catalysts of Co-Mo, Ni-Mo or a combination thereof in alumina. It takes place at temperatures above 300 °C and pressures between 20 and 100 atm. This process has been proven to be effective for sulfur removal down to 500 ppm for gasoline and diesel but becomes unproductive for deep desulfurization [11,19].

To reduce sulfur levels to the desired levels of 15-10 ppm, it requires much higher pressures, hydrogen-to-feed ratio and higher hydrogen purity [9]. If a single-stage HDS unit were converted to a deep desulfurization unit process, some operational solutions would be required, such as an increase in hydrogen partial pressure and improvements to the reactors, which would significantly increase the cost of the process [9,11].

Because the legislation regarding the limits of sulfur compounds is getting stricter and that the conventional desulfurization process often does not reach these limits, it is, therefore, necessary to develop new techniques for the removal of refractory compounds.

2.2. TECHNIQUES TO REDUCE THE CONTENT OF SULPHUR COMPOUNDS

Various techniques have been developed to reduce the content of dense sulfur compounds in liquid fuels: extractive desulfurization (EDS) [36], adsorptive desulfurization (ADS) [37], biodesulfurization (BDS) [38] and oxidative desulfurization (ODS) [11,19, 26,39].

In ADS, sulfur compounds in fuel are adsorbed to the surface of a solid sorbent [11]. The advantages of this technique include that its operation under ambient conditions and a high reaction rate. Sulfur compounds can be removed by physical adsorption, chemisorption and π -complexation adsorption [40].

Another method widely studied in this field is EDS, mainly because of its easiness and simplicity. In EDS, sulfur compounds are selectively extracted from fuel using solvents [41]. For this purpose, it is necessary to use solvents with suitable properties, such as (i) high solubility and selectivity for sulfur compounds in aromatic hydrocarbons and other compounds, (ii) pronounced boiling point or other properties that allow efficient regeneration, (iii) thermal stability, and others [11].

However, among the mentioned techniques, ODS stands out for requiring mild temperature ($<100^{\circ}\text{C}$) and pressure ($P=P_{\text{atm}}$) conditions [42], in addition to dispensing the use of hydrogen, thus being a promising and economical process in the field of treatment of fossil fuels. Another advantage is that ODS can be combined with other techniques, such as ultrasound, plasma and microwave [40].

2.3. OXIDATIVE DESULFURIZATION (ODS)

The first article on ODS was published in 1964 in the Journal of Organic Chemistry by Thomas J. Wallace, Harvey Pobiner and Alan Schriesheim [43]. Since then, work on the subject has only increased in the early 20th century, when laws regarding limits on sulfur in fuels became more stringent [19]. Figure 7 shows the number of publications on ODS and HDS in the Web of Science database from 1964 to 2022.

The basic principle of ODS is to change the chemical properties of refractory sulfur compounds, such as DBT, through chemical reactions. With this method, some properties of the molecules can be transformed to facilitate their removal [11]. ODS consists of 2 main steps: (a) the oxidation of sulfur-containing compounds into sulfoxides and sulfones; (b) the removal of the oxidized products by adsorption or extraction [31]. The use of ODS facilitates the removal of denser aromatic and sulfur compounds due to the high electron density of the sulfur atom, making it an excellent alternative to complement or even replace HDS [19]. It is possible to note that in recent years the publications of ODS have already exceeded the number of publications of the conventional method of treatment.

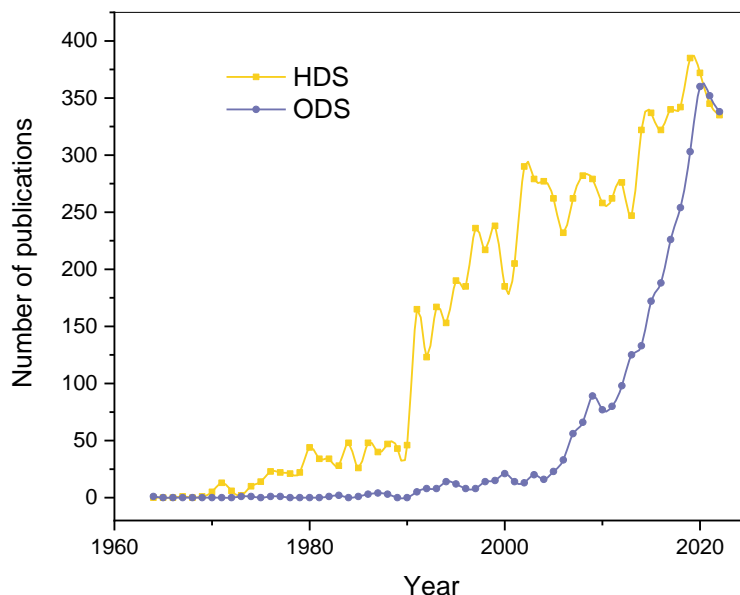


Figure 7 - Papers published on ODS and HDS over the years until December/2022. Source: Web of Science with the keywords “oxidative desulfurization” and “hydrodesulfurization”; search date of February 09th, 2023

2.3.1. OXIDATION PROCESS

Over time, various types of oxidants have been described in the literature, such as H₂O₂, molecular O₂, organic peracids, ozone, among others. Among these, hydrogen peroxide is highlighted as a better oxidizing agent since it has a high efficiency per weight and leaves as by-products only water, fitting into the principles of green chemistry [26,44]. Another advantage of its use is that hydrogen peroxide can be converted, by catalysis, into hydroxyl radicals whose oxidizing power is exceeded only by fluorine. Table 1 shows the most important oxidizing agents and their respective oxidation potentials, and Table 2 shows the most frequently used oxidizing agents in ODS. Easiness of handling, mild temperature and pressure conditions, low cost, and good miscibility with water are other advantages that can be cited when using this reagent [45,46].

Table 1- Most important oxidizing agents and their respective oxidation potentials

Oxidant agent	Oxidation Power (eV)
Fluorine	3.00
Hydroxyl radical	2.80
Atomic oxygen	2.42
Ozone	2.07
Hydrogen peroxide	1.78

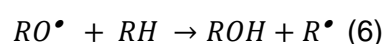
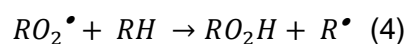
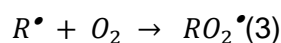
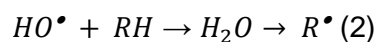
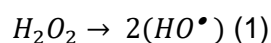
Source: Adapted from Dantas, T.L.P.P., (2005) [47]

Table 2- Most frequently used oxidizing agents in ODS

Oxidant	Active Oxygen (%)
H ₂ O ₂ at 30 wt%	14.1
Ozone	33.3
t-BuOOH	17.8

Source: Adapted from Mjalli, F.S., (2014) [11]

In aqueous system and using suitable catalysts, hydrogen peroxide is converted into hydroxyl radicals, which will lead to the oxidation of sulfur compounds, as demonstrated in reactions 1 to 7, where “R” is the organic sulfur chain that will be oxidized.



In reactions 1, 2 and 3, the initiation phase takes place, in which the hydroxyl radical is formed by the decomposition of hydrogen peroxide under the action of a catalyst [47]. From there, the propagation stage begins (reactions 4, 5 and 6) where the radicals react with other molecules, leading to other types of radicals and the desired product (reaction 7). For sulfur-containing compounds, the desired product would, initially, be the sulfoxide intermediate [4].

Refractory sulfur compounds are first oxidized to the sulfoxide form and later to the sulfone form [31], as shown in Figure 8. In the ODS process carried out using hydrogen peroxide, a two-phase system is formed, since the hydrogen peroxide is present in an aqueous-phase, whereas the organosulfur compounds are located in the oily phase. Due to the increased polarity of the sulfoxide and sulfone forms of the parent organosulfur compound, they can be extracted to the aqueous phase, or removed by adsorption.

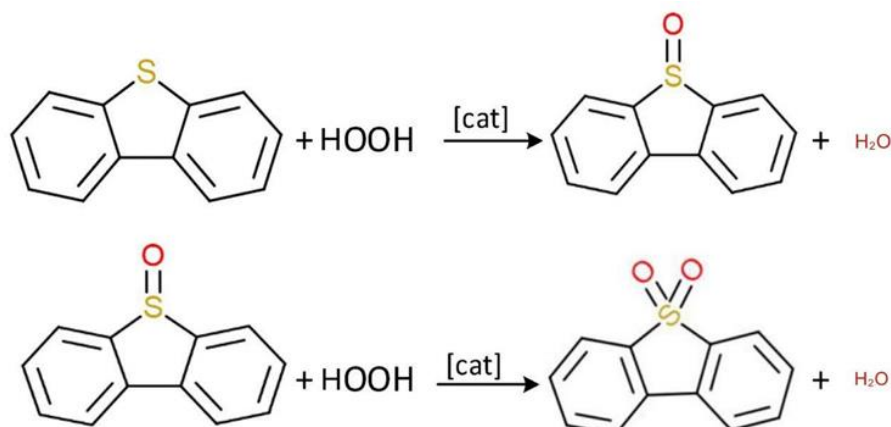


Figure 8 - Oxidation of DBT in ODS. Adapted from Houda, S. et al., (2018) [26]

2.3.2. SEPARATION PROCESS: EXTRACTION OR ADSORPTION

After the oxidation, the oxidized organosulfur molecules have physical and chemical properties remarkably different from those of the hydrocarbons in the fuel and they can, therefore, be more easily removed from the oil phase [43]. Some ways to perform this separation are extraction or adsorption.

The extraction process requires an extractant with high selectivity and is usually chosen because of its mild operating conditions, solvent recyclability, high speed and easiness of separation of the refined fuel from the solvent [47]. Nevertheless, it poses some challenges for implementation on an industrial scale. The loss of sufficient compost due to evaporation and the difficulty of regeneration are some of the factors that highlight these drawbacks [48].

The adsorption process is based on the ability of a solid adsorbent to selectively adsorb organic sulfur compounds from refinery streams [49]. It has the advantage of being carried out at room temperature and under low pressure. Several types of solid adsorbents have already been studied for the adsorption of sulfur compounds. These materials are usually transition metal complexes supported by porous materials such as zeolites or activated carbons [2,50].

Using H₂O₂ as an oxidizing agent, a two-phase system is formed and it is necessary to use a material that acts at the interface of the formed phases and allows mass transfer, such as a selective adsorbent [2]. Hybrid materials are very suitable for two-phase reactions. Due to their amphiphilic properties, they can interact simultaneously with the aqueous and the oily phase, facilitating mass transfer [51].

2.3.3. CATALYSIS IN ODS

There are two main factors that directly affect removal efficiency in the ODS process: the choice of the oxidant agent and the production of an effective, selective catalyst that can be easily recovered [50].

Catalysts can be categorized as homogeneous and heterogeneous. According to Van Leeuwen [52], homogeneous catalysis refers to a catalytic system in which the substrates for a reaction and the catalyst components are brought together in one phase, most often the liquid phase. Carboxylic acids (acetic acid, formic acid) and polyoxometalates are among the most important homogeneous catalysts in ODS, whose main advantages are low cost without significant resistance to mass transfer, high selectivity and reactivity [53]. However, its use has been limited due to the difficulty of its regeneration and separation from the reaction environment [54].

Considering this, heterogeneous catalysts have gained importance as an essential tool for achieving more sustainable methods. Heterogeneous catalysis refers to the form of catalysis in which the phase of the catalyst differs from that of the reactants [55]. One of the most important properties of heterogeneous catalysts is their easiness of separation, their large surface area - which promotes an increase in the interaction of the pollutant with the catalyst, and an increase in the separation efficiency. Furthermore, their chemical and thermal stability during the reaction is also an advantage [54].

In the ODS process, several types of catalysts have been explored, such as metal oxides (MO), metal complexes (MC), metal-free (MF), metal-organic frameworks (MOFs), polyoxometalates (POMs), titanosilicates (TS), porous aromatic frameworks (PAFs), covalent organic frameworks (COFs), ionic liquids (ILs), Fenton and Fenton-like catalysts (FFL), and biocatalysts (BioC) [55]. Among them, the solid catalysts are prominent, and the catalytic activity is mostly ascribed to noble metals or rare earth metals, such as nickel, iridium, tungsten, palladium, cobalt, scandium, yttrium and lanthanum [56], and also polyoxometalates [57].

However, these isolated components are not suitable for catalytic reactions because (i) they are unevenly distributed, (ii) have low mechanical strength, and (iii) have poor thermal stability and conductivity, being unstable and susceptible to external influences. In the case of polyoxometalates, they are homogeneous catalysts, as mentioned earlier. Therefore, the deposition of active metals on suitable surface substrates, such as alumina (Al_2O_3) and carbon-based materials is an important step in the preparation of the catalyst [57]. Another important characteristic for catalysts in ODS is to display

amphiphilic properties. Amphiphilic materials can simultaneously interact with aqueous and oily phases. In ODS reactions, they would allow promoting the formation of oxidizing radicals in aqueous phase while simultaneously interacting with the sulfur compounds in the oil phase, favoring mass transfer between phases.

One type of material that has been enlightened in heterogeneous catalytic reactions is nanostructured carbon-based materials. In the past three decades, many carbon-based nanostructures have been discovered, including fullerene, CNTs, graphene, and mesoporous carbon [58]. Some of these structures can be seen in Figure 9. Among them, CNTs have attracted attention for a series of reasons. They have shown better catalytic performance than conventional metal catalysts in many fields, such as hydrocarbon conversion, fine chemical production, fuel cells, and solar energy [59]. In 2011, a global estimate of carbon nanomaterial production was about 3500 tons and is estimated to expand. According to some studies, only the CNT market will exceed 70.000 tons of annual demand by 2032 [60,61]. CNTs have also the advantage of being easily tuned, allowing to introduce surface groups to alter their hydrophilic-hydrophobic characteristics, being suitable candidates for ODS applications [62].

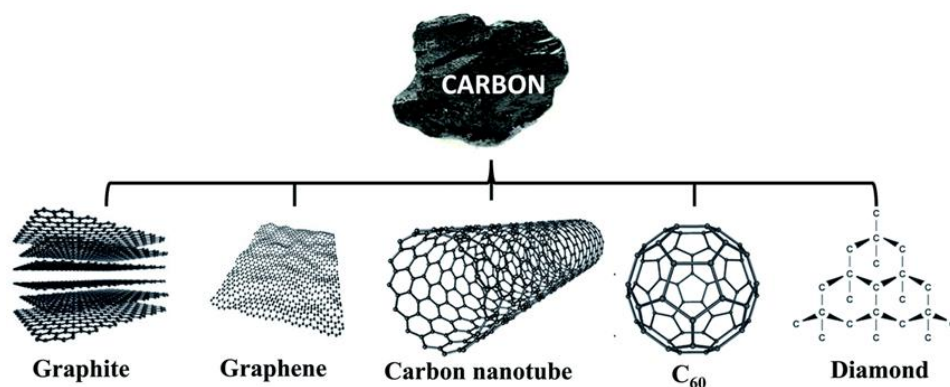


Figure 9 - Examples of different types of carbon-based nanostructures. Collected from Khan., M.E. (2021) [14]

2.3.3.1. CNTs AS CATALYSTS AND ADSORBENTS

Originally reported by Iijima in 1991, carbon nanotubes (CNTs) are highly attractive constituents for many technological applications [14,63]. Due to its high tensile strength, high elasticity, flexibility and other unique structural, mechanical, electrical and physicochemical properties, this material is increasingly reported as an effective catalyst and adsorbent in the field of analytical chemistry [51].

Nanotubes are long, slender fullerenes whose tube walls consist of hexagonal carbon (graphite structure) and are often closed at both ends. They can be formed of a single

wall (Single-Walled Nanotubes) or multiple walls (Multi-Walled Nanotubes) and are considered nearly one-dimensional structures according to their high length-to-diameter ratio (Fig.10) [64,65].

As some interesting features (in addition to their diameter on the order of nanometers and length on the order of micrometers), they have excellent thermal and electrical properties: thermal stability up to 2800 °C in vacuum, twice as thermally efficient as diamond, and they transmit electricity 1000 times faster than copper [4,65]. Because of these and other properties, there are numerous applications for these cylindrical carbon molecules in nanotechnology, electronics, energy devices, optics, and medical applications, among others [66,67].

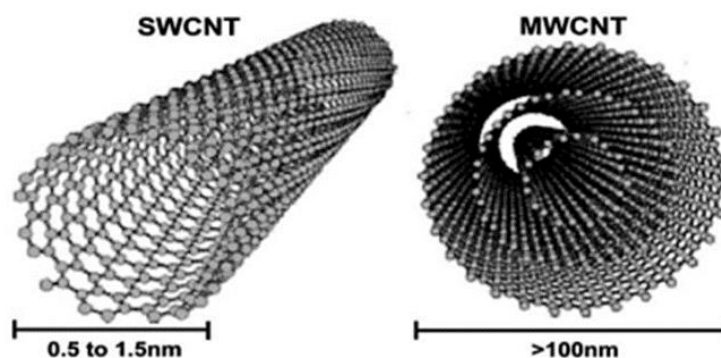


Figure 10 - Schematic representation of single walled carbon nanotube (SWCNT) and multiwalled carbon nanotube (MWCNT). Collected from Ribeiro, B. et al., (2016) [69]

In the field of catalysis, CNTs have been extensively investigated due to their high mechanical strength, high thermal stability, and considerable specific surface area. Due to its inert properties, extremely hollow and porous structures, large surface area, and strong interaction with organic molecules, it has been studied as a promising technology in the ODS process [54,68].

CNTs have a graphitic structure with unsaturated carbon atoms at the edges, as well as defects in the basal plane, which contribute significantly to surface reactivity with heteroatoms. Therefore, their surface has suitable active sites for adsorption of sulfur-containing compounds, making this material also an excellent adsorbent [62]. Table 3 summarizes some of the work done at ODS using CNTs as hybrid materials.

Table 3- Examples of works using CNTs in ODS

Ref.	Catalyst	Oxidizing Agent	Organic Phase	Pollutant	Results
[69]	W/CNT	H ₂ O ₂	n-hexane	DBT	95% of conversion and initial sulfur concentration of less than 600 mg L ⁻¹
[70]	CNT-SZ, CNT-TS, CNT-CD	Molecular Oxygen	n-dodecane	Benzothiophenic compounds (BT, DBT, 4,6-DMBT)	100% of conversion
[71]	POM@CNTs and CNTs@PDDA@POM	Molecular Oxygen	n-Octane	DBT	99.4% of conversion
[72]	MnOx/FMWNT	H ₂ O ₂	Naphta	Sulfur-compounds	99.8% of conversion
[51]	Fe/C700 and Fe/C900	H ₂ O ₂	oily solution (80% mineral oil, 20% toluene)	DBT and Quinoline	DBT removal of 38 and 10% (Fe/C700 and Fe/C900); QN removal of 100% (Fe/C700 and Fe/C900)
[51]	FeMo/C700 and FeMo/900	H ₂ O ₂	oily solution (80% mineral oil, 20% toluene)	DBT and Quinoline	DBT removal of 63% (FeMo/C700); QN removal of 100% (Fe/Mo/C700 and FeMo/C900)
[73]	CoW/CNT and CoW/CNF	H ₂ O ₂	<i>n-decane</i>	DBT	100% of removal
[74]	VO-MoO ₂ @NC	Cumene Hydroo	n-octane	DBT and 4,6-DMDBT	100% of removal
[75]	Pd/FMWNT	H ₂ O ₂	Real naphtha	Sulphur Compounds	More than 90% of removal

2.4. PRODUCTION OF CNTs

As CNTs have become a favorable area to be studied for their various potential applications, many methods have been developed to grow CNTs, such as laser ablation, arc discharge, solar energy, and chemical vapor deposition (CVD) [4,76].

Although all carbon nanotube synthesis and processing methods are constantly evolving, the CVD process is the most promising and preferred method. It is economically and industrially viable, can be easily scaled up and enables mass production [2,4]. As defined by Pierson [77], Chemical Vapor Deposition can be defined as the deposition of a solid on a heated surface from a chemical reaction in the vapor phase, which is currently widely used to produce new and modified catalysts [78]. During CVD, the thermal decomposition of a carbon-rich precursor occurs in the presence of a metal catalyst promoting the growth of nanoparticles [13]. In its simplest version, it requires only an oven, a tubular reactor, and a set of mass flow controllers to feed the gas mixture, being considered a simple and low-cost method [4,79].

Another advantage of the CVD process is the large number of parameters that can still be varied and investigated, both during catalyst treatment and CNT growth. Such factors can influence both the yield and quality of CNTs [80].

One of the factors that can directly influence the production of CNTs is the choice and synthesis of the metal catalyst. Since transition metals are able to dissolve carbon at higher temperatures and have a high diffusion rate of carbon, they are often used as a catalyst in powder form [81]. CNTs are usually produced using transition metal catalysts such as Fe, Ni and Co supported on silica, calcium carbonate, zeolites, or magnesium oxide [13,82]. The development of several Ni-based bi/trimetallic catalysts has been investigated, such as Ni-Co, Ni-Mg, Ni-Mo, Ni-Cu-Mo, Ni-Mg-Al, among others. According to some studies, bimetallic catalysts have a higher catalytic activity and excellent regenerative properties compared to monometallic catalyst [83]. Since Ni has a high capacity to break C-C and C-H bonds and Fe has economic advantages [82]. Nickel Ferrite is one commonly used CVD catalyst.

Another important factor in the synthesis of CNTs is the choice of a carbon source. In general, hydrocarbons such as methane, ethylene, and acetylene have been used as carbon sources for CNT synthesis [85]. Methanol, for example, as a renewable, low-cost and highly available source, has been studied as a viable option for application in the production of CNTs [2].

In addition to these hydrocarbons, waste polymers are also an alternative that is environmentally friendly and economically advantageous for CNT production. A variety of studies have been performed on converting virgin or waste plastics into high-value carbon nanomaterials [85]. Since the conventional treatment of polymeric wastes, such as incineration and landfilling, does not fully solve the problem of plastic waste

accumulation and is still associated with other types of environmental pollution, the use of plastic solid waste in the production of CNTs is a viable and desired alternative [84].

2.5. WASTE PLASTICS AS LOW-COST FEEDSTOCKS FOR CNT GROWTH

In the last 50 years, plastics have become an integral part of everyday life. Properties such as low density, resistance, robustness, design/manufacturing possibilities and low cost make them an easily accessible material with many possible applications [85]. Some of the most common uses for plastics are in packaging, construction, transportation/automotive, and electrical components. Since they are widely used and low-cost materials, they can be easily disposed of after use [86].

Worldwide, Plastic Solid Waste (PSW) is produced in massive quantities, reaching 150 million tons a year [87]. Data published in Our World in Data [88] shows that 9.5 billion tons of plastic have been produced globally until 2019, as shown in Figure 11.

Considering the mentioned data, waste management has been the subject of numerous studies in the past few decades. Some of the solutions proposed over the years are in continuous development, such as recycling and recovery technologies, investment in infrastructure, creation of viable markets, and industry/government/consumer participation. The most common alternatives include recycling (mechanical, chemical, and thermal), incineration and landfilling [88,89].

Nevertheless, there are some problems associated with these methods, such as: (i) constantly decreasing available landfill space; (ii) contamination of groundwater or aquifers — or both — due to leaks during the use of landfills or at the end of their activities; (iii) the lack of access to recycling facilities, (iv) the complexity of waste identification, separation and cleaning and (v) air pollution is the main consequence of burning plastic waste (incineration) in open fields [88,90]. Since more than 60% of post-consumer plastics end up in landfills or are incinerated, new treatment alternatives need to be investigated [91].

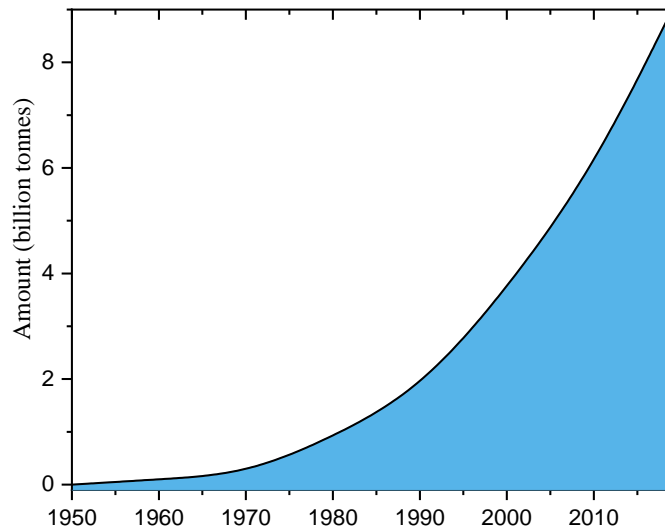


Figure 11 - Cumulative global production of plastics (polymers and fibers) until 2019. Adapted from Our World in Data [88]

One of them is *Upcycling*: an efficient way to transform plastic waste into high-value products that can significantly reduce the environmental impact of plastic production and consumption. The pyrolysis of plastics is an example of upcycling that has been widely used to produce carbon nanotubes (CNTs) [92,93].

The idea of using polymers as precursors for the growth of CNTs was first mentioned two decades ago [88]. Since then, thermal and catalytic pyrolysis of plastics have been studied in detail in different reactors and operating conditions. Generally, this process uses a heat source to catalytically decompose plastics and the products, either in liquid or gaseous form, serve as carbon sources for the growth of CNTs on catalysts [91]. The first stage of pyrolysis is reported to be where plastics are thermally degraded to produce a wide range of volatile hydrocarbons that serve as a carbon-rich feedstock. The products are then transferred to a second catalytic stage for carbon vapor deposition at high temperatures (typically 800 °C) [84]. Table 4 summarizes some of the work on CNT synthesis using different types of plastic as a carbon source.

Table 4- Works on the production of CNTs using different types of plastic as carbon source

Ref.	Catalyst	Polymer	Method	Conditions
[94]	Ni/Al ₂ O ₃ and Ni/AAO	High-density polyethylene (HDPE)	Two-stage catalytic thermal chemical conversion reaction	First Stage: 500°C Second Stage: 700°C; N ₂ as carrier gas
[95]	Ni/Cordierite; Fe/Cordierite; Ni-Mg/Cordierite	Recycled polypropylene (PP)	Two-stage pyrolysis reactor	Second Stage: 750°C at heating rate of 40°C/min; First Stage: 500°C at the rate of 10°C min; N ₂ as carrier gas; Different pressures (0.5 MPa, 1.0 MPa, 1.25MPa) were investigated
[96]	Co-Mo-MgO	A mixture of pure plastics: polypropylene (70 wt%, PP), low-density polyethylene (6 wt%, LDPE) and high-density polyethylene (24 wt%, HDPE)	Tandem catalytic process with CVD	Pyrolysis of plastics at 450 °C followed by non-catalytic cracking of volatiles at 530 °C (90 min); Synthesis temperature: 1000°C
[97]	Ni/MgAl ₂ O ₄	PolyLactic Acid, PLA	Two-stage pyrolysis reactor	Pyrolytic and Catalytic temperatures were operated at 500 °C and 500–700 °C; N ₂ as carrier gas (0.4 L/min)
[98]	Ni/ceramic	Waste high density polyethylene plastics (HDPE) with high purity (~90%)	Two-stage catalytic thermal-chemical conversion reaction system	Pyrolysis temperature: 500°C (first stage); Second Stage: Different reaction temperatures were used (600, 700 and 800 °C); N ₂ as carrier gas (100 mL/min)
[99]	Ni-Mo/Al ₂ O ₃	HDPE, LDPE, PET, PP and PS are used individually	Two-stage reaction system	First Stage: 700°C; Second Stage: 650°C (decomposition of the evolved gases)
[100]	NiMo-supported CaTiO ₃	Waste of polypropylene (PP)	Single-stage chemical vapor deposition technique	Different calcination temperatures were investigated (600,700 and 800°C)

As shown in Table 4, several types of polymers can be used in the process, such as polyethylene (PE), polypropylene (PP), polystyrene (PS), polyvinyl alcohol (PVA), polyvinyl chloride (PVC), polytetrafluoroethylene (PTFE), polycarbosilane, and polyethylene terephthalate (PET).

Figure 12 shows the plastics most in demand in Europe. Polypropylene (PP), low-density polyethylene (LDPE), high-density polyethylene (HDPE) and polystyrene (PS), represent almost 30% percent of all the plastic demand [17].

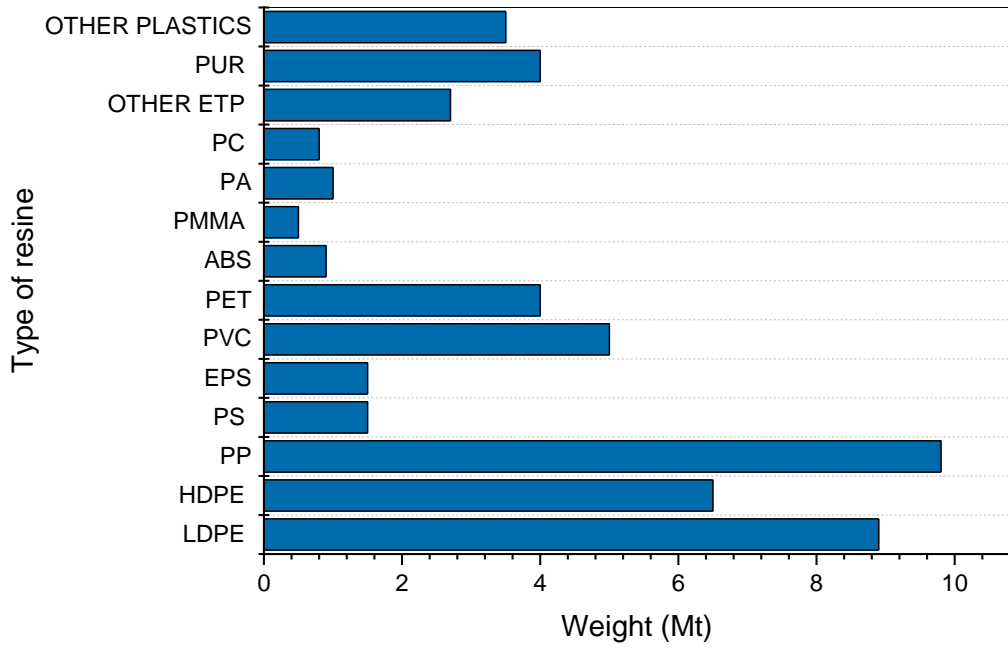


Figure 12 - Distribution of European plastic demand by resin type in 2019. Adapted from: *Plastics Europe Market Research Group* [17]

3. MATERIALS AND METHODS

3.1. REACTANTS AND EQUIPMENT

3.1.1. REACTANTS

- Aluminum oxide (Al_2O_3 , 99.7%) was provided by *Thermo Scientific*;
- High Density Polyethylene (HDPE; Melt Index 2.2g/10min; 190°C/2.16 kg), Low Density Polyethylene (LDPE; Average Mw ~35.000 by GPC, Average Mn ~7.700 by GPC) and Polypropylene (PP; Average Mw ~250.000; Average Mn ~67.000) were provided by *Sigma-Aldrich Chemistry*;
- Polystyrene (PS; Average Mw – 192,000), Dibenzothiophene sulfone ($\text{C}_{12}\text{H}_8\text{O}_2\text{S}$, 97%) and Titanium(IV) oxysulfate solution (TiOSO_4 , 99.99% trace metal basis) were provided by *Sigma-Aldrich*;
- n-Hexadecane ($\text{CH}_3(\text{CH}_2)_{14}\text{CH}_3$, 99%) was provided by *Alfa Aesar*;
- Hydrochloric acid (HCl, 37%) and Sodium chloride (NaCl, 98%) were provided by *VWR Chemicals*;
- Iron (III) chloride tetrahydrate ($\text{FeCl}_3 \cdot 6\text{H}_2\text{O}$, ACS reagent), Dibenzothiophene (98%), and Ammonia solution (NH_4OH , 28-30%) were provided by *Merck Chemicals*;
- Sulfuric Acid (H_2SO_4 , 98%), Sodium hydroxide pearls (NaOH, 98%), and Formic Acid (CH_2O_2 , 98%) were provided by *Labkem*;
- 2,2,4-Trimethylpentane (C_8H_{18} , 99.5%), Cyclohexane (C_6H_{12} , 99.99%), Acetonitrile ($\text{C}_2\text{H}_3\text{N}$, 99.9%), Propan-2-ol ($\text{C}_3\text{H}_8\text{O}$, 99.8%), Ethanol absolute ($\text{C}_2\text{H}_6\text{O}$, 99.8%), Nickel (II) chloride hexahydrate ($\text{NiCl}_2 \cdot 6\text{H}_2\text{O}$, Analytical reagent) and Hydrogen Peroxide (H_2O_2 , 60% w/v) were provided by *Fisher Scientific*;
- Nitric Acid (HNO_3 , 69%) was provided by *PanReac AppliChem*;
- Potassium bromide (KBr, 99%) was provided by *Acros Organics*;
- Phenolphthalein ($\text{C}_{20}\text{H}_{14}\text{O}_4$);
- Spray Mount, provided by *3M*

3.1.2. EQUIPMENT

- Magnetic stirrers, model C-MAG HS 7, provide by IKA
- Bath shaker, provided by OVAN;
- Oven (drying and heating chambers) provided by BINDER
- Synthesis Vertical Oven, model TH/TV, provided by *Termolab*.
- Furnace; provided by *THERMCONCEPT*;

- Muffle; model 6000 furnace, provided by *Thermolyne*
- Thermometer, model ETS-D5, provided by IKA;
- Fume hood with a control flow provided by ECRO CE;
- pHmeter, model IDS, provided by *WTW*;
- Hydraulic press, provided by *Specac*;
- Digester block, model HI 839800, provided by *Hanna instruments*;
- UV-Vis Spectrometer, model T70, provided by *PG Instrument Ltd*;
- FT-IR Spectrometer, model Spectrum Two, provided by *PerkinElmer*
- Gas Chromatograph System, model CP-3800, provided by *Varian*, equipped with a FID detector and a chromatographic column Supelcowax 10 (30mx0.25mmx0.25 μ m).
- TOC-L total organic carbon analyzer with the ASI-L autosampler all of them were provided by *SHIMADZU*.
- Pore Analyzer; model Nova Touch LX4, provided by *Quantachrome Ltd*;
- High-performance liquid chromatography (HPLC) coupled with a column of specification "RESTEK Ultra Biphenyl Column" (15cm x 2.1mm, particle size 5 μ m), and a UV detector (UV-2075 plus) and Quaternary Gradient Pump (PU-2089 Plus);
- Atomic absorption spectrometer, model SpectrAA, provided by *Varian*;
- Raman spectrometer, model Senterra, provided by *Bruker*
- Equipment for thermogravimetric analysis, model DTG60H, provided by *SHIMADZU*

3.2. PRODUCTION OF MATERIALS

3.2.1. NICKEL FERRITE

The co-precipitation method was used to synthesize the metallic catalyst, Nickel Ferrite, supported in alumina ($\text{NiFe}_2\text{O}_4/\text{Al}_2\text{O}_3$). To prepare the solution, 0.81 g of $\text{NiCl}_2 \cdot 6\text{H}_2\text{O}$ and 1.87 g of $\text{FeCl}_3 \cdot 6\text{H}_2\text{O}$ were added to approximately 200 mL of distilled water to obtain 20% of NiFe_2O_4 considering 4 g as the basis. The mixture was well-stirred, and 3.2 g of alumina was added and stirred for an hour. Then, ammonium hydroxide (1 mol L⁻¹) was added at a rate of 1 mL min⁻¹ until the pH reached 9, followed by an additional hour of stirring.

The mixture was left undisturbed for about an hour, allowing the solid to precipitate. The resulting catalyst was washed with distilled water until the pH reached 7, and then ethanol was used for further washing. After drying the catalyst in an oven at 60°C, it was

subjected to thermal treatment for calcination. The calcination process involved heating the catalyst in a muffle at a temperature of 800°C for three hours. The resulting material was used for the production of carbon nanotubes.

3.2.2. CNTs

Three carbon nanotube (CNTs) types were produced using the chemical vapor deposition (CVD) technique. The three types were CNT-PS, which used polystyrene as the carbon source, CNT-MIX, which used a mixture of polyolefins (LDPE:HDPE:PP; 35:25:40 – mass basis) as the carbon source; and CNT-MIX-PS, which used a combination of both polyolefins and polystyrene (LDPE:HDPE:PP:PS 31:23:35:11, mass basis). The goal was to produce approximately 3 grams of each type of CNT by conducting three syntheses for each material.

The CVD process was performed in a vertical oven (TH/TV, TERMOLAB), with the metal catalyst placed at the bottom and the polymer source at the top. For the synthesis of CNTs, 1 g of the catalyst was loaded in the lower crucible and 5 g of the desired polymer (or a mixture of polymers) in the upper crucible. The furnace was divided into three temperature control regions, T1, T2, and T3. The syntheses were carried out under an inert atmosphere of N₂ (50 mL min⁻¹) at a temperature of 800 °C in the T3 region, which was maintained for one hour after reaching the desired temperature.

After each synthesis, the produced material was subjected to an acid wash with 50% v/v H₂SO₄ (140°C, 3 h under reflux) to remove any excess metallic material bound to the structure. The material was then filtered and washed with distilled water until reaching a neutral pH, followed by drying in a muffle at 60°C. Finally, the materials were washed with nitric acid (69%, 130°C for 24 hours under reflux) washed with distilled water until the neutrality of rinsing waters, and dried.

To study the impact of functional groups incorporated into the material's surface, 1.5 g of CNT-MIX was treated in an inert atmosphere (N₂; 100 mL min⁻¹) by a temperature ramp of 120 °C h⁻¹ until 800°C was reached. It occurred for approximately 10 hours in an oven (brand *THERMCONCEPT*), forming CNT-MIX-800. Figure 13 demonstrates the appearance of a CNT synthesized from polymers.



Figure 13 - Appearance of a CNT synthesized by polymers (CNT-PS)

3.3. MATERIALS CHARACTERIZATIONS

3.3.1. FOURIER TRANSFORM INFRARED SPECTROSCOPY (FTIR)

Fourier Transform Infrared Spectroscopy was employed to analyze the materials on a PerkinElmer spectrophotometer. KBr pellets were prepared, each incorporating a specific material. The measurements covered various relevant spectral regions over 450 to 4000 cm^{-1} . All measurements were carried out at room temperature.

3.3.2. ACIDIC CHARACTERIZATION

A sample weighing 0.1g was combined with 25 mL of a 0.02 mol L^{-1} NaOH solution to determine acidic sites. The resulting mixture was agitated at 200 rpm for 48 hours. Afterward, the mixture was filtered, and 5 mL of the filtrate was titrated using 0.01 mol L^{-1} HCl, with phenolphthalein serving as the basic indicator site. A sample weighing 0.1g was combined with 25 mL of a 0.02 mol L^{-1} HCl solution to determine basic sites. The resulting mixture was agitated at 200 rpm for 48 hours. Afterward, the mixture was filtered, and 5 mL of the filtrate was titrated using 0.01 mol L^{-1} NaOH, with phenolphthalein serving as the indicator.

Also, the determination of the Point of Zero Charge (pH_{PZC}) value for each material was performed. Six dilutions of 0.01 mol L^{-1} NaCl were prepared to create various pH conditions. The pH of each dilution was adjusted to specific values, namely 2, 4, 6, 7, 10, and 12, by carefully adding HCl and NaOH solutions at concentrations of 0.02 mol L^{-1} . In each flask, 25 mg of the material was introduced. All the flasks were then agitated at 200 rpm for 24 hours. After completion, the mixture was filtered, and the final pH (pH_{F}) was determined. The pH of the point zero charge was found by the interception between the curve $\text{pH}_0 \times \text{pH}_{\text{F}}$ and the identity curve.

3.3.3. SURFACE AND PORE ANALYZER

The N₂ adsorption-desorption isotherms at a temperature of 77 K were utilized to determine the textural properties of the materials. These isotherms were obtained using a Quantachrome instrument NOVA TOUCH LX4, employing long cells with a bulb and an outer diameter measuring 9 mm. The materials were subjected to outgassing at 200 °C for 4 hours. The specific surface area (S_{BET}) was calculated using the BET method by employing Quantachrome TouchWin software. The calculations were performed within the range of p/p_0 0.05 – 0.35 and total pore volume was estimated at $p/p_0 = 0.98$.

This technique enables the classification of materials based on their adsorption isotherms, as well as the determination of loop hysteresis according to IUPAC standard, as shown in Figure 14 (A and B, respectively).

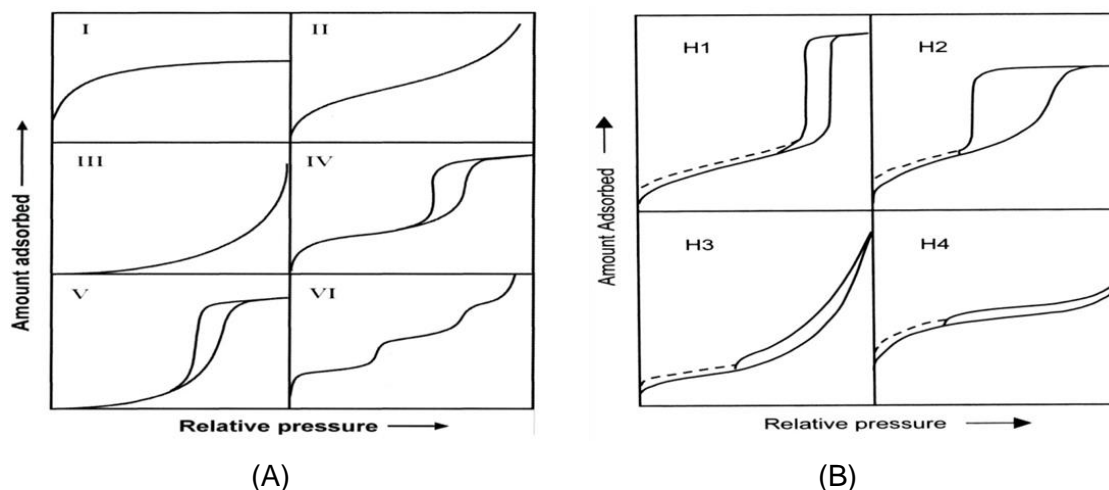


Figure 14 - Classification of isotherms and loop hysteresis according to IUPAC. Adapted from AL Othman, Z. A. (2012) [101]

3.3.4. CONTACT ANGLE

The contact angle of the samples was determined by following a methodology reported elsewhere [101]. Briefly, a glass slide was covered with the powdered material with a spray adhesive. The adhesive was allowed to dry, and any loose solid was gently removed from the glass slide. Three distinct measurements were performed for the contact angle in each slide, and the recorded images were processed using ImageJ software. The reported values are an average of the three distinct measurements.

3.3.5. METAL AND ASH CONTENT

The atomic absorption technique was employed to determine nickel and iron in the ashes of the samples. Approximately 200 mg of all materials underwent heat treatment in a muffle furnace at 800 °C for 8 hours in previously calcined crucibles for 1 hour at 550 °C. Following this, about 6 mg of ash from each sample was digested in 5 mL of aqua regia (3HCl:1HNO₃, v/v). The digestion process was carried out in triplicate, and the resulting solutions were left in a digester block for 9 hours at 105 °C. Afterward, the solutions were separately filtered and diluted with 5% v/v nitric acid in 50 mL flasks. The samples were analyzed using an atomic absorption spectrometer, and the results were obtained by utilizing a calibration curve for iron and nickel within the range of 0-10 ppm. The constructed curves (Figure 15) exhibited R² values of 0.9917 and 0.9909, respectively, indicating a remarkable linear correlation between the variables.

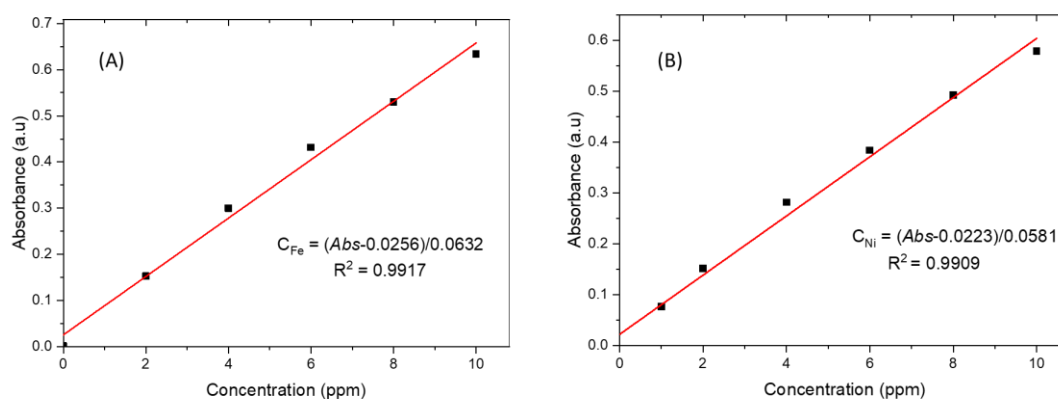


Figure 15 - Calibration curves for (A) Fe determination and (B) Ni determination

3.4. ANALYTICAL METHODS

3.4.1. UV-VIS SPECTROPHOTOMETRY

Quartz cells with dimensions of 10 x 10 mm and a UV-Vis Spectrometer (model T70) provided by PG Instrument Ltd were used for the UV-Vis analyses. To quantify the concentration of hydrogen peroxide in the aqueous phase, a reaction sample was appropriately diluted and then supplemented with TiOSO₄ and 0.5 M H₂SO₄, by a colorimetric method [102].

The solution was analyzed at a specific wavelength of 405 nm to determine the hydrogen peroxide concentration. This measurement was made using a calibration curve generated from a concentration range from 1 g L⁻¹ to 12 g L⁻¹. The calibration curve obtained with this procedure presented an R² value of 0.9992, considered an excellent

value for linear adjustments. Figure 16 visually depicts the curve obtained, showcasing the relationship between the measured values and the corresponding concentrations.

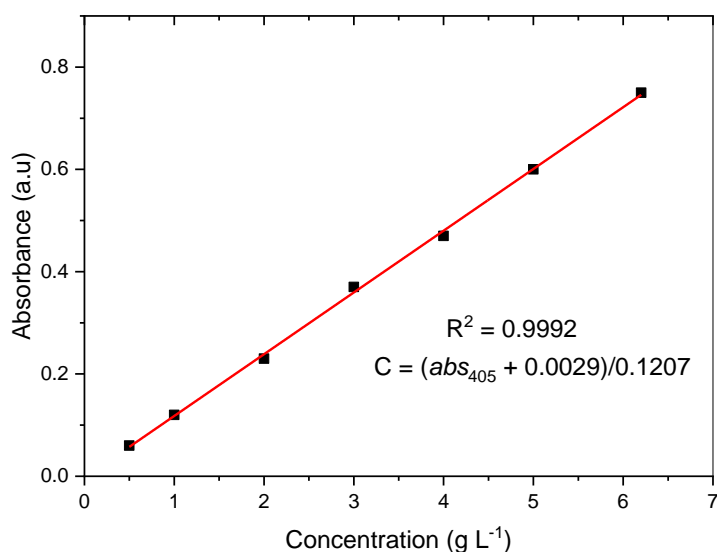


Figure 16 - Calibration curve for H₂O₂ determination

During the adsorption tests, the concentration of DBT was determined by diluting a 0.1 mL aliquot of the organic phase with 20 mL of isopropyl alcohol in a flask. The resulting solution was measured at a wavelength of 235 nm, and the concentration of DBT was determined using a calibration curve with a concentration range from 1 ppm to 2.5 ppm. The value of R² was found to be 0.9993, which shows a good fit for the linear regression. Figure 17 visually depicts the curve obtained.

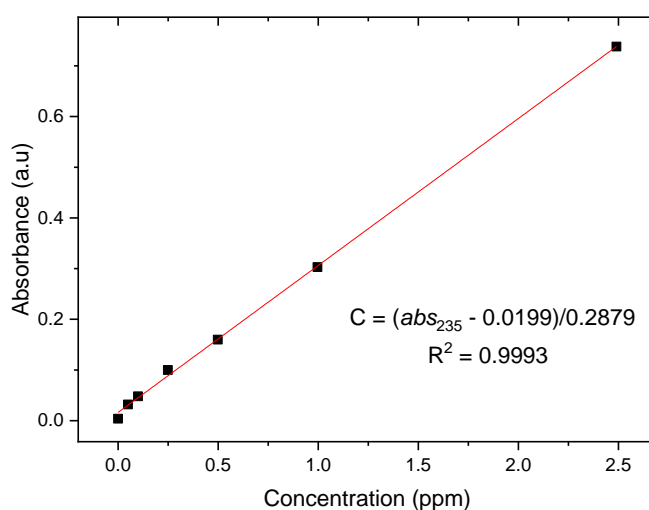


Figure 17 - Calibration curve for DBT determination

3.4.2. GAS CHROMATOGRAPHY WITH A FLAME IONIZATION DETECTOR (GC-FID)

Samples for chromatographic analysis were prepared by mixing 200 μL of the internal standard (n-hexadecane in cyclohexane 1 mg mL^{-1}) in an aliquot of 1 mL of the organic phase. The operation conditions used for GC analysis were a helium flow (carrier gas) of 1 mL min^{-1} and an initial oven temperature of 50 $^{\circ}\text{C}$, which was held for 1 min. Then, a first ramp was done up to 270 $^{\circ}\text{C}$ at 15 $^{\circ}\text{C min}^{-1}$ rate, which was held for 2 min, leading to a total running time of 16 min. The injection temperature was 250 $^{\circ}\text{C}$, and the detector temperature was 200 $^{\circ}\text{C}$, and all the analysis were made in the splitless mode.

The calibration curve was constructed within the 10 to 500 ppm concentration range. It was established by analyzing the ratio between the areas obtained from the internal standard and the DBT (Y-axis) and plotting it against the internal standard and the DBT (X-axis) concentration. The R^2 value of 0.9942 indicates a strong linear approximation, providing evidence of a robust relationship between the variables. Figure 18 depicts the resulting curve.

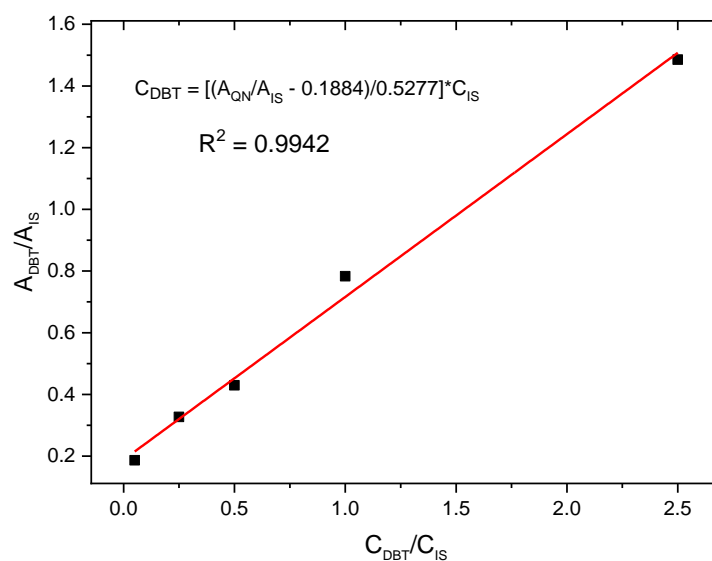


Figure 18 - Calibration curve for DBT determination by GC-FID

3.4.3. HIGH PERFORMANCE LIQUID CHROMATOGRAPHY (HPLC)

HPLC (High-performance liquid chromatography) was used to identify DBT and possible intermediaries in the extractant phase. For this method, a column "RESTEK Ultra Biphenyl Column" (15cm x 2.1mm, particle size 5 μm) and a mobile phase with 50% of acetonitrile and 50% of ultrapure water with orthophosphoric acid (1 mL L^{-1}) were used.

All the analyses were done in an isocratic system at a flow of 0.3 mL min⁻¹, and DBT was detected at a wavelength of 235 nm. The calibration curve was constructed within the 0.1 to 50 ppm concentration range. The R² value of 0.9990 indicates a strong linear approximation and a good fitting for the experimental data. Figure 19 depicts the resulting curve.

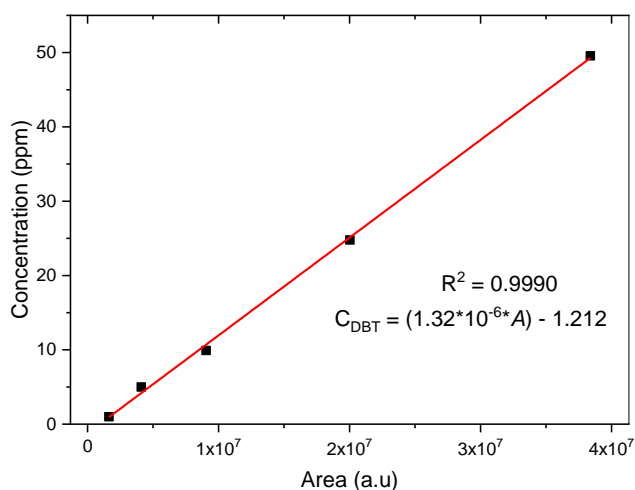


Figure 19 - Calibration curve for the determination of DBT concentration in the extractant phase by HPLC

To quantify dibenzothiophene sulfone (DBT_{SO₂}) in the extractant phase, a calibration curve was generated within a range of 1-50 ppm. The constructed curve (Figure 20) exhibited a R² value 0.99954, indicating a highly accurate linear approximation.

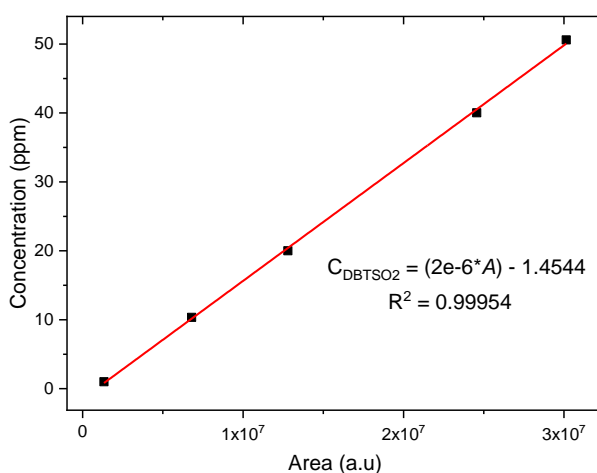


Figure 20 - Calibration curve for the determination of DBT_{SO₂} concentration in the extractant phase by HPLC

3.5. ADSORPTION OF DBT

3.5.1. IN OILY PHASE

A solution containing 500 ppm of DBT in isooctane was prepared. Next, 0.125 g of CNT-PS was added to a reaction flask containing 50 mL DBT-isooctane solution. The mixture was heated to 80 °C and stirred for 24 hours. Aliquots of 0.5 mL were collected at different time intervals (0, 30, 60, 120, 240, and 480 min) to monitor the adsorption and diluted with ethanol for subsequent UV-Vis analysis. The absorbance of each sample was measured at a wavelength of 235 nm. This same procedure was performed for CNT-MIX, CNT-MIX-PS, and Nickel Ferrite.

3.5.2. BIPHASIC MEDIUM

To conduct adsorption tests in a biphasic medium, approximately 0.125 g of the catalyst was added to a 250 mL flask containing 10 mL of aqueous phase (H₂O; pH = 3) and 40 mL of the organic phase (isooctane-DBT with a concentration of 500 ppm). The pH of the aqueous phase was adjusted using sulfuric acid (0.5 M). The system was stirred at 80 °C for 8 hours. At various time intervals (0, 60, 120, 240, and 480 minutes), aliquots of 1 mL from the organic phase and 0.25 mL from the aqueous phase were extracted. For subsequent UV-Vis analysis, the organic phase was diluted with ethanol. The absorbance of each sample was measured using UV-Vis spectroscopy at wavelengths of 235 nm to detect DBT. This adsorption test was performed for all three types of synthesized CNT and the metallic catalyst.

3.6. OXIDATIVE DESULFURIZATION OF DBT

A catalyst weighing 0.25 g was placed into a 250 mL flask for desulfurization oxidation tests. The flask was filled with 20 mL of aqueous phase (H₂O; pH = 3) and 80 mL of organic phase (isooctane-DBT). The system was stirred at 80 °C. The initial time of reaction was established after adding 0.37 mL of H₂O₂ (60% w/v) (C_{H₂O₂} = 11.1 g L⁻¹), followed by the addition of the catalyst. Subsequently, aliquots of 2 mL from the organic phase and 0.5 mL from the aqueous phase were collected at intervals of 0, 30, 60, 120, 240, and 480 min. The concentration of hydrogen peroxide was determined for the aqueous phase and analyzed by UV-Vis at a wavelength of 405 nm, and the oily phase was analyzed by GC-FID to determine the concentration of DBT. This test was conducted for all materials. Figure 21 exemplifies an experimental setup for the reactions.



Figure 21 - Setup for the experimental trials

Furthermore, an additional set of ODS trials was conducted utilizing CNT-MIX, changing parameters such as the extractant phase and the oxidant. Table 5 presents comprehensive information regarding the specific reagents employed in each test.

Table 5- Conditions and reagents used in the additional set of experiments with CNT-MIX

Trial	Extractant phase	Oxidant	The proportion between hydrogen peroxide and formic acid (vol./vol.)
A*	Water	H ₂ O ₂ :H-COOH	1:1
B	Acetonitrile	H ₂ O ₂	-
C	Acetonitrile	H ₂ O ₂ :H-COOH	1:1

* Ultrapure water was used in this trial (pH = 7).

3.7. NON CATALYTIC TRIALS

To conduct the non-catalytic test, a 250 mL flask was filled with 20 mL of the organic phase (DBT-Isooctane) and 80 mL of the aqueous phase (H₂O; pH = 3) and heated to 80 °C. Next, 0.37 mL of hydrogen peroxide (C_{H₂O₂} = 11.1 g L⁻¹) was added to the solution, stirring for 8 hours. Aliquots of 2 mL from the organic phase and 0.5 mL from the aqueous phase were collected at intervals of 0, 30, 60, 120, 240, and 480 min.

For UV-Vis analysis of the aqueous phase, samples were analyzed at a wavelength of 405 nm to measure the concentration of hydrogen peroxide. GC-FID analyzed the oily phase to determine the concentration of DBT.

4. RESULTS AND DISCUSSION

4.1. SYNTHESIS OF MATERIALS

Four syntheses of nickel ferrite were conducted to produce approximately 16 g of catalyst. The average yield obtained in the syntheses was approximately 84.6%, resulting in a total production of 13.5 g of metallic catalyst, successfully used to synthesize different CNTs. In order to evaluate the efficiency of the CNT synthesis, the yield was calculated by considering the carbon content in both the carbon source (polymer) and the structure of the CNTs. The carbon content was obtained from the mass obtained after the CVD process, and changes in the mass of the metallic catalyst were not considered. Equation 1 was used for the calculation.

$$CVD\ Yield = \frac{Carbon\ in\ the\ CNTs\ synthesized}{Carbon\ in\ the\ polymer} \times 100 \quad (1)$$

The conversion yield of the polymers into each type of CNT can be seen in Figure 22. The synthesis of CNT-MIX-PS showed the highest yield (25.2%) followed by the synthesis of CNT-MIX (21.6%) and then CNT-PS (21.3%) Factors such as the carbon source, the pyrolysis temperature and the type of catalyst directly influence the synthesis yield, as already well established in several studies [103,104,105]. The mean values obtained, considering the components used, correspond to values already reported in the literature [106,107,108]. Even though the gas compositions differed, the results can be comparable, given the low standard deviations observed (3.162, 1.154 and 0.849 for CNT-PS, CNT-MIX and CNT-MIX-PS, respectively) [109].

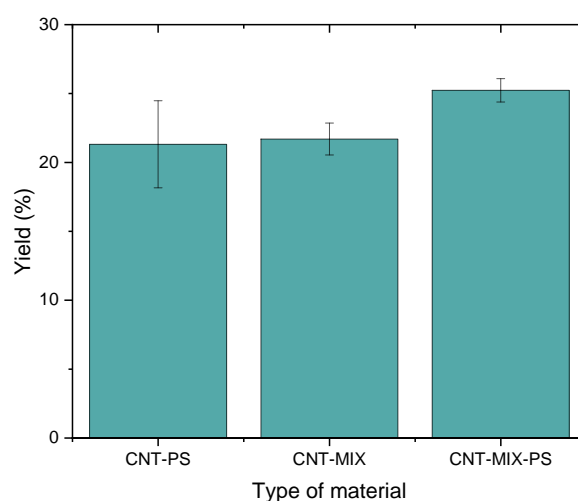


Figure 22 - Carbon onversion yields in the CVD process

After the production of the carbon nanotubes, an acid wash with sulfuric acid was employed. This procedure offers multiple advantages. Firstly, it enables the functionalization of the CNTs surface, which may enhance adsorption properties. Secondly, it effectively purifies the compound by removing any residual metallic materials. This purification step is crucial in preventing the potential leaching of metallic compounds, thereby contributing to environmental safety and protection [110]. Other studies report that the acidic wash can also remove amorphous carbon from crude materials [111]. Subsequently, an additional wash with nitric acid was carried out to eliminate residual alumina in the materials.

Figure 23 presents the corresponding percentage of mass loss achieved after each acid wash stage.

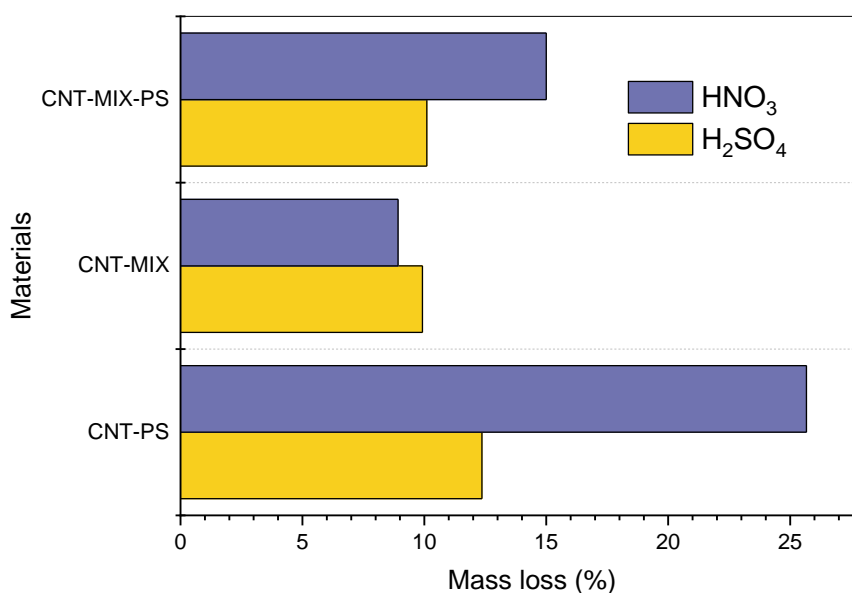


Figure 23 - Mass loss after each acidic wash

The mass loss after each acidic wash presented varied results across the materials. For CNT-MIX, it did not exhibit significant variations across different washes, (9.92 and 8.91% for H₂SO₄ and HNO₃, respectively). However, for the CNT-PS and CNT-MIX-PS materials, the nitric acid wash exhibited a higher mass loss compared to the sulfuric acid wash. For CNT-MIX-PS, the mass loss between washes exhibited a percentage difference of 5% (10.10 and 15.00% for H₂SO₄ and HNO₃, respectively). In contrast, CNT-PS demonstrated a more significant difference, with a value of 13.28% (12.35 and 25.6% for H₂SO₄ and HNO₃, respectively). This observation suggests a potential inclination towards greater hydrophilicity in materials synthesized from polystyrene, as they exhibited stronger interactions with the acid, resulting in a higher removal of metallic

content (the predominant components targeted for elimination). The obtained values align with reported data, indicating that CNTs treated with H_2SO_4/HNO_3 can undergo substantial weight reduction ranging from 17 to 100%, depending on the concentrations of the acids involved [112].

4.2. CHARACTERIZATION OF THE MATERIALS

The prepared materials were characterized by Fourier Transformed Infra-Red (FTIR), metal and ash content, acidity/basicity determination, adsorption-desorption isotherms of N_2 and contact angle.

4.2.1. FOURIER TRANSFORM INFRARED SPECTROSCOPY (FTIR)

The FTIR spectra obtained by analysis of the different materials are depicted in Figure 24.

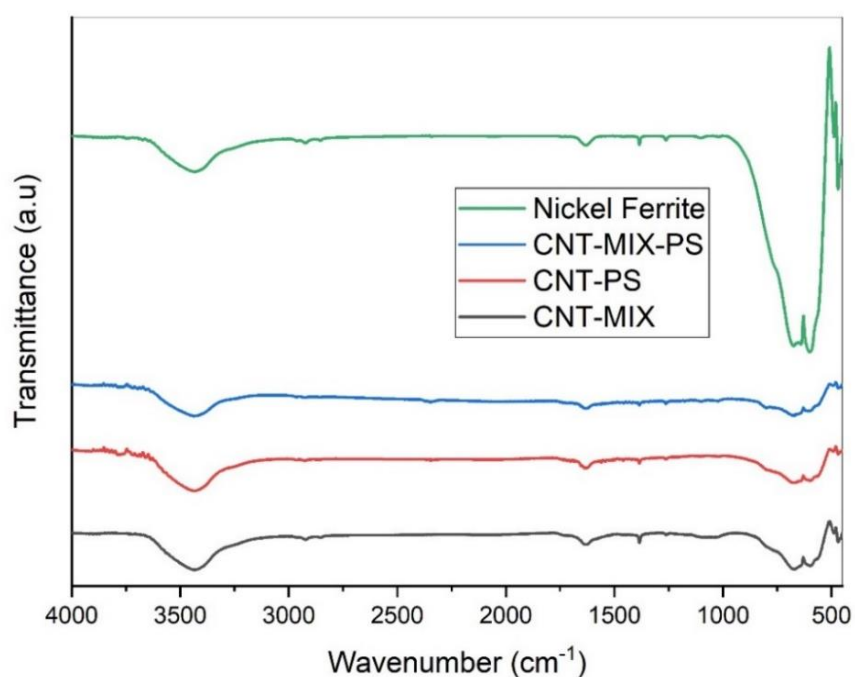


Figure 24 - FTIR Spectra of the prepared materials

Upon observing the FTIR spectrum of Nickel Ferrite, it is possible to readily identify prominent absorption bands within the 400-600 cm^{-1} range. According to literature, the FT-IR bands of solids in the range of 1000-100 cm^{-1} are commonly associated with the vibration of ions within the crystal lattice [113].

The most significant band located around 600 cm^{-1} can be attributed to the intrinsic stretching of the $NiFe_2O_4$ at the tetrahedral vibration site [114,115]. Conversely, the

smaller band at approximately 500 cm^{-1} corresponds to the octahedral stretching vibration of the complex, a characteristic feature found in all spinels and especially in ferrites [116,117]. Additionally, notable bands are observed at approximately 1600 cm^{-1} and 3400 cm^{-1} , which correspond, respectively, to the bending mode of H_2O molecules and the stretching mode of H_2O molecules and OH groups [118], likely due to adsorbed water at the materials' surface.

The FTIR spectra of the synthesized CNTs exhibited similar results for all samples. The band at 3400 cm^{-1} could be attributed to the presence of the COOH peak [119] and the peak at approximately 1600 cm^{-1} could be attributed to conjugated C=C bonds [120], as previously reported for carbon materials.

Nevertheless, there is a noticeable resemblance between the spectral bands of the metallic catalyst and the carbon materials. A discernible decrease in band intensity can be observed in the CNTs compared to the catalyst, indicating the growth of carbon materials. Since complete elimination of metallic components was not achieved, it is plausible to associate the detected bands in the CNTs with the catalyst that remains in the structure of the carbon nanotubes.

4.2.2. ACIDIC CHARACTERIZATION

Depending on their functionalization and treatment, CNTs can have both acidic and basic sites on their surface. In this work, nitric acid (69% v/v) and sulfuric acid (50% v/v) were used to functionalize the materials to remove metallic particles and impact their hydrophobic surface.

Another critical parameter that significantly affects the adsorption of substances into carbon nanotubes is pH_{pzc} . At the point of zero charge (pH_{pzc}), the total positive charges at the surface of the CNT balance the total negative charges [121]. Consequently, below the pH_{pzc} , the surface exhibits a positive charge, while above the pH_{pzc} , the surface becomes negatively charged. Understanding the pH_{pzc} is fundamental as it indicates the sorbent's efficacy in relation to the pH of the medium being treated [122]. This information is crucial for optimizing adsorption and ensuring the desired result. The pH_{pzc} values were determined using the methodology described, and the resulting curve is depicted in Figure 25.

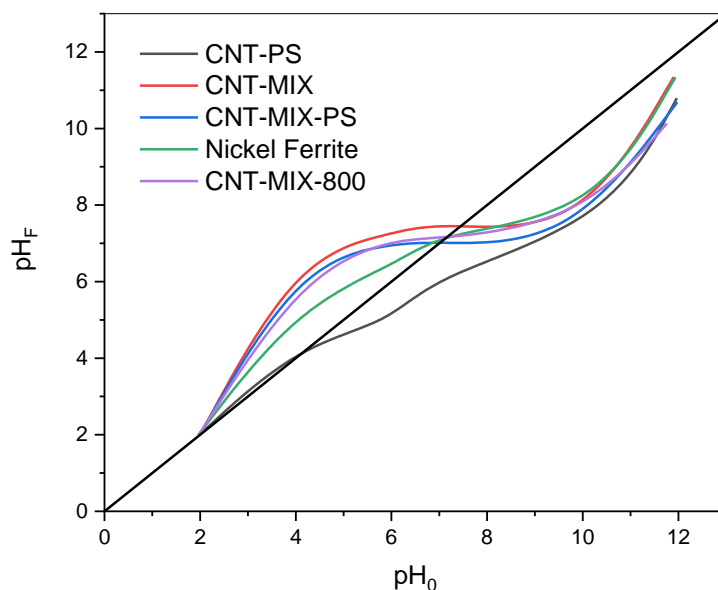


Figure 25 - pH_{pzc} curves for the materials

Table 6 displays the measured values for the acidic and basic sites (determined by titration) alongside the corresponding pH_{pzc} values for the materials.

Table 6- Results of the acidic characterization

Samples	Acidity ($\mu\text{mol/g}$)	Basicity ($\mu\text{mol/g}$)	pH_{pzc}
CNT-PS	195	50	4.10
CNT-MIX	100	0	7.45
CNT-MIX-PS	199	40	7.04
CNT-MIX-800	190	25	7.09
Nickel Ferrite	50	65	7.16

The obtained acidity and basicity values indicate a higher concentration of acidic sites in the materials. This finding aligns with the applied methodology, where the materials underwent treatment with acidic substances. This characterization was adapted from the Boehm titration methodology [123], which may introduce certain limitations, such as potential errors arising from the influence of CO_2 during the analyses. Examining Table 6, it is noteworthy that the material with the lowest pH_{pzc} (CNT-PS) also exhibited a relatively high count of acidic sites, aligning with findings in literature [124].

On the other hand, CNT-MIX-PS displayed the highest number of acid sites, yet its pH_{pzc} value was closer to neutral. It is important to emphasize that the quantity of acidic sites

alone does not determine the overall acidity of a material, as acidity can vary in terms of type of acidic groups, concentration, amount of CNTs, treatment methods and operating temperature [125]. Additional characterization tests would be essential to validate this assert.

Based on the results, it is evident that the materials synthesized using polystyrene exhibited the highest number of acid sites. This observation highlights the notable impact of the polymer's structure, indicating that materials made with polystyrene may have a distinct tendency to incorporate various acidic groups compared to the other polymers used in the synthesis. This information is further supported by the distinctive value of pH_{PZC} exhibited by CNT-PS, distinguishing it from the other materials.

The oxidation tests conducted in this work were primarily performed at an initial pH of 3, leading to intriguing findings regarding the materials' pH_{PZC} . Given that the pH of the aqueous phase is lower than the pH_{PZC} of all materials, it is plausible to assume that the catalyst in contact with the aqueous phase acquires positive charges. This phenomenon may facilitate the adsorption of negatively charged intermediates, such as dibenzothiophene sulfone, which can potentially be produced during oxidation tests, providing evidence of a synergy between the catalyst, solvent and oxidizing agent in the oxidation-extraction process for DBT removal from the oil phase [126]. In general, the acid characterization allowed obtaining a preview of the reactivity of the materials and their surface modifications.

4.2.3. METAL AND ASH CONTENT

As stated in the existing literature, prior observations have indicated that carbon nanotubes continue to retain residual metallic catalyst nanoparticles despite undergoing a rigorous washing procedure involving high-temperature treatment with nitric acid. This persistence can be ascribed to the presence of multiple graphene sheets that encapsulate these metallic nanoparticles, rendering their complete removal a challenging task [127]. The findings obtained from this analysis align with this established phenomenon, as the materials examined exhibited final metallic content ranging from 0.6 to 4.9% for iron and 0 to 1.7% for nickel.

As shown in Figure 26, it is possible to see that the values found for the metallic content in the ashes of the materials and each material specifically followed the same trend.

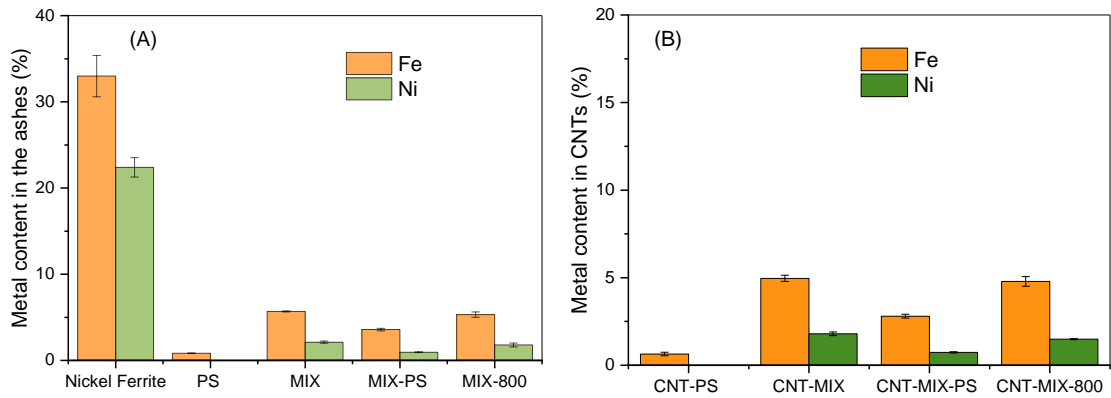


Figure 26 - Metal content in the ashes (A) and in the CNTs (B)

Notably, the material synthesized with polystyrene exhibited lower iron and nickel content after the acid treatments, corroborating the significant mass loss observed during the washes. The CNT-MIX and CNT-MIX-800 materials displayed similar metal content, which aligns with expectations since the heat treatment of CNT-MIX-800 should have minimal impact on the metal content. In comparison, the CNT-MIX-PS material demonstrated intermediate results when compared to CNT-MIX and CNT-PS, indicating that the combination of polymers in CNT synthesis can result in intermediate characteristics regarding surface characteristics. CNT-MIX showcased the highest residual nickel and iron contents, further supporting the findings of minimal mass loss during heat treatments along with the fewest acidic sites.

Figure 27 provides a visual representation of the ash content for each material following heat treatment.

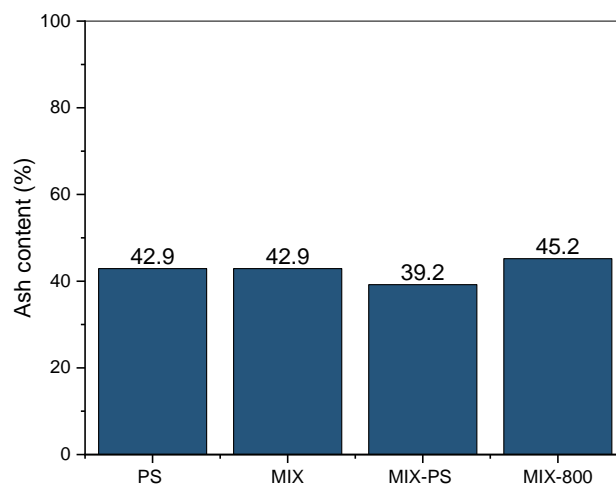


Figure 27 - Ash content of the materials

The quantities of ashes obtained align with the yields achieved during the synthesis of each material. The synthesis of CNT-MIX-PS yielded the highest result, resulting in the lowest ash content among the other materials. Furthermore, by comparing these values with the metallic content obtained from the ashes, it becomes apparent that the acid treatment exhibited greater effectiveness in removing metals than the potential removal of alumina, which served only as a support material during the synthesis of nickel ferrite.

4.2.4. SURFACE AND PORE ANALYSIS

Figure 28 shows the adsorption isotherms of N₂ at 77 K on the prepared materials.

By analyzing Figure 28, it is evident that the material with the highest adsorption capacity was CNT-PS, followed by CNT-MIX and MIX-PS. On the other hand, CNT-MIX-800, which underwent heat treatment, exhibited the lowest adsorption capacity among the carbon materials. Thermal treatment can induce thermal decomposition or chemical transformations in functional groups, directly impacting the surface modifications of CNTs. This finding is consistent with expectations, as functionalized materials typically exhibit higher adsorption capacity [128][129].

The difference in the obtained adsorption capacity values signifies variations in the material's surface properties when employing different carbon sources [130]. Interestingly, the CNT-MIX-PS material, derived from a combination of CNT-PS and CNT-MIX precursors, exhibited intermediate characteristics compared to the other two materials. It displayed a curve profile closely resembling the one of CNT-PS while demonstrating a closer adsorption capacity to CNT-MIX.

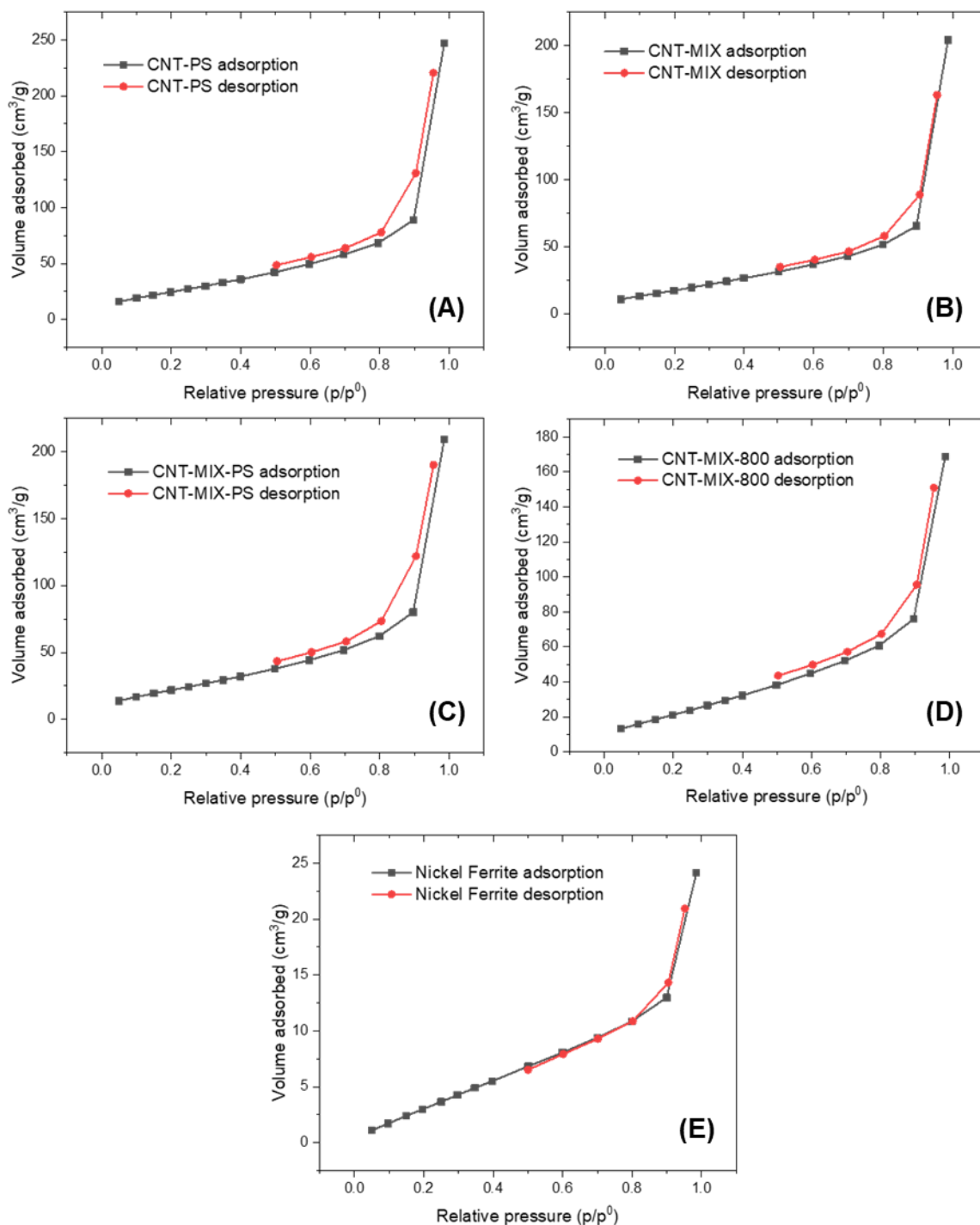


Figure 28 - Adsorption isotherms of N₂ at 77 K of the A) CNT-PS, B) CNT-MIX, C) CNT-MIX-PS, D) CNT-MIX-800 and E) Nickel Ferrite

Based on the IUPAC classification, it can be concluded that the carbon materials exhibit similar profiles, closely resembling the IV(a) curve. Materials exhibiting this profile are typically associated with adsorbents that possess mesoporous characteristics. This observation aligns with existing literature, which frequently reports the presence of mesoporous structures in carbon nanotube materials [131,132]. The shape of the curve

is a consequence of the monolayer-multilayer adsorption, followed by pore condensation. The materials exhibited a type III hysteresis, a commonly observed phenomenon for this type of curve, indicating the presence of materials with pore diameters larger than 4 nm [133] and associated with the tensile strength effect [133]. Based on the obtained results for nickel ferrite, a curve resembling the type III isotherm is observed, indicating the presence of a non-porous material. There is no evidence of monolayer formation in this scenario, and the interactions between the adsorbent and adsorbate are relatively weak [134].

The results of S_{BET} and pore volume obtained from the adsorption isotherms are shown in Table 7.

Table 7- Textural properties of the prepared materials

Material	S_{BET} (m ² g ⁻¹)	Total pore volume (mm ³ g ⁻¹)
CNT-PS	98	382
CNT-MIX	73	316
CNT-MIX-PS	88	324
CNT-MIX-800	89	261
Nickel Ferrite	18	37

Upon analyzing Table 7, it becomes apparent that the material with the highest adsorption capacity, CNT-PS, also exhibited the largest BET surface area. Conversely, CNT-MIX displayed the smallest surface area alongside a smaller pore volume. The CNT-MIX-PS material presented intermediate results, thus corroborating the findings observed in the adsorption curves. Furthermore, the S_{BET} values obtained are comparable to those reported in literature for CNTs synthesized from polymers [135]–[137]. Again, an evident increase in the BET surface area of the CNT-MIX-800 compared to its precursor can be observed. This phenomenon can be attributed to the reducing atmosphere that the material was exposed, as previous records indicate that this procedure can modify material surfaces and enhance their surface area [138]. The determined surface area values for the metallic catalyst also align with the values reported in literature, which typically range from 5 to 50 m² g⁻¹, depending on the specific synthesis conditions [139,140].

4.2.5. CONTACT ANGLE

Table 8 displays the results of the contact angle measurements obtained for the materials using ultrapure water as solvent.

The contact angle is a fundamental property employed to examine the surface wettability of materials. In the context of this study, it holds great significance as it provides valuable insights into the surface properties that influence the performance of CNTs in adsorption tests [141,142]. The techniques employed for measuring contact angles in powders have inherent limitations, primarily influenced by the material's composition, geometric microstructure, and the characteristics of the contact surface [143]. In this study, the adhesion technique using a glass plate was employed, as it provides more realistic values for the surface energy of the powders compared to the packed plate approach [101].

Table 8- Results for the contact angle measurements of the materials

Material	Contact angle (°)	Image description
CNT-MIX	129 ± 8	
CNT-MIX-800	120 ± 10	
CNT-MIX-PS	52 ± 8	
CNT-PS	~0*	

*In the case of CNT-PS, although it is possible to observe the water droplet in the figure, the droplet rapidly disappeared (<2 s), and it was estimated that the contact angle approaches 0°

The obtained results for the contact angle measurements, using water as solvent, reveal a trend towards increased hydrophilicity in the materials synthesized with polystyrene. CNT-PS exhibited high hydrophilicity, with its contact angle practically approaching zero across all three measurements. On the other hand, CNT-MIX and CNT-MIX-800 demonstrated the highest contact angles, indicating greater hydrophobicity. CNT-MIX-PS, synthesized by combining the precursors of the other two materials, displayed an intermediate contact angle of 52°, indicating an intermediate level of hydrophilicity. These findings are consistent with the existing literature on carbon nanotubes. Kakade *et al.* [144] reported a contact angle of approximately 120° for CNTs functionalized with a mixture of nitric and sulfuric acid. Similarly, other studies have documented a decrease in the contact angle between 50° to 100° after functionalization [143].

It is crucial to emphasize that this analysis, conducted under identical conditions for all materials, is solely intended for sample comparison purposes and may not provide an accurate absolute value for this measurement.

4.3. EXPERIMENTAL REACTIONS

4.3.1. ADSORPTION OF DBT

The adsorption tests (organic and biphasic medium) were conducted to examine the potential adsorption of DBT by the CNTs and to accurately measure the efficacy of the oxidation process in removing this pollutant through oxidation and extraction rather than relying solely on adsorption.

Figure 29 shows the results obtained for DBT removal in the organic medium using the different materials prepared.

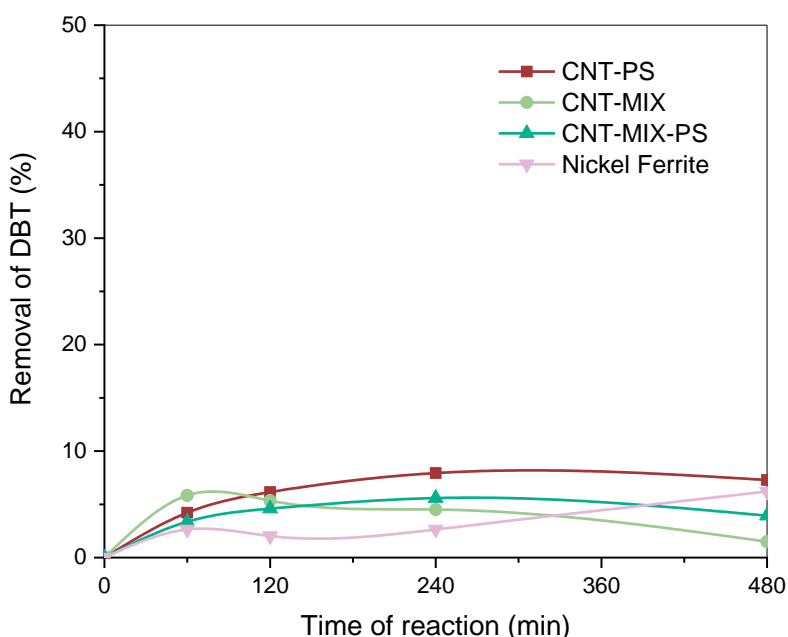


Figure 29 - Adsorption of DBT on the CNTs over time (80 °C, $C_{CNT} = 2.5 \text{ g L}^{-1}$, $C_{DBT} = 500 \text{ mg L}^{-1}$ in isooctane). The lines are only intended to guide the eyes.

These findings show that the average DBT removal across the materials exhibited relatively low values ranging from 2 to 8%. Previous studies have reported higher removal rates of 30 to 40% for adsorption-based desulfurization of dibenzothiophene in diesel models using carbon nanotubes [145]. However, it is important to note that those studies employed an amount of material 16 times higher than the quantity used in the current study. This disparity in results could also be attributed to variations in the types of carbon nanotubes and metallic catalysts employed.

Nevertheless, a consistent trend was observed with all materials, wherein a higher removal rate was observed within the first hour, followed by a decline or stabilization in

subsequent hours. This behavior can be attributed to the initial abundance of vacant sites on the adsorbent surface during the early adsorption stage, suggesting the formation of a monolayer coverage of DBT on the adsorbent surface, in alignment with reported data [146]. Furthermore, the CNT-PS material exhibited the highest pollutant removal capacity. This fact could be attributed to its larger surface area and to the higher number of acid sites since the basicity of thiophene compounds facilitates stronger interactions with the acid sites, resulting in improved adsorption performance [147]. It is curious to note that the CNT-MIX-PS material demonstrates an intermediate behavior between CNT-PS and CNT-MIX. This observation further emphasizes the influence of polymer mixture on the overall performance. Lastly, it is worth mentioning that the observed increase in DBT removal for the metallic catalyst could be ascribed with possible gradual evaporation of the solvent during the reaction time. Even low amounts of evaporation could result in an overestimation of the concentration of DBT in the organic phase, affecting the results.

Figure 30 illustrates the results obtained for DBT removal in the biphasic medium using the different materials prepared.

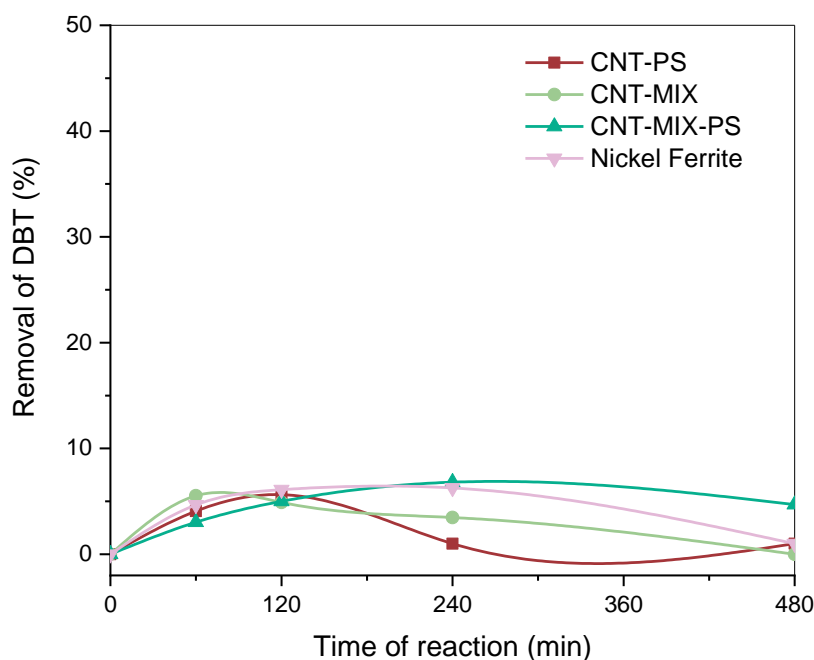


Figure 30 - Adsorption of DBT on the CNTs under a biphasic system (80 °C, $C_{CNT} = 2.5 \text{ g L}^{-1}$, $C_{DBT} = 500 \text{ mg L}^{-1}$ in isooctane). The lines are only intended to guide the eyes.

The results show a consistent trend of increased adsorption within the first two hours of testing, similar to the observations in the organic medium tests. Interestingly, CNT-MIX-PS exhibited the highest DBT removal capacity, which could be attributed to its

intermediate polarity, as the contact angle tests validated. The presence of this material at the phase interface likely facilitated enhanced DBT mass transfer, thereby supporting the findings obtained. It is essential to highlight that the DBT (octanol-water) partition coefficient possesses a value higher than 1 ($K_{OW} = 4.8$) [148] indicating a higher affinity of the substance towards the oil phase. The presence of the adsorbents at the interface plays a significant role in these tests as it promotes efficient mass transfer.

The removal values obtained in the biphasic medium tests (2-6%) were comparable to those observed in tests conducted with an oily medium, indicating relatively low values. Notably, adsorption tests in a biphasic medium for DBT removal are rarely reported in the literature. In general, authors report the removal in the biphasic medium by oxidation tests and the effect of adsorption under a biphasic medium is not measured. This fact could represent a drawback as the actual contribution of oxidation may be overestimated. Therefore, the values obtained in this study can serve as a valuable benchmark to compare the results of oxidative tests in similar setups.

4.3.2. OXIDATIVE DESULFURIZATION OF DBT

The oxidative desulfurization runs were measured by monitoring DBT and hydrogen peroxide concentration over time. The results for different materials and the non-catalytic run are shown in Figure 31.

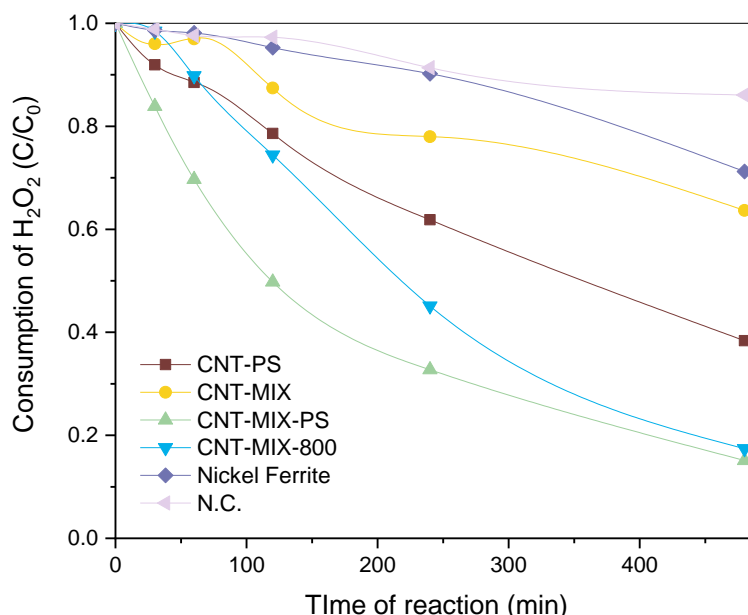


Figure 31 - Decomposition of hydrogen peroxide in the biphasic oxidation runs (80 °C, $pH_0 = 3.0$, $C_{DBT} = 500 \text{ mg L}^{-1}$ in isoctane, $C_{CNT} = 2.5 \text{ g L}^{-1}$, $C_{H_2O_2} = 11 \text{ g L}^{-1}$). The lines are only intended to guide the eyes.

The non-catalytic run resulted in the decomposition of only 13% of H_2O_2 . For the same tests using the CNTs, results of 36.3, 61.6, 82.5 and 84.9% of decomposition were obtained for the materials CNT-MIX, CNT-PS, CNT-MIX-800 and CNT-MIX-PS at the end of the tests, respectively. These results are consistent with expectations, as carbon materials are known for their catalytic performance in the degradation of hydrogen peroxide. The surface reactions on these materials lead to short-lived hydroxyl radicals, which have a high propensity for resonance stabilization at the carbon surfaces [149].

CNT-MIX-PS and CNT-MIX-800 demonstrated the most rapid and extensive degradation among the tested materials. Within just two hours of reaction, over 50% of hydrogen peroxide had already undergone decomposition. Similarly, for CNT-PS, which exhibited the third highest H_2O_2 decomposition rate, approximately 40% of the peroxide was transformed into oxidizing radicals after four hours of reaction. Notably, this degradation pattern aligns with the materials that possessed the highest number of acidic sites, indicated by their higher functionalization index. Literature supports this observation, as studies have reported that functionalized CNT surfaces facilitate faster degradation of H_2O_2 [150]. It is crucial to highlight that rapid degradation of hydrogen peroxide does not always guarantee improved results, as unintended reactions can take place between hydroxyl radicals and other components within the medium, including hydrogen peroxide itself and the carbon material. These parasitic reactions need to be considered when studying the overall effectiveness of the process.

To monitor the removal of DBT, the analysis of the oil phase was conducted at different time points using GC-FID. Figure 32 provides a visual representation of the varying effectiveness of different materials in removing DBT from the oil phase.

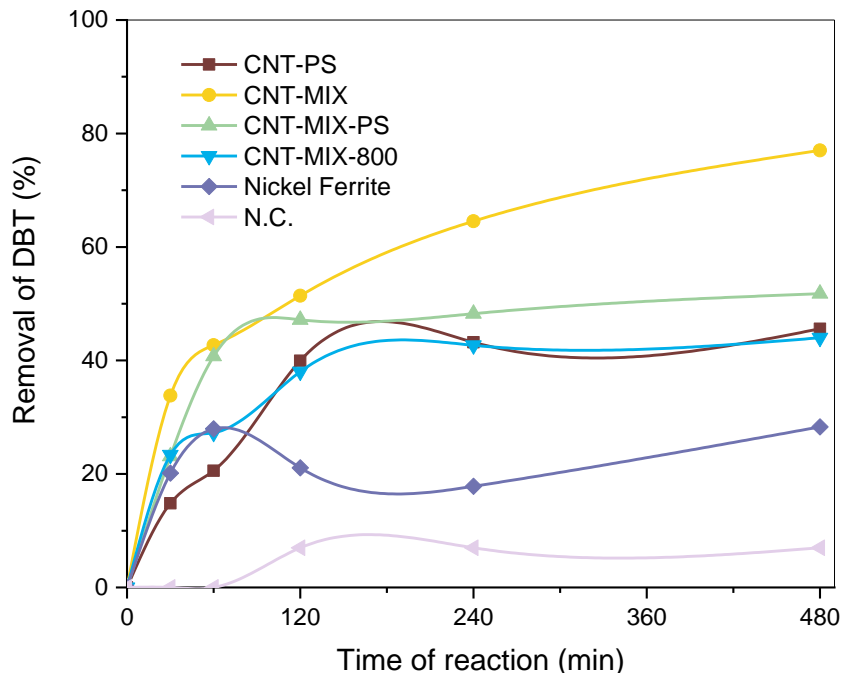


Figure 32 - Removal of DBT in oxidative desulfurization using H_2O_2 (80 °C, $C_{CNT} = 2.5 \text{ g L}^{-1}$, $C_{DBT} = 500 \text{ mg L}^{-1}$ in isooctane; $C_{O_{H_2O_2}} = 11 \text{ g L}^{-1}$). The lines are only intended to guide the eyes.

Observations from the experiments reveal significant differences in the removal of DBT from the oil phase. In the non-catalytic test, DBT removal was minimal, with 93% of the pollutant still present in the isooctane phase at the end of the run. Similarly, the test using only the metallic catalyst resulted in a modest 28% removal. These outcomes align with expectations explained in the previous section, as DBT exhibits a strong affinity for the oil phase, and materials with suitable properties are necessary to facilitate mass transfer and increase the removal of DBT.

In contrast, the oxidation tests involving carbon nanotubes exhibited remarkable performance in DBT removal. CNT-MIX exhibited the highest efficiency, removing 51% of DBT within only a 2-hour timeframe and achieving a removal of 77% at the end of the 8 hours-experiment. This result was followed by CNT-MIX-PS with 52% of removal and CNT-PS with 46% of removal.

These results can be elucidated by considering the surface chemistry of the materials. CNT-PS exhibited the lowest pH_{pzc} value and a higher concentration of acidic sites on its surface. In contrast, materials like CNT-MIX and CNT-MIX-PS were found to be less acidic. According to previous reports [151], materials that contain functionalities with acidic oxygen tend to exhibit limited catalytic activity. This factor may have contributed to the lower efficiency observed in DBT removal when employing CNT-PS. Conversely,

the higher rate of DBT removal observed for CNT-MIX and CNT-MIX-PS can be attributed to basic active sites or to a lower abundance of acidic sites. Furthermore, in the case of CNT-MIX, the controlled decomposition rate of hydrogen peroxide likely facilitated the production of activated hydroxyl radicals, which may have contributed to the improved DBT removal efficiency.

Another factor contributing to the variation in DBT removal among the materials is their hydrophilic/hydrophobic characteristics. Particularly, CNT-PS exhibited a unique behavior during the experiments, showing enhanced diffusion in the aqueous medium as confirmed by contact angle measurements, indicating higher hydrophilicity. This outcome can be attributed to structural defects in the nanotube walls, which likely increased the material's interaction with the acid, compounded by the mass loss in the washes. Consequently, the material accumulated in the aqueous phase, impeding its contact with DBT and limiting its catalytic activity. Conversely, materials like CNT-MIX and CNT-MIX-PS tend to aggregate at the interface. This observation suggests that these materials may enable more effective removal of DBT. Another noteworthy factor to consider is the presence of Fe and Ni in the materials after the washing process. In the case of CNT-PS, all nickel and iron were completely removed through the washes. Conversely, CNT-MIX exhibited the highest residual amount of Fe and Ni after the washes. This finding can further elucidate the superior catalytic activity of this material, as the metallic components play a vital role in the catalytic process by directly influencing the overall catalysis.

The conversion/removal of DBT, achieved through the use of carbon compounds in two-phase systems involving water as the extracting phase and hydrogen peroxide as the oxidant, can exhibit a wide range of values, typically from 20 to 100% [152]–[155]. However, the above percentages may vary depending on several parameters, including catalyst type and reaction conditions.

It is crucial to highlight that the highest documented removal rates, using biphasic systems, often employ solvents like methanol, chloroform or acetonitrile to enhance the extraction percentage. In contrast, the tests conducted here solely used water as the extracting phase to minimize the generation of toxic residues. The results obtained in this study fall within the expected range of typical values. Particularly, the application of CNT-MIX in ODS yielded a final concentration of S in the simulated fuel of 20 ppm, showcasing the distinct advantage of employing this specific material. It is worth noting that this approach has the potential to incorporate solid plastic waste into the synthesis process, offering an additional benefit in terms of sustainability and waste management.

4.3.3. CNT-MIX: ADDITIONAL CHARACTERIZATIONS

TG and RAMAN characterizations were conducted to assess additional properties of CNT-MIX, given its superior performance in ODS tests.

For TG analysis, the material was heated from 25 to 900°C at a rate of 10°C per minute under a N₂ atmosphere of 50 mL min⁻¹. Figure 33 illustrates the TG and DTG profiles obtained from this analysis.

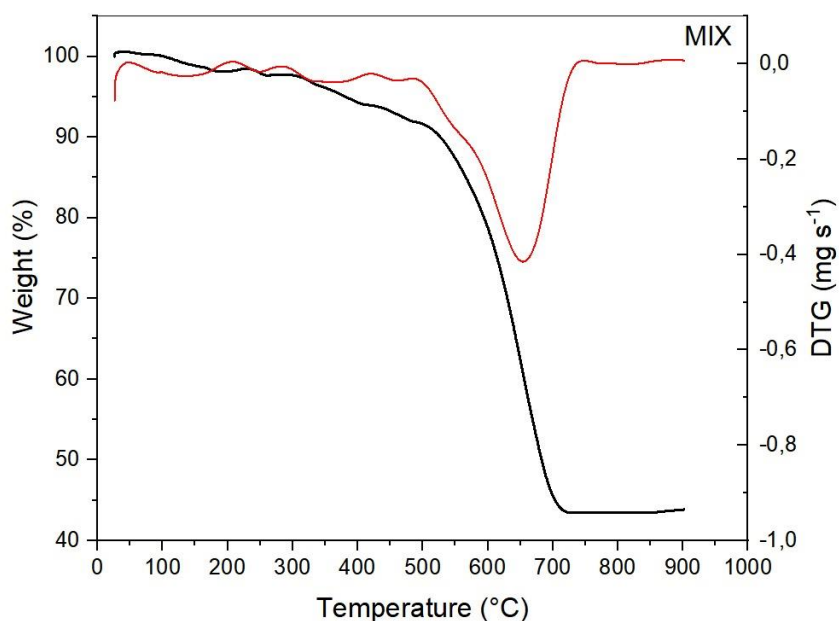


Figure 33 -TG and DTG profiles for CNT-MIX

The DTG curve reveals a slight weight loss within the temperature range of 410-490 °C, which could be attributed to the carbon sources employed during the synthesis of this material, namely polypropylene and polyethylene (high and low density). According to literature [156], polypropylene typically experiences mass loss around 420°C, while polyethylene exhibits it around 460°C under N₂ atmosphere. These findings align with the experimental results obtained in this study.

Notably, the material exhibits its most substantial mass loss at around 700°C, a characteristic behavior of carbon nanotubes [157]. This fact indicates the efficiency of the CVD process employed in achieving this outcome. Approximately 40% of the mass was lost at this temperature, while 60% of metallic residues remained in the material.

The obtained value for metallic residues aligns with the expected results, as no significant mass loss was observed during the acid washes conducted on this material. It is worth noting that despite having only 40% carbon content, the material displayed

hydrophobic characteristics, as confirmed by contact angle measurements. This suggests a high degree of material dispersion at the catalyst surface, thereby enhancing its hydrophobic nature.

The exceptional performance of this material in the ODS tests can be attributed to its excellent dispersion and the favorable ratio between carbon and metallic content, as demonstrated by the TG analysis. This optimal ratio promotes the catalytic decomposition of peroxide and facilitates the aggregation of the material at the interface of the phases.

For the Raman measurements, a Bruker Senterra Raman spectrometer, equipped with a CCD detector, was used. The spectrometer has an optical microscope (OLYMPUS BX51) attached to focus the laser beam on the sample and to collect backscattered light. To excite the sample, a laser at a wavelength of 633 nm was used. Figure 34 illustrates the Raman spectra obtained from this analysis.

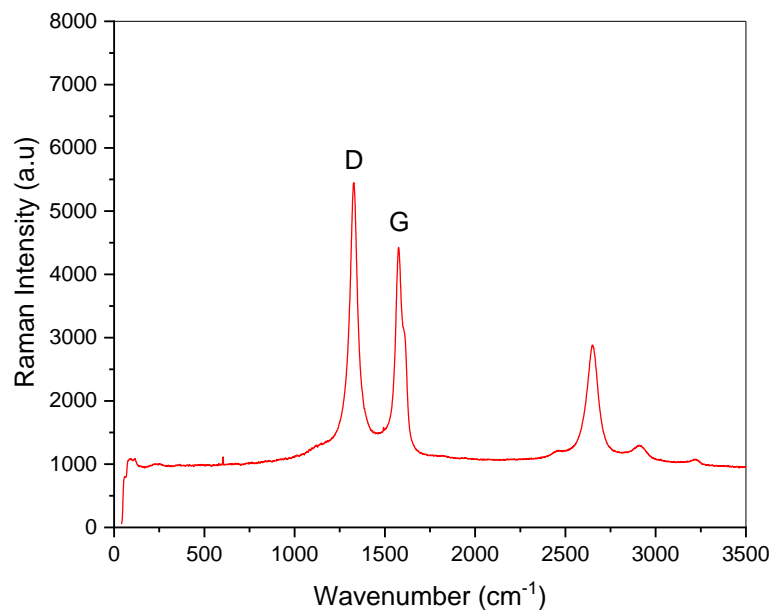


Figure 34 - Raman spectra for CNT-MIX

The Raman spectrum reveals the distinct G and D bands in the figure. The G band, also referred to as the Graphitic mode, appeared within the 1524–1643 cm⁻¹ range, indicating the presence of sp² hybridized carbon atoms in the CNT lattice, aligned along the nanotube's circumferential direction [158]. On the other hand, the D band (disorder mode) appears in the range of 1248-1422 cm⁻¹, signifying the existence of defects in the CNT structure. This band's presence may also be associated with the occurrence of amorphous carbons, which result from the conversion of carbon states centers from sp²

to sp^3 hybridization, potentially arising due to a break in the symmetry of the graphite plane [108].

The G/D ratio is utilized to determine carbon graphitization and serves as an indicator of defect content in CNTs. A higher G/D ratio indicates a lower presence of defects, signifying more crystalline and organized CNTs. Conversely, a lower G/D ratio suggests a higher abundance of defects. For the sample in question, the G/D ratio was calculated from the intensity of the G and D bands [159], resulting in a value of 0.814. The obtained value closely aligns with values documented in the literature for acid-treated carbon nanotubes, as reported by Liu et al [160] in the range of 0.95-1.18. However, it is comparatively lower than values observed in materials without pretreatment [108]. It is worth noting that these defects may have played a significant role in enhancing the material's activity by creating additional active centers, thereby contributing to its superior performance.

4.3.4. OXIDATIVE DESULFURIZATION OF DBT: ADDITIONAL EXPERIMENTS WITH CNT-MIX

The material with the most effective DBT removal performance from the desulfurization oxidation tests, CNT-MIX, was selected to enhance the experimental results through modifications in the experimental conditions, specifically the extractant phase and the oxidant. Figure 35 depicts the results obtained through the monitoring of DBT concentration in these experiments.

In run A, ultra-pure water was considered as the extractant phase, accompanied by hydrogen peroxide and formic acid as the chosen oxidizing agents. This combination was specifically selected due to substantial improvements documented in the literature regarding the use of this mixture in desulfurization tests [161]. In run B, acetonitrile was selected as the extraction solvent due to its well-documented effectiveness in extracting DBT from fuel oils [162] and H_2O_2 was employed as the oxidizing reagent due to its favorable miscibility with the aforementioned solvent. Finally, in run C, acetonitrile was employed as the extracting solvent, while a combination of formic acid and hydrogen peroxide was applied as the oxidizing agents. These experimental setups were designed to compare the activity of the material produced in this work and try to elucidate the individual interference of each component in the respective tests.

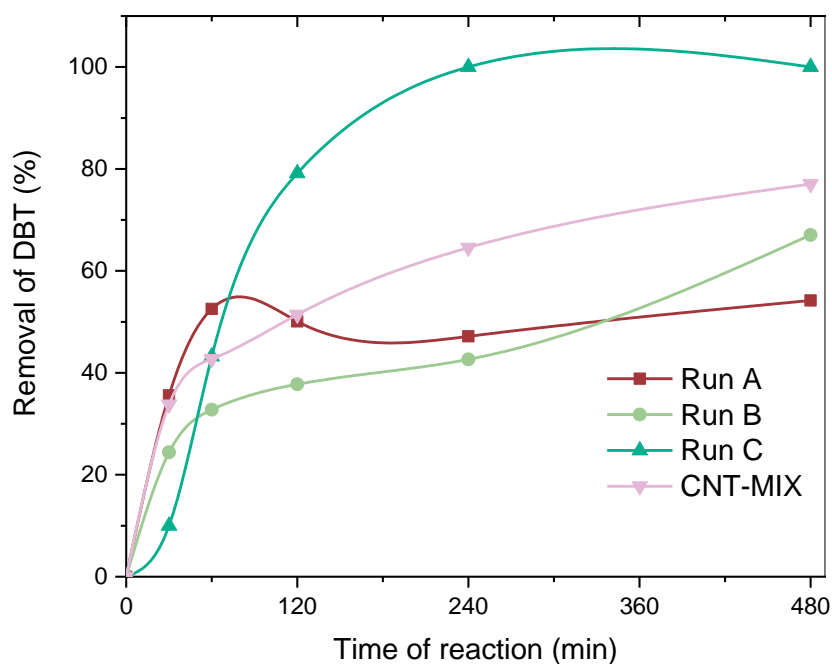


Figure 35 - Removal of DBT in ODS using different systems (Run A: Extractant: ultrapure water; Oxidizing Agents: H₂O₂ and HCOOH; Run B: Extractant: acetonitrile; Oxidizing Agent: H₂O₂; Run C: Extractant: acetonitrile; Oxidizing agent: H₂O₂ and HCOOH; CNT MIX: Extractant: Water (pH=3); Oxidizing Agent: H₂O₂). The lines are only intended to guide the eyes.

Upon comparing the results obtained from runs A and B, a notable disparity in removal efficiency becomes apparent. Acetonitrile in combination with H₂O₂ as the oxidant exhibits a significantly higher removal rate compared to the use of water as the extracting solvent along with the mixture of formic acid and H₂O₂ as the oxidants. The 19.4% variance in removal between the runs highlights the superior effectiveness of acetonitrile as a solvent for extracting DBT from the oil phase.

Upon observing the results obtained in run C, it becomes evident that the system employing acetonitrile in conjunction with the combination of formic acid and hydrogen peroxide as oxidants, with the application of CNT-MIX as the catalyst/adsorbent, exhibits the most outstanding performance in terms of DBT removal. Remarkably, this system achieves an efficiency of 100%, ensuring the complete elimination of DBT from the oily phase.

While the exact mechanism of hydrogen peroxide oxidation in the presence of acids is not fully understood, experimental evidence indicates that combining these components results in the formation of peroxy acid. The presence of this acid plays a crucial role in polarizing the O-O bond of the peroxide, effectively accelerating the oxidation reaction [163].

Several studies have already reported results using similar systems. For instance, Haghghat et al. [164] achieved a significant 97% sulfur removal using the same combination. However, their methodology involved a liquid-liquid extraction process and a higher quantity of acetonitrile (2.5 times more than the amount used in this work). In another investigation by Akopyan et al. [165] hybrid catalysts based on polyoxometalate with sulfuric acid and ionic liquid components were employed, leading to a noteworthy DBT conversion rate of 71% under optimal conditions. Additionally, some studies have used carbon nanotubes, water, formic acid and hydrogen peroxide, reporting DBT conversion results ranging from 14.5 to 82%, depending on the synthesis temperature of the CNTs [2]. Hence, the results obtained using this particular type of material align with those reported in the existing literature and offer various advantages, including solvent savings, high efficiency and the potential for recycling.

Another significant observation from Figure 35 is that the test conducted solely using water as the extracting phase and hydrogen peroxide as the oxidant yielded the second-best result, surpassing the removals achieved in runs A and B. This finding highlights the possibility of obtaining excellent experimental results using this material while minimizing the use of toxic compounds.

HPLC was used to monitor the concentration of DBT in acetonitrile for experiments B and C. The results obtained are depicted in Figure 36.

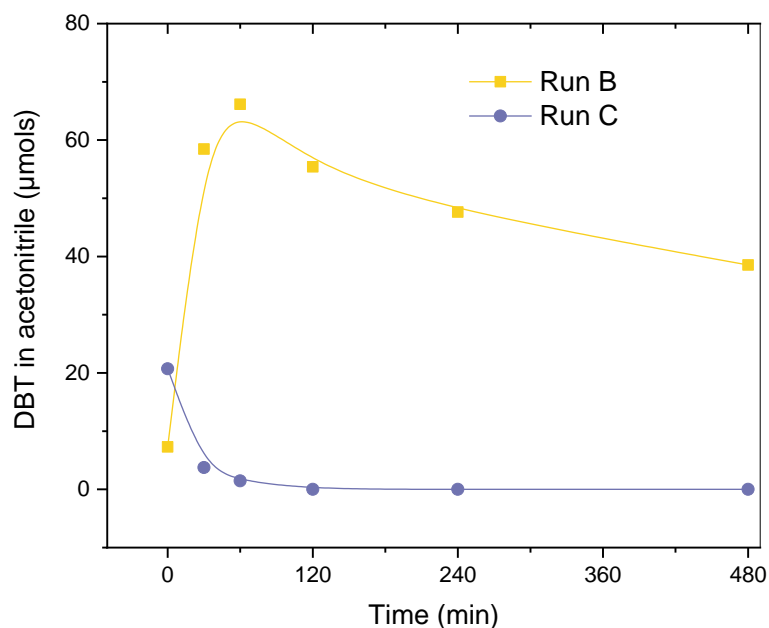


Figure 36 - Presence of DBT in acetonitrile (Run B: ACN with H_2O_2 ; Run C: ACN with H_2O_2 and $HCOOH$; $80\text{ }^\circ\text{C}$, $C_{CNT} = 2.5\text{ g L}^{-1}$, $C_{DBT} = 500\text{ mg L}^{-1}$ in isooctane; $C_{H_2O_2} = 11\text{ g L}^{-1}$, $C_{HCOOH} = 22\text{ g L}^{-1}$). The lines are only intended to guide the eyes.

It is apparent from both tests that DBT is present in the acetonitrile phase even before the catalyst is added (t_0). Acetonitrile, with a relative polarity (*R.P.*) value of 0.46, exhibits a stronger affinity for interacting with hydrophobic substances like DBT compared to water (*R.P.* = 1). This property explains why acetonitrile is chosen as an extractant for DBT, as it enables efficient extraction by favorably interacting with the component. Tao B et al. [166] conducted a study to determine the solubility of DBT in various organic solvents. At 297 K, the solubility of DBT in acetonitrile was found to be 0.0143 in molar fraction. This value is significantly higher compared to the reported solubility of DBT in water, which is documented in the literature as 0.0015 g L⁻¹ (8.15 μmol L⁻¹). Despite achieving significant results in DBT removal through extractive tests using acetonitrile alone [162] studies indicate that this system is inefficient when considering a fuel matrix. Acetonitrile lacks selectivity towards other aromatic hydrocarbons [167] highlighting the necessity for a selective oxidative system.

Based on Figure 36, visible differences emerge when formic acid is introduced into the system. During Run B, a notable amount of DBT is initially detected within the first four hours, which can be attributed to the extractive effect of acetonitrile. However, the concentration of DBT undergoes a significant decrease in the subsequent hours, indicating the potential oxidation of DBT by hydrogen peroxide. This information is further supported by the quantification of DBT in its sulphonated form in acetonitrile (Figure 37). Conversely, in Run C, a distinct profile is evident, with no significant concentrations of DBT observed in the extracting solvent throughout the test. This effect can be attributed to the presence of formic acid, which, when combined with H₂O₂, leads to the predominant formation of sulfones [163]. As a result, rapid oxidation of DBT into sulfone takes place in this system, which also has been corroborated by the quantification of this compound using HPLC analysis, as depicted in Figure 37.

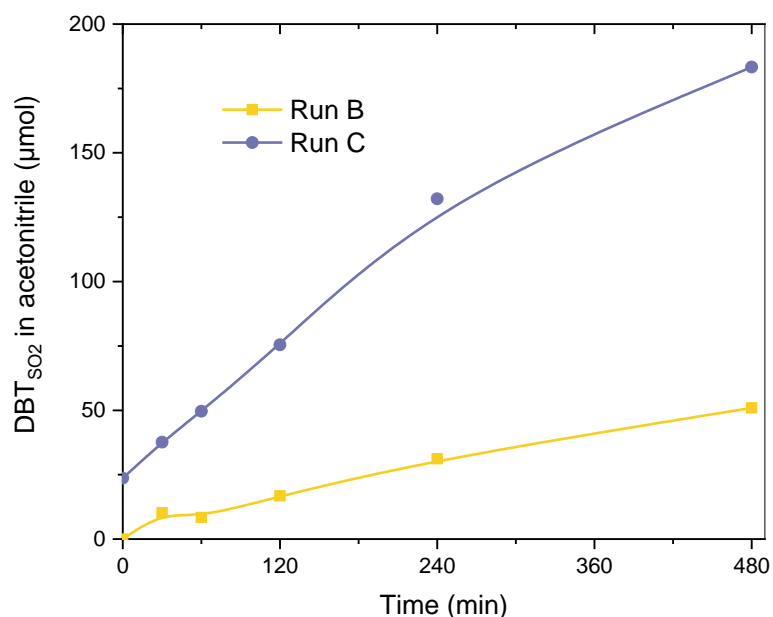


Figure 37 - Presence of DBT_{SO₂} in acetonitrile (Run B: ACN with H₂O₂; Run C: ACN with H₂O₂ and HCOOH; 80 °C, C_{CNT} = 2.5 g L⁻¹, C_{DBT} = 500 mg L⁻¹ in isooctane; C_{H₂O₂} = 11 g L⁻¹, C_{HCOOH} = 22 g L⁻¹). The lines are only intended to guide the eyes.

The curves depicted in Figures 35 and 36 reveal a discernible correlation. In Run B, - without addition of formic acid, the predominant mechanism for DBT removal is extraction. However, in Run C, where formic acid was introduced, DBT removal occurs through the oxidation of intermediates, particularly to its sulfonated form. Dibenzothiophene sulfone, with a predicted partition coefficient (octanol-water) of 2.74, exhibits a greater affinity for polar solvents compared to its original molecule (partition coefficient octanol-water of 4.8). Consequently, its extraction with acetonitrile is considerably more favored when compared for instance with water.

In addition to the aforementioned results, the presence of an additional intermediate compound (not identified) was detected in runs A, B and C in acetonitrile, as confirmed by HPLC.

Figure 38 shows the temporal evolution of this compound in each run.

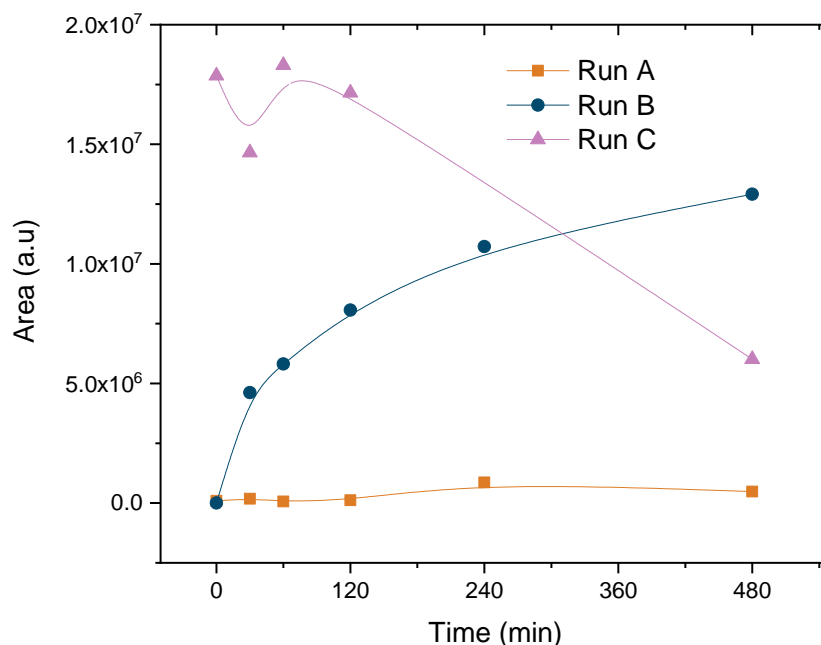


Figure 38 - Reaction intermediate identified by the same retention time in HPLC (80 °C, $C_{CNT} = 2.5 \text{ g L}^{-1}$, $C_{DBT} = 500 \text{ mg L}^{-1}$ in isooctane, $C_{H_2O_2} = 11 \text{ g L}^{-1}$, $C_{HCOOH} = 22 \text{ g L}^{-1}$). The lines are only intended to guide the eyes.

Once again, a correlation can be observed between the presence of an intermediate compound, potentially identified as DBT sulfoxide, and the coexistence of DBT and DBT sulfone in the systems. As previously demonstrated in other studies, sulfone formation typically proceeds through an intermediate stage involving the formation of sulfoxides. This information is exemplified in run C, where an initial peak in the intermediate formation is observed within the first two hours, followed by a subsequent decrease. This decline can be attributed to the concurrent increase in sulfone formation, which becomes more prominent after this period. In contrast, run B results in an accumulation of this intermediate, further indicating the role of formic acid in DBT sulfone formed compared to sulfoxide.

By comparing the results presented in Figures 35, 36, 37 and 38 it becomes evident that the application of the materials proposed in this study yielded remarkable outcomes. Notably, in the case of CNT-MIX tested in scenario C, a complete removal of DBT from the oil phase was achieved, accompanied by significant detection of DBT sulfone in the extractant phase. These findings provide strong evidence of the material's effectiveness as a catalyst, adsorbent, and potentially as a phase-transfer catalyst for biphasic reaction runs.

5. CONCLUSIONS AND FUTURE WORK

5.1. CONCLUSIONS

The main conclusion of this study is that the materials synthesized from polymers and polyolefin mixtures have proven to be effective in removing DBT in a two-phase system, with water serving as the extracting phase, as initially proposed. Particularly, the outstanding performance of the CNT-MIX material highlights the potential of synthesizing such materials using plastic residues, thereby achieving a significant percentage of removal without the need for toxic solvents.

The synthesized materials demonstrate that the choice of precursor directly impacts the carbon nanotubes' characteristics. In particular, the CNT-MIX-PS material, synthesized from a combination of polyolefins and polystyrene, exhibits intermediate properties (surface area, pH_{pzc} , water contact angle and others) when compared to both CNT-MIX and CNT-PS. Thus, different characteristics can be attained by correctly selecting the starting polymer, allowing to design specific catalysts for specific applications.

Moreover, when comparing the carbon materials with the metallic catalyst, it becomes evident that the catalytic activity significantly enhances with the growth of nanotubes. This improvement in catalytic performance is particularly noteworthy in oxidative tests, underscoring the potential of these materials for such applications.

Lastly, this study has successfully demonstrated a substantial increase in the yields of DBT removal when using acetonitrile as the extracting phase in combination with formic acid and hydrogen peroxide as oxidizing agents. The quantification of key intermediates in the DBT oxidation reaction using HPLC has provided strong evidence supporting the proposed pathway for removing this component through oxidative desulfurization (ODS).

5.2. FUTURE WORK

Based on the results obtained in this study, several promising approaches for future research can be identified, including:

- Development of methodologies to accurately quantify compounds adsorbed on catalysts, enabling a comprehensive understanding of the adsorption process and its impact on catalytic efficiency.
- Exploration of alternative reaction conditions, such as investigating the potential of using a mixture of water and acetonitrile as extracting phases. Optimizing the

proportion between these components could lead to enhanced DBT extraction efficiency while minimizing toxic waste generation.

- Evaluation of the impact on DBT removal of different reaction conditions, such as hydrogen peroxide concentration, catalyst concentration, temperature, oil-water ratio, DBT concentration, hydrogen peroxide-formic acid proportion, pH of the aqueous phase.
- Study the formation of Pickering emulsions in the presence of the materials and the impact of carrying out the reaction under an emulsified system.
- Investigation of organic carbon content in the aqueous phases to achieve a comprehensive mass balance involving the phase transfer of DBT. Understanding the fate and distribution of organic carbon compounds can provide valuable insights into the overall process efficiency.
- Utilization of real plastic waste as a feedstock for synthesizing carbon nanotubes. This approach would not only address environmental concerns associated with plastic waste but also contribute to the development of sustainable and eco-friendly catalyst materials.
- Assessment of the proposed methodology using real fossil fuels, which would provide a more realistic representation of the challenges and complexities involved in desulfurization processes.

6. REFERENCES

- [1] The Statistical Review, 'Statistical Review of World Energy 2022'. (Accessed Feb. 11, 2023).
- [2] R. Mambrini, 'Sistemas magnéticos nanoestruturados para a remoção seletiva de compostos sulfurados e nitrogenados do petróleo', Belo Horizonte, 2013.
- [3] E. Stauffer, J. Dolan, and R. Newman, *Fire Debris Analysis*. Academic Press, 2007.
- [4] L. De and G. Piccinin, 'Catalytic application of carbon nanotubes obtained from plastic solid waste in the removal of quinoline from isooctane by selective oxidation with hydrogen peroxide', Bragança, 2022.
- [5] 'Effects of Acid Rain'. <https://www.epa.gov/acidrain/effects-acid-rain> (Accessed Feb. 11, 2023).
- [6] A. Demirbas and H. S. Bamufleh, 'Optimization of crude oil refining products to valuable fuel blends', *Pet Sci Technol*, vol. 35, no. 4, pp. 406–412, Feb. 2017, doi: 10.1080/10916466.2016.1261162.
- [7] S. Du *et al.*, 'Molecular simulation on mechanism of thiophene hydrodesulfurization on surface of Ni₂P', *Energy Exploration & Exploitation*, vol. 39, no. 3, pp. 975–992, May 2021, doi: 10.1177/0144598721994950.
- [8] D. Duayne Whitehurst, T. Isoda, and I. Mochida, 'Present State of the Art and Future Challenges in the Hydrodesulfurization of Polyaromatic Sulfur Compounds', 1998, pp. 345–471. doi: 10.1016/S0360-0564(08)60631-8.
- [9] W. Min, 'A Unique Way to Make Ultra Low Sulfur Diesel', 2002.
- [10] M. N. Hossain, M. K. Choi, and H. S. Choi, 'A Review of the Desulfurization Processes Used for Waste Tire Pyrolysis Oil', *Catalysts*, vol. 11, no. 7, p. 801, Jun. 2021, doi: 10.3390/catal11070801.
- [11] F. S. Mjalli, O. U. Ahmed, T. Al-Wahaibi, Y. Al-Wahaibi, and I. M. AlNashef, 'Deep oxidative desulfurization of liquid fuels', *Reviews in Chemical Engineering*, vol. 30, no. 4, pp. 337–378, Aug. 2014, doi: 10.1515/revce-2014-0001.
- [12] M. N. Abbas and H. A. Alalwan, 'Catalytic oxidative and adsorptive desulfurization of heavy naphtha fraction', *Korean Chemical Engineering Research*, vol. 57, no. 2, pp. 283–288, Apr. 2019, doi: 10.9713/kcer.2019.57.2.283.
- [13] L. M. Hoyos-Palacio, A. G. García, J. F. Pérez-Robles, J. González, and H. v Martínez-Tejada, 'Catalytic effect of Fe, Ni, Co and Mo on the CNTs production', *IOP Conf Ser Mater Sci Eng*, vol. 59, p. 012005, Jun. 2014, doi: 10.1088/1757-899X/59/1/012005.
- [14] M. E. Khan, 'State-of-the-art developments in carbon-based metal nanocomposites as a catalyst: photocatalysis', *Nanoscale Adv*, vol. 3, no. 7, pp. 1887–1900, 2021, doi: 10.1039/D1NA00041A.
- [15] B. G. Mwanza and C. Mbohwa, 'Drivers to Sustainable Plastic Solid Waste Recycling: A Review', *Procedia Manuf*, vol. 8, pp. 649–656, 2017, doi: 10.1016/j.promfg.2017.02.083.

- [16] C. Wang, Y. Liu, W. Chen, B. Zhu, S. Qu, and M. Xu, 'Critical review of global plastics stock and flow data', *J Ind Ecol*, vol. 25, no. 5, pp. 1300–1317, Oct. 2021, doi: 10.1111/jiec.13125.
- [17] PlasticsEurope, 'Plastics-the Facts 2021 An analysis of European plastics production, demand and waste data'. (Accessed Feb. 11, 2023).
- [18] B. Bertleff *et al.*, 'Extractive Catalytic Oxidative Denitrogenation of Fuels and Their Promoting Effect for Desulfurization Catalyzed by Vanadium Substituted Heteropolyacids and Molecular Oxygen', *Energy & Fuels*, vol. 34, no. 7, pp. 8099–8109, Jul. 2020, doi: 10.1021/acs.energyfuels.0c00864.
- [19] A. Rajendran, T. Cui, H. Fan, Z. Yang, J. Feng, and W. Li, 'A comprehensive review on oxidative desulfurization catalysts targeting clean energy and environment', *J Mater Chem A Mater*, vol. 8, no. 5, pp. 2246–2285, 2020, doi: 10.1039/C9TA12555H.
- [20] M. Nishioka, 'Aromatic sulfur compounds other than condensed thiophenes in fossil fuels: enrichment and identification', *Energy & Fuels*, vol. 2, no. 2, pp. 214–219, Mar. 1988, doi: 10.1021/ef00008a019.
- [21] S. R. M. Ibrahim, H. M. Abdallah, A. M. El-Halawany, and G. A. Mohamed, 'Naturally occurring thiophenes: isolation, purification, structural elucidation, and evaluation of bioactivities', *Phytochemistry Reviews*, vol. 15, no. 2, pp. 197–220, Apr. 2016, doi: 10.1007/s11101-015-9403-7.
- [22] A. , M. Santos, 'Estudo Atomístico da Formação de Interfaces Orgânico-Inorgânico: Tiofenos sobre Óxido de Titânio', Doutorado, Universidade de São Paulo, São Paulo, 2008.
- [23] S. Wang, Y. Patehebieke, Z. Zhou, Z. Zhang, and X. Wang, 'Catalyst-free biphasic oxidation of Thiophenes in continuous-flow', *J Flow Chem*, vol. 10, no. 4, pp. 597–603, Dec. 2020, doi: 10.1007/s41981-020-00102-9.
- [24] S. Sitamraju, M. J. Janik, and C. Song, 'Selectivity of adsorption of thiophene and its derivatives on titania anatase surfaces: A density functional theory study', in *Topics in Catalysis*, Jun. 2012, pp. 229–242. doi: 10.1007/s11244-012-9807-1.
- [25] S. Houda, C. Lancelot, P. Blanchard, L. Poinel, and C. Lamonier, 'Oxidative Desulfurization of Heavy Oils with High Sulfur Content: A Review', *Catalysts*, vol. 8, no. 9, p. 344, Aug. 2018, doi: 10.3390/catal8090344.
- [26] X. Zeng, J. Lin, J. Liu, and Y. Yang, 'Speciation Distribution of Polycyclic Aromatic Sulfur Heterocycles in Crude Oil', *Chinese Journal of Analytical Chemistry*, vol. 34, no. 11, pp. 1546–1551, Nov. 2006, doi: 10.1016/S1872-2040(07)60014-0.
- [27] PubChem, 'Dibenzothiophene (Compound)'. <https://pubchem.ncbi.nlm.nih.gov/compound/dibenzothiophene#section=Safety-and-Hazards> (Accessed Feb. 11, 2023).
- [28] Wikipedia, 'Dibenzothiophene'. <https://en.wikipedia.org/wiki/Dibenzothiophene> (Accessed Feb. 11, 2023).
- [29] C. Song and X. Ma, 'New design approaches to ultra-clean diesel fuels by deep desulfurization and deep dearomatization', *Appl Catal B*, vol. 41, no. 1–2, pp. 207–238, Mar. 2003, doi: 10.1016/S0926-3373(02)00212-6.

- [30] F. F. Roman, J. L. Diaz de Tuesta, A. M. T. Silva, J. L. Faria, and H. T. Gomes, 'Carbon-Based Materials for Oxidative Desulfurization and Denitrogenation of Fuels: A Review', *Catalysts*, vol. 11, no. 10, p. 1239, Oct. 2021, doi: 10.3390/catal11101239.
- [31] M. J. Grossman, M. K. Lee, R. C. Prince, V. Minak-Bernero, G. N. George, and I. J. Pickering, 'Deep Desulfurization of Extensively Hydrodesulfurized Middle Distillate Oil by *Rhodococcus* sp. Strain ECRD-1', *Appl Environ Microbiol*, vol. 67, no. 4, pp. 1949–1952, Apr. 2001, doi: 10.1128/AEM.67.4.1949-1952.2001.
- [32] CME Group, 'A Look into the Refining Process'.
<https://www.cmegroup.com/education/courses/introduction-to-refined-products/a-look-into-the-refining-process.html> (Accessed Feb. 11, 2023).
- [33] PennState College of Earth and Mineral Sciences, 'Fluid Catalytic Cracking (FCC)'.
<https://www.e-education.psu.edu/fsc432/content/fluid-catalytic-cracking-fcc> (Accessed Feb. 11, 2023).
- [34] G. W. Huber and A. Corma, 'Synergies between Bio- and Oil Refineries for the Production of Fuels from Biomass', *Angewandte Chemie International Edition*, vol. 46, no. 38, pp. 7184–7201, Sep. 2007, doi: 10.1002/anie.200604504.
- [35] M. Bachrach, T. J. Marks, and J. M. Notestein, 'Understanding the Hydrodenitrogenation of Heteroaromatics on a Molecular Level', *ACS Catal*, vol. 6, no. 3, pp. 1455–1476, Mar. 2016, doi: 10.1021/acscatal.5b02286.
- [36] S. Xizhou, L. Zhiqiang, F. Liuya, S. Hao, G. Feng, and S. Zhi, '61 · China Petroleum Processing and Petrochemical Technology', 2019.
- [37] H. Tang *et al.*, 'Adsorptive desulfurization of diesel with mesoporous aluminosilicates', *Sci China B Chem*, vol. 52, no. 3, pp. 276–281, Mar. 2009, doi: 10.1007/s11426-009-0061-8.
- [38] F. Li, P. Xu, C. Ma, Y. Zheng, and Y. Qu, 'Biodesulfurization of Dibenzothiophene by a Newly Isolated Bacterium *Mycobacterium* sp. X7B', *JOURNAL OF CHEMICAL ENGINEERING OF JAPAN*, vol. 36, no. 10, pp. 1174–1177, 2003, doi: 10.1252/jcej.36.1174.
- [39] F. Boshagh, M. Rahmani, and W. Zhu, 'Recent Advances and Challenges in Developing Technological Methods Assisting Oxidative Desulfurization of Liquid Fuels: A Review', *Energy & Fuels*, vol. 36, no. 21, pp. 12961–12985, Nov. 2022, doi: 10.1021/acs.energyfuels.2c03218.
- [40] H. Tang *et al.*, 'Adsorptive desulfurization of diesel with mesoporous aluminosilicates', *Sci China B Chem*, vol. 52, no. 3, pp. 276–281, Mar. 2009, doi: 10.1007/s11426-009-0061-8.
- [41] T.-J. Ren, J. Zhang, Y.-H. Hu, J.-P. Li, M.-S. Liu, and D.-S. Zhao, 'Extractive desulfurization of fuel oil with metal-based ionic liquids', *Chinese Chemical Letters*, vol. 26, no. 9, pp. 1169–1173, Sep. 2015, doi: 10.1016/j.ccllet.2015.05.023.
- [42] M. Taghizadeh, E. Mehrvarz, and A. Taghipour, 'Polyoxometalate as an effective catalyst for the oxidative desulfurization of liquid fuels: a critical review', *Reviews in Chemical Engineering*, vol. 36, no. 7, pp. 831–858, Oct. 2020, doi: 10.1515/revce-2018-0058.

- [43] T. J. Wallace, H. Pobiner, and A. Schriesheim, 'Mercaptan Oxidations. VII. Oxidative Desulfurization of Benzyl Mercaptan, Benzyl Disulfide, and Related Species', *J Org Chem*, vol. 29, no. 4, pp. 888–891, Apr. 1964, doi: 10.1021/jo01027a031.
- [44] J. Piera and J.-E. Bäckvall, 'Catalytic Oxidation of Organic Substrates by Molecular Oxygen and Hydrogen Peroxide by Multistep Electron Transfer—A Biomimetic Approach', *Angewandte Chemie International Edition*, vol. 47, no. 19, pp. 3506–3523, Apr. 2008, doi: 10.1002/anie.200700604.
- [45] I. L. de Mattos, K. A. Shiraishi, A. D. Braz, and J. R. Fernandes, 'Peróxido de hidrogênio: importância e determinação', *Quim Nova*, vol. 26, no. 3, pp. 373–380, May 2003, doi: 10.1590/S0100-40422003000300015.
- [46] R. F. Muniz Moreira Co-orientador and H. Jorge José, 'Tirzhá Lins Porto Dantas DECOMPOSIÇÃO DE PERÓXIDO DE HIDROGÊNIO EM UM CATALISADOR HÍBRIDO E OXIDAÇÃO AVANÇADA DE EFLUENTE TÊXTIL POR REAGENTE FENTON MODIFICADO'.
- [47] F. R. Moghadam, S. Azizian, M. Bayat, M. Yarie, E. Kianpour, and M. A. Zolfigol, 'Extractive desulfurization of liquid fuel by using a green, neutral and task specific phosphonium ionic liquid with glyceryl moiety: A joint experimental and computational study', *Fuel*, vol. 208, pp. 214–222, Nov. 2017, doi: 10.1016/j.fuel.2017.07.025.
- [48] R. Abro *et al.*, 'Extractive desulfurization of fuel oils using deep eutectic solvents – A comprehensive review', *J Environ Chem Eng*, vol. 10, no. 3, p. 107369, Jun. 2022, doi: 10.1016/j.jece.2022.107369.
- [49] M. Cerutti, 'Dessulfurização da gasolina por adsorção em Zéolitas "Y" trocadas com cobre', Universidade Federal de Santa Catarina, Florianópolis, 2007.
- [50] Y. Xu *et al.*, 'Fast determination of sulfonamides from egg samples using magnetic multiwalled carbon nanotubes as adsorbents followed by liquid chromatography–tandem mass spectrometry', *Food Chem*, vol. 140, no. 1–2, pp. 83–90, Sep. 2013, doi: 10.1016/j.foodchem.2013.02.078.
- [51] R. v. Mambrini, C. Z. Maia, J. D. Ardisson, P. P. de Souza, and F. C. C. Moura, 'Fe/C and FeMo/C hybrid materials for the biphasic oxidation of fuel contaminants', *New Journal of Chemistry*, vol. 41, no. 1, pp. 142–150, 2017, doi: 10.1039/C6NJ02718K.
- [52] P. W. N. M. van Leeuwen, 'Catalysis, Homogeneous', in *Encyclopedia of Physical Science and Technology*, Elsevier, 2003, pp. 457–490. doi: 10.1016/B0-12-227410-5/00085-5.
- [53] M. Haghghi and S. Gooneh-Farahani, 'Insights to the oxidative desulfurization process of fossil fuels over organic and inorganic heterogeneous catalysts: advantages and issues', *Environmental Science and Pollution Research*, vol. 27, no. 32, pp. 39923–39945, Nov. 2020, doi: 10.1007/s11356-020-10310-4.
- [54] F. Boshagh, M. Rahmani, K. Rostami, and M. Yousefifar, 'Key Factors Affecting the Development of Oxidative Desulfurization of Liquid Fuels: A Critical Review', *Energy & Fuels*, vol. 36, no. 1, pp. 98–132, Jan. 2022, doi: 10.1021/acs.energyfuels.1c03396.
- [55] Q. Zhao *et al.*, 'Metal-free carbon materials-catalyzed sulfate radical-based advanced oxidation processes: A review on heterogeneous catalysts and applications', *Chemosphere*, vol. 189, pp. 224–238, Dec. 2017, doi: 10.1016/j.chemosphere.2017.09.042.

- [56] S. Wei, H. He, Y. Cheng, C. Yang, G. Zeng, and L. Qiu, 'Performances, kinetics and mechanisms of catalytic oxidative desulfurization from oils', *RSC Advances*, vol. 6, no. 105. Royal Society of Chemistry, pp. 103253–103269, 2016. doi: 10.1039/c6ra22358c.
- [57] M. Ahmadian and M. Anbia, 'Oxidative Desulfurization of Liquid Fuels Using Polyoxometalate-Based Catalysts: A Review', *Energy and Fuels*, vol. 35, no. 13. American Chemical Society, pp. 10347–10373, Jul. 01, 2021. doi: 10.1021/acs.energyfuels.1c00862.
- [58] C. Ampelli, S. Perathoner, and G. Centi, 'Carbon-based catalysts: Opening new scenario to develop next-generation nano-engineered catalytic materials', *Chinese Journal of Catalysis*, vol. 35, no. 6, pp. 783–791, Jun. 2014, doi: 10.1016/S1872-2067(14)60139-X.
- [59] A. D. Purceno *et al.*, 'Magnetic amphiphilic hybrid carbon nanotubes containing N-doped and undoped sections: powerful tensioactive nanostructures', *Nanoscale*, vol. 7, no. 1, pp. 294–300, 2015, doi: 10.1039/C4NR04005H.
- [60] C. Zhuo, J. O. Alves, J. A. S. Tenorio, and Y. A. Levendis, 'Synthesis of Carbon Nanomaterials through Up-Cycling Agricultural and Municipal Solid Wastes', *Ind Eng Chem Res*, vol. 51, no. 7, pp. 2922–2930, Feb. 2012, doi: 10.1021/ie202711h.
- [61] Dr Richard Collins and Dr Alex Holland, 'Carbon Nanotubes 2022-2032: Market, Technology, Players'. <https://www.idtechex.com/en/research-report/carbon-nanotubes-2022-2032-market-technology-players/859> (accessed Feb. 12, 2023).
- [62] R. Rocha, O. Soares, J. Figueiredo, and M. Pereira, 'Tuning CNT Properties for Metal-Free Environmental Catalytic Applications', *C (Basel)*, vol. 2, no. 3, p. 17, Jun. 2016, doi: 10.3390/c2030017.
- [63] C. Vallés, M. Pérez-Mendoza, M. T. Martínez, W. K. Maser, and A. M. Benito, 'CVD production of double-wall and triple-wall carbon nanotubes', *Diam Relat Mater*, vol. 16, no. 4–7, pp. 1087–1090, Apr. 2007, doi: 10.1016/j.diamond.2006.11.007.
- [64] E. T. Thostenson, Z. Ren, and T.-W. Chou, 'Advances in the science and technology of carbon nanotubes and their composites: a review', *Compos Sci Technol*, vol. 61, no. 13, pp. 1899–1912, Oct. 2001, doi: 10.1016/S0266-3538(01)00094-X.
- [65] T. Belin and F. Epron, 'Characterization methods of carbon nanotubes: a review', *Materials Science and Engineering: B*, vol. 119, no. 2, pp. 105–118, May 2005, doi: 10.1016/j.mseb.2005.02.046.
- [66] U. Kumar, 'Carbon Nanotube Radio', in *Carbon Nanotubes - From Research to Applications*, InTech, 2011. doi: 10.5772/17251.
- [67] M. Endo, T. Hayashi, Y. A. Kim, and H. Muramatsu, 'Development and Application of Carbon Nanotubes', *Jpn J Appl Phys*, vol. 45, no. 6A, pp. 4883–4892, Jun. 2006, doi: 10.1143/JJAP.45.4883.
- [68] O. O. Sadare and M. O. Daramola, 'Adsorptive desulfurization of dibenzothiophene (DBT) in model petroleum distillate using functionalized carbon nanotubes', *Environmental Science and Pollution Research*, vol. 26, no. 32, pp. 32746–32758, Nov. 2019, doi: 10.1007/s11356-019-05953-x.
- [69] N. D. V. Quyen, T. N. Tuyen, D. Q. Khieu, H. V. M. Hai, D. X. Tin, and K. Itatani, 'Oxidation of dibenzothiophene using the heterogeneous catalyst of tungsten-based

- carbon nanotubes', *Green Processing and Synthesis*, vol. 8, no. 1, pp. 68–77, Jan. 2019, doi: 10.1515/gps-2017-0189.
- [70] W. Zhang, H. Zhang, J. Xiao, Z. Zhao, M. Yu, and Z. Li, 'Carbon nanotube catalysts for oxidative desulfurization of a model diesel fuel using molecular oxygen', *Green Chem.*, vol. 16, no. 1, pp. 211–220, 2014, doi: 10.1039/C3GC41106K.
- [71] Y. Gao, R. Gao, G. Zhang, Y. Zheng, and J. Zhao, 'Oxidative desulfurization of model fuel in the presence of molecular oxygen over polyoxometalate based catalysts supported on carbon nanotubes', *Fuel*, vol. 224, pp. 261–270, Jul. 2018, doi: 10.1016/j.fuel.2018.03.034.
- [72] N. Mohammadi Meman, M. Pourkhalil, A. Rashidi, and B. ZareNezhad, 'Synthesis, characterization and operation of a functionalized multi-walled CNT supported MnOx nanocatalyst for deep oxidative desulfurization of sour petroleum fractions', *Journal of Industrial and Engineering Chemistry*, vol. 20, no. 6, pp. 4054–4058, Nov. 2014, doi: 10.1016/j.jiec.2014.01.004.
- [73] S. Hasannia, M. Kazemini, A. Seif, and A. Rashidi, 'Investigations of the ODS process utilizing CNT- and CNF-based WO₃ catalysts for environmental depollution: experimental and theoretical aspects', *Environmental Science and Pollution Research*, Nov. 2022, doi: 10.1007/s11356-022-23943-4.
- [74] J. Zou, Y. Lin, S. Wu, Y. Zhong, and C. Yang, 'Molybdenum Dioxide Nanoparticles Anchored on Nitrogen-Doped Carbon Nanotubes as Oxidative Desulfurization Catalysts: Role of Electron Transfer in Activity and Reusability', *Adv Funct Mater*, vol. 31, no. 22, p. 2100442, May 2021, doi: 10.1002/adfm.202100442.
- [75] N. M. Meman, B. Zarenezhad, A. Rashidi, Z. Hajjar, and E. Esmaeili, 'Application of palladium supported on functionalized MWNTs for oxidative desulfurization of naphtha', *Journal of Industrial and Engineering Chemistry*, vol. 22, pp. 179–184, Feb. 2015, doi: 10.1016/j.jiec.2014.07.008.
- [76] N. M. Mubarak, E. C. Abdullah, N. S. Jayakumar, and J. N. Sahu, 'An overview on methods for the production of carbon nanotubes', *Journal of Industrial and Engineering Chemistry*, vol. 20, no. 4, pp. 1186–1197, Jul. 2014, doi: 10.1016/j.jiec.2013.09.001.
- [77] H. O. Pierson, 'Fundamentals of Chemical Vapor Deposition', in *Handbook of Chemical Vapor Deposition (CVD)*, Elsevier, 1999, pp. 36–67. doi: 10.1016/B978-081551432-9.50005-X.
- [78] A. Kiadó and B. Vol, 'PREPARATION AND CHARACTERIZATION OF HIGHLY DISPERSED V₂O₅/SiO₂ PREPARED BY A CVD METHOD', Kluwer Academic Publishers, 2002.
- [79] A. A. S. Oliveira, I. F. Teixeira, T. Christofani, J. C. Tristão, I. R. Guimarães, and F. C. C. Moura, 'Biphasic oxidation reactions promoted by amphiphilic catalysts based on red mud residue', *Appl Catal B*, vol. 144, pp. 144–151, Jan. 2014, doi: 10.1016/j.apcatb.2013.07.015.
- [80] J.-P. Tessonier and D. S. Su, 'Recent Progress on the Growth Mechanism of Carbon Nanotubes: A Review', *ChemSusChem*, vol. 4, no. 7, pp. 824–847, Jul. 2011, doi: 10.1002/cssc.201100175.

- [81] V. Sivamaran, V. Balasubramanian, M. Gopalakrishnan, V. Viswabaskaran, and A. G. Rao, 'Identification of appropriate catalyst system for the growth of multi-walled carbon nanotubes via catalytic chemical vapor deposition process in a single step batch technique', *Mater Res Express*, vol. 6, no. 10, p. 105620, Sep. 2019, doi: 10.1088/2053-1591/ab3cbb.
- [82] D. Yao, H. Yang, Q. Hu, Y. Chen, H. Chen, and P. T. Williams, 'Carbon nanotubes from post-consumer waste plastics: Investigations into catalyst metal and support material characteristics', *Appl Catal B*, vol. 280, p. 119413, Jan. 2021, doi: 10.1016/j.apcatb.2020.119413.
- [83] Y. Shen, W. Gong, B. Zheng, and L. Gao, 'Ni–Al bimetallic catalysts for preparation of multiwalled carbon nanotubes from polypropylene: Influence of the ratio of Ni/Al', *Appl Catal B*, vol. 181, pp. 769–778, Feb. 2016, doi: 10.1016/j.apcatb.2015.08.051.
- [84] J. Gong *et al.*, 'Converting mixed plastics into mesoporous hollow carbon spheres with controllable diameter', *Appl Catal B*, vol. 152–153, pp. 289–299, Jun. 2014, doi: 10.1016/j.apcatb.2014.01.051.
- [85] B. G. Mwanza and C. Mbohwa, 'Drivers to Sustainable Plastic Solid Waste Recycling: A Review', *Procedia Manuf*, vol. 8, pp. 649–656, 2017, doi: 10.1016/j.promfg.2017.02.083.
- [86] C. Zhuo and Y. A. Levendis, 'Upcycling waste plastics into carbon nanomaterials: A review', *J Appl Polym Sci*, vol. 131, no. 4, p. n/a-n/a, Feb. 2014, doi: 10.1002/app.39931.
- [87] N. Singh, D. Hui, R. Singh, I. P. S. Ahuja, L. Feo, and F. Fraternali, 'Recycling of plastic solid waste: A state of art review and future applications', *Compos B Eng*, vol. 115, pp. 409–422, Apr. 2017, doi: 10.1016/j.compositesb.2016.09.013.
- [88] by Hannah Ritchie and Max Roser, 'Plastic Pollution'. <https://ourworldindata.org/plastic-pollution> (Accessed Feb. 12, 2023).
- [89] S. M. Al-Salem, P. Lettieri, and J. Baeyens, 'Recycling and recovery routes of plastic solid waste (PSW): A review', *Waste Management*, vol. 29, no. 10, pp. 2625–2643, Oct. 2009, doi: 10.1016/j.wasman.2009.06.004.
- [90] R. Verma, K. S. Vinoda, M. Papireddy, and A. N. S. Gowda, 'Toxic Pollutants from Plastic Waste- A Review', *Procedia Environ Sci*, vol. 35, pp. 701–708, 2016, doi: 10.1016/j.proenv.2016.07.069.
- [91] D. Yao, Y. Zhang, P. T. Williams, H. Yang, and H. Chen, 'Co-production of hydrogen and carbon nanotubes from real-world waste plastics: Influence of catalyst composition and operational parameters', *Appl Catal B*, vol. 221, pp. 584–597, Feb. 2018, doi: 10.1016/j.apcatb.2017.09.035.
- [92] X. Zhao *et al.*, 'Plastic waste upcycling toward a circular economy', *Chemical Engineering Journal*, vol. 428, p. 131928, Jan. 2022, doi: 10.1016/j.cej.2021.131928.
- [93] C. Wu, M. A. Nahil, N. Miskolczi, J. Huang, and P. T. Williams, 'Processing Real-World Waste Plastics by Pyrolysis-Reforming for Hydrogen and High-Value Carbon Nanotubes', *Environ Sci Technol*, vol. 48, no. 1, pp. 819–826, Jan. 2014, doi: 10.1021/es402488b.
- [94] X. Liu, B. Shen, P. Yuan, D. Patel, and C. Wu, 'Production of carbon nanotubes (CNTs) from thermochemical conversion of waste plastics using Ni/anodic aluminum oxide

- (AAO) template catalyst', *Energy Procedia*, vol. 142, pp. 525–530, Dec. 2017, doi: 10.1016/j.egypro.2017.12.082.
- [95] J. Wang, B. Shen, M. Lan, D. Kang, and C. Wu, 'Carbon nanotubes (CNTs) production from catalytic pyrolysis of waste plastics: The influence of catalyst and reaction pressure', *Catal Today*, vol. 351, pp. 50–57, Jul. 2020, doi: 10.1016/j.cattod.2019.01.058.
- [96] A. Veksha, W. Chen, L. Liang, and G. Lisak, 'Converting polyolefin plastics into few-walled carbon nanotubes via a tandem catalytic process: Importance of gas composition and system configuration', *J Hazard Mater*, vol. 435, p. 128949, Aug. 2022, doi: 10.1016/j.jhazmat.2022.128949.
- [97] S. Prabu and K.-Y. Chiang, 'Highly active Ni–Mg–Al catalyst effect on carbon nanotube production from waste biodegradable plastic catalytic pyrolysis', *Environ Technol Innov*, vol. 28, p. 102845, Nov. 2022, doi: 10.1016/j.eti.2022.102845.
- [98] X. Liu *et al.*, 'Producing carbon nanotubes from thermochemical conversion of waste plastics using Ni/ceramic based catalyst', *Chem Eng Sci*, vol. 192, pp. 882–891, Dec. 2018, doi: 10.1016/j.ces.2018.07.047.
- [99] A. A. Aboul-Enein, A. E. Awadallah, A. A.-H. Abdel-Rahman, and A. M. Haggag, 'Synthesis of multi-walled carbon nanotubes via pyrolysis of plastic waste using a two-stage process', *Fullerenes, Nanotubes and Carbon Nanostructures*, vol. 26, no. 7, pp. 443–450, Jul. 2018, doi: 10.1080/1536383X.2018.1447929.
- [100] H. U. Modekwe, M. A. Mamo, M. O. Daramola, and K. Moothi, 'Catalytic Performance of Calcium Titanate for Catalytic Decomposition of Waste Polypropylene to Carbon Nanotubes in a Single-Stage CVD Reactor', *Catalysts*, vol. 10, no. 9, p. 1030, Sep. 2020, doi: 10.3390/catal10091030.
- [101] J. W. Dove, G. Buckton A', and C. Doherty, 'international journal of pharmaceuticals A comparison of two contact angle measurement methods and inverse gas chromatography to assess the surface energies of theophylline and caffeine', 1996.
- [102] H. T. G. J. M. T. P. and J. L. D. D. T. C. M. Masso, 'Valorization of compost in the production of carbon-based materials for the treatment of contaminated wastewater', Polytechnic Institute of Bragança, Bragança, 2018.
- [103] M. A. Hazan *et al.*, 'Waste NR Latex Based-Precursors as Carbon Source for CNTs Eco-Fabrications', *Polymers (Basel)*, vol. 13, no. 19, p. 3409, Oct. 2021, doi: 10.3390/polym13193409.
- [104] X.-D. Wang, K. Vinodgopal, and G.-P. Dai, 'Synthesis of Carbon Nanotubes by Catalytic Chemical Vapor Deposition', in *Perspective of Carbon Nanotubes*, IntechOpen, 2019. doi: 10.5772/intechopen.86995.
- [105] M. Hussein, A. Jaafar, A. Yahaya, M. Masarudin, and Z. Zainal, 'Formation and Yield of Multi-Walled Carbon Nanotubes Synthesized via Chemical Vapour Deposition Routes Using Different Metal-Based Catalysts of FeCoNiAl, CoNiAl and FeNiAl-LDH', *Int J Mol Sci*, vol. 15, no. 11, pp. 20254–20265, Nov. 2014, doi: 10.3390/ijms151120254.
- [106] J. C. Acomb, C. Wu, and P. T. Williams, 'Control of steam input to the pyrolysis-gasification of waste plastics for improved production of hydrogen or carbon nanotubes', *Appl Catal B*, vol. 147, pp. 571–584, Apr. 2014, doi: 10.1016/j.apcatb.2013.09.018.

- [107] C. Zhuo, B. Hall, H. Richter, and Y. Levendis, 'Synthesis of carbon nanotubes by sequential pyrolysis and combustion of polyethylene', *Carbon N Y*, vol. 48, no. 14, pp. 4024–4034, Nov. 2010, doi: 10.1016/j.carbon.2010.07.007.
- [108] A. Orbaek White *et al.*, 'On the Use of Carbon Cables from Plastic Solvent Combinations of Polystyrene and Toluene in Carbon Nanotube Synthesis', *Nanomaterials*, vol. 12, no. 1, p. 9, Dec. 2021, doi: 10.3390/nano12010009.
- [109] L. F. Sanches, 'Valorisation of carbon-rich solid wastes into nanostructured catalysts for wet peroxide oxidation of contaminants of emerging concern', Polytechnic Institute of Bragança, Bragança, 2021.
- [110] M. U. Khan, K. R. Reddy, T. Snguanwongchai, E. Haque, and V. G. Gomes, 'Polymer brush synthesis on surface modified carbon nanotubes via in situ emulsion polymerization', *Colloid Polym Sci*, vol. 294, no. 10, pp. 1599–1610, Oct. 2016, doi: 10.1007/s00396-016-3922-7.
- [111] R. Dubey, D. Dutta, A. Sarkar, and P. Chattopadhyay, 'Functionalized carbon nanotubes: synthesis, properties and applications in water purification, drug delivery, and material and biomedical sciences', *Nanoscale Adv*, vol. 3, no. 20, pp. 5722–5744, 2021, doi: 10.1039/D1NA00293G.
- [112] N. Sezer and M. Koç, 'Oxidative acid treatment of carbon nanotubes', *Surfaces and Interfaces*, vol. 14, pp. 1–8, Mar. 2019, doi: 10.1016/j.surfin.2018.11.001.
- [113] K. Nejati and R. Zabihi, 'Preparation and magnetic properties of nano size nickel ferrite particles using hydrothermal method', *Chem Cent J*, vol. 6, no. 1, Mar. 2012, doi: 10.1186/1752-153X-6-23.
- [114] S. Sagadevan, Z. Z. Chowdhury, and R. F. Rafique, 'Preparation and characterization of nickel ferrite nanoparticles via co-precipitation method', *Materials Research*, vol. 21, no. 2, 2018, doi: 10.1590/1980-5373-mr-2016-0533.
- [115] M. N. Ashiq, M. F. Ehsan, M. J. Iqbal, and I. H. Gul, 'Synthesis, structural and electrical characterization of Sb³⁺ substituted spinel nickel ferrite (NiSb_xFe_{2-x}O₄) nanoparticles by reverse micelle technique', *J Alloys Compd*, vol. 509, no. 16, pp. 5119–5126, Apr. 2011, doi: 10.1016/j.jallcom.2011.01.193.
- [116] S. B. Gopale, G. N. Kakade, G. D. Kulkarni, V. Vinayak, S. P. Jadhav, and K. M. Jadhav, 'X-ray diffraction, infrared and magnetic studies of NiFe₂O₄ nanoparticles', in *Journal of Physics: Conference Series*, IOP Publishing Ltd, Oct. 2020. doi: 10.1088/1742-6596/1644/1/012010.
- [117] R. Sen, P. Jain, R. Patidar, S. Srivastava, R. S. Rana, and N. Gupta, 'Synthesis and Characterization of Nickel Ferrite (NiFe₂O₄) Nanoparticles Prepared by Sol- Gel Method', in *Materials Today: Proceedings*, Elsevier Ltd, 2015, pp. 3750–3757. doi: 10.1016/j.matpr.2015.07.165.
- [118] H. Moradmard and S. F. Shayesteh, 'The Variation of Magnetic Properties of Nickel Ferrite by Annealing', *Manufacturing Science and Technology*, vol. 3, no. 4, pp. 141–145, Dec. 2015, doi: 10.13189/mst.2015.030411.
- [119] S. A. Girei *et al.*, 'Effect of –COOH Functionalized Carbon Nanotubes on Mechanical, Dynamic Mechanical and Thermal Properties of Polypropylene Nanocomposites', *Journal of Thermoplastic Composite Materials*, vol. 25, no. 3, pp. 333–350, May 2012, doi: 10.1177/0892705711406159.

- [120] A. Basheer, M. Hanafiah, M. Alsaadi, W. Wan Yaacob, and Y. Al-Douri, 'Synthesis, Characterization, and Analysis of Hybrid Carbon Nanotubes by Chemical Vapor Deposition: Application for Aluminum Removal', *Polymers (Basel)*, vol. 12, no. 6, p. 1305, Jun. 2020, doi: 10.3390/polym12061305.
- [121] C. Rodríguez and E. Leiva, 'Enhanced Heavy Metal Removal from Acid Mine Drainage Wastewater Using Double-Oxidized Multiwalled Carbon Nanotubes', *Molecules*, vol. 25, no. 1, p. 111, Dec. 2019, doi: 10.3390/molecules25010111.
- [122] M. Pashai Gatabi, H. Milani Moghaddam, and M. Ghorbani, 'Point of zero charge of maghemite decorated multiwalled carbon nanotubes fabricated by chemical precipitation method', *J Mol Liq*, vol. 216, pp. 117–125, Apr. 2016, doi: 10.1016/j.molliq.2015.12.087.
- [123] S. L. Goertzen, K. D. Thériault, A. M. Oickle, A. C. Tarasuk, and H. A. Andreas, 'Standardization of the Boehm titration. Part I. CO₂ expulsion and endpoint determination', *Carbon N Y*, vol. 48, no. 4, pp. 1252–1261, Apr. 2010, doi: 10.1016/j.carbon.2009.11.050.
- [124] M. T. Pinho, R. S. Ribeiro, H. T. Gomes, J. L. Faria, and A. M. T. Silva, 'Screening of Activated Carbons for the Treatment of Highly Concentrated Phenol Solutions Using Catalytic Wet Peroxide Oxidation: The Effect of Iron Impurities on the Catalytic Activity', *Catalysts*, vol. 10, no. 11, p. 1318, Nov. 2020, doi: 10.3390/catal10111318.
- [125] L. Y. Jun, N. M. Mubarak, L. S. Yon, C. H. Bing, M. Khalid, and E. C. Abdullah, 'Comparative study of acid functionalization of carbon nanotube via ultrasonic and reflux mechanism', *J Environ Chem Eng*, vol. 6, no. 5, pp. 5889–5896, Oct. 2018, doi: 10.1016/j.jece.2018.09.008.
- [126] L. F. Ramírez-Verduzco, J. A. De los Reyes, and E. Torres-García, 'Solvent Effect in Homogeneous and Heterogeneous Reactions To Remove Dibenzothiophene by an Oxidation–Extraction Scheme', *Ind Eng Chem Res*, vol. 47, no. 15, pp. 5353–5361, Aug. 2008, doi: 10.1021/ie701692r.
- [127] M. Pumera, 'Carbon Nanotubes Contain Residual Metal Catalyst Nanoparticles even after Washing with Nitric Acid at Elevated Temperature Because These Metal Nanoparticles Are Sheathed by Several Graphene Sheets', *Langmuir*, vol. 23, no. 11, pp. 6453–6458, May 2007, doi: 10.1021/la070088v.
- [128] A. A. Farghali, H. A. Abdel Tawab, S. A. Abdel Moaty, and R. Khaled, 'Functionalization of acidified multi-walled carbon nanotubes for removal of heavy metals in aqueous solutions', *J Nanostructure Chem*, vol. 7, no. 2, pp. 101–111, Jun. 2017, doi: 10.1007/s40097-017-0227-4.
- [129] Y.-D. Dai, K. J. Shah, C. P. Huang, H. Kim, and P.-C. Chiang, 'Adsorption of Nonylphenol to Multi-Walled Carbon Nanotubes: Kinetics and Isotherm Study', *Applied Sciences*, vol. 8, no. 11, p. 2295, Nov. 2018, doi: 10.3390/app8112295.
- [130] J. C. Acomb, C. Wu, and P. T. Williams, 'Control of steam input to the pyrolysis-gasification of waste plastics for improved production of hydrogen or carbon nanotubes', *Appl Catal B*, vol. 147, pp. 571–584, Apr. 2014, doi: 10.1016/j.apcatb.2013.09.018.
- [131] D. Y. Kim *et al.*, 'Controllable pore structures of pure and sub-millimeter-long carbon nanotubes', *Appl Surf Sci*, vol. 566, p. 150751, Nov. 2021, doi: 10.1016/j.apsusc.2021.150751.

- [132] Y. H. Hu and E. Ruckenstein, 'Pore Size Distribution of Single-Walled Carbon Nanotubes', 2004, doi: 10.1021/ie030757.
- [133] Z. AlOthman, 'A Review: Fundamental Aspects of Silicate Mesoporous Materials', *Materials*, vol. 5, no. 12, pp. 2874–2902, Dec. 2012, doi: 10.3390/ma5122874.
- [134] M. Thommes *et al.*, 'Physisorption of gases, with special reference to the evaluation of surface area and pore size distribution (IUPAC Technical Report)', *Pure and Applied Chemistry*, vol. 87, no. 9–10, pp. 1051–1069, Oct. 2015, doi: 10.1515/pac-2014-1117.
- [135] J. Zhang, J. Du, Y. Qian, and S. Xiong, 'Synthesis, characterization and properties of carbon nanotubes microspheres from pyrolysis of polypropylene and maleated polypropylene', *Mater Res Bull*, vol. 45, no. 1, pp. 15–20, Jan. 2010, doi: 10.1016/j.materresbull.2009.09.007.
- [136] J.-T. Yeh *et al.*, 'Ultradrawing properties of ultra-high molecular weight polyethylene/functionalized carbon nanotube fibers', *Polym Eng Sci*, vol. 51, no. 4, pp. 687–696, Apr. 2011, doi: 10.1002/pen.21871.
- [137] Y. Zheng, H. Zhang, S. Ge, J. Song, J. Wang, and S. Zhang, 'Synthesis of Carbon Nanotube Arrays with High Aspect Ratio via Ni-Catalyzed Pyrolysis of Waste Polyethylene', *Nanomaterials*, vol. 8, no. 7, p. 556, Jul. 2018, doi: 10.3390/nano8070556.
- [138] S. Bandi, S. Ravuri, D. R. Peshwe, and A. K. Srivastav, 'Graphene from discharged dry cell battery electrodes', *J Hazard Mater*, vol. 366, pp. 358–369, Mar. 2019, doi: 10.1016/j.jhazmat.2018.12.005.
- [139] D. Li, Y. Sun, P. Gao, X. Zhang, and H. Ge, 'Structural and magnetic properties of nickel ferrite nanoparticles synthesized via a template-assisted sol-gel method', *Ceram Int*, vol. 40, no. 10, pp. 16529–16534, Dec. 2014, doi: 10.1016/j.ceramint.2014.08.006.
- [140] M. M. Rashad and O. A. Fouad, 'Synthesis and characterization of nano-sized nickel ferrites from fly ash for catalytic oxidation of CO', *Mater Chem Phys*, vol. 94, no. 2–3, pp. 365–370, Dec. 2005, doi: 10.1016/j.matchemphys.2005.05.028.
- [141] H. Liu, J. Zhai, and L. Jiang, 'Wetting and anti-wetting on aligned carbon nanotube films', *Soft Matter*, vol. 2, no. 10, p. 811, 2006, doi: 10.1039/b606654b.
- [142] J. Wang *et al.*, 'Wettability of carbon nanotube-grafted carbon fibers and their interfacial properties in polypropylene thermoplastic composite', *Compos Part A Appl Sci Manuf*, vol. 159, p. 106993, Aug. 2022, doi: 10.1016/j.compositesa.2022.106993.
- [143] M. Pavese, S. Musso, S. Bianco, M. Giorcelli, and N. Pugno, 'An analysis of carbon nanotube structure wettability before and after oxidation treatment', *Journal of Physics: Condensed Matter*, vol. 20, no. 47, p. 474206, Nov. 2008, doi: 10.1088/0953-8984/20/47/474206.
- [144] B. A. Kakade and V. K. Pillai, 'Tuning the wetting properties of multiwalled carbon nanotubes by surface functionalization', *Journal of Physical Chemistry C*, vol. 112, no. 9, pp. 3183–3186, Mar. 2008, doi: 10.1021/jp711657f.
- [145] O. O. Sadare and M. O. Daramola, 'Adsorptive desulfurization of dibenzothiophene (DBT) in model petroleum distillate using functionalized carbon nanotubes', *Environmental Science and Pollution Research*, vol. 26, no. 32, pp. 32746–32758, Nov. 2019, doi: 10.1007/s11356-019-05953-x.

- [146] O. O. Sadare, 'Development and Evaluation of Adsorption coupling Biodesulphurization (AD/BDS) process for the desulphurization of South African Petroleum Distillates', 2018.
- [147] A. M. Moreira, H. L. Brandão, F. V. Hackbarth, D. Maass, A. A. Ulson de Souza, and S. M. A. Guelli U. de Souza, 'Adsorptive desulfurization of heavy naphthenic oil: Equilibrium and kinetic studies', *Chem Eng Sci*, vol. 172, pp. 23–31, Nov. 2017, doi: 10.1016/j.ces.2017.06.010.
- [148] P. Saranjampour and K. Armbrust, 'Repeatability of n-octanol/water partition coefficient values between liquid chromatography measurement methods', *Environmental Science and Pollution Research*, vol. 25, no. 15, pp. 15111–15119, May 2018, doi: 10.1007/s11356-018-1729-4.
- [149] C. H. L. S. Z. Z. YU Guo-xian, 'Catalysis of Activated Carbon in Oxidative Removal of Dibenzothiophene with Hydrogen Peroxide', *Journal of East China University of Science and Technology*, vol. 32, no. 1, pp. 1–6, Jan. 2006.
- [150] K. Voitko *et al.*, 'Catalytic performance of carbon nanotubes in H₂O₂ decomposition: Experimental and quantum chemical study', *J Colloid Interface Sci*, vol. 437, pp. 283–290, Jan. 2015, doi: 10.1016/j.jcis.2014.09.045.
- [151] R. S. Ribeiro, A. M. T. Silva, J. L. Figueiredo, J. L. Faria, and H. T. Gomes, 'Catalytic wet peroxide oxidation: a route towards the application of hybrid magnetic carbon nanocomposites for the degradation of organic pollutants. A review', *Appl Catal B*, vol. 187, pp. 428–460, Jun. 2016, doi: 10.1016/j.apcatb.2016.01.033.
- [152] V. Tamborrino *et al.*, 'Catalytic oxidative desulphurization of pyrolytic oils to fuels over different waste derived carbon-based catalysts', *Fuel*, vol. 296, p. 120693, Jul. 2021, doi: 10.1016/j.fuel.2021.120693.
- [153] R. Ghubayra, C. Nuttall, S. Hodgkiss, M. Craven, E. F. Kozhevnikova, and I. V. Kozhevnikov, 'Oxidative desulfurization of model diesel fuel catalyzed by carbon-supported heteropoly acids', *Appl Catal B*, vol. 253, pp. 309–316, Sep. 2019, doi: 10.1016/j.apcatb.2019.04.063.
- [154] L. Liu, Y. Zhang, and W. Tan, 'Ultrasound-assisted oxidation of dibenzothiophene with phosphotungstic acid supported on activated carbon', *Ultrason Sonochem*, vol. 21, no. 3, pp. 970–974, May 2014, doi: 10.1016/j.ultsonch.2013.10.028.
- [155] L. Liu, Y. Zhang, and W. Tan, 'Synthesis and characterization of phosphotungstic acid/activated carbon as a novel ultrasound oxidative desulfurization catalyst', *Front Chem Sci Eng*, vol. 7, no. 4, pp. 422–427, Dec. 2013, doi: 10.1007/s11705-013-1353-2.
- [156] H. M. Ng, N. M. Saidi, F. S. Omar, K. Ramesh, S. Ramesh, and S. Bashir, 'Thermogravimetric Analysis of Polymers', in *Encyclopedia of Polymer Science and Technology*, John Wiley & Sons, Inc., 2018, pp. 1–29. doi: 10.1002/0471440264.pst667.
- [157] L. S. K. Pang, J. D. Saxby, and S. P. Chatfield, 'Thermogravimetric Analysis of Carbon Nanotubes and Nanoparticles', 1993. [Online]. Available: <https://pubs.acs.org/sharingguidelines>
- [158] D. A. S. Costa, R. V. Mambrini, L. E. Fernandez-Outon, W. A. A. Macedo, and F. C. C. Moura, 'Magnetic adsorbent based on cobalt core nanoparticles coated with carbon filaments and nanotubes produced by chemical vapor deposition with ethanol', *Chemical Engineering Journal*, vol. 229, pp. 35–41, Aug. 2013, doi: 10.1016/j.cej.2013.05.099.

- [159] A. Jorio, E. H. M. Ferreira, M. V. O. Moutinho, F. Stavale, C. A. Achete, and R. B. Capaz, 'Measuring disorder in graphene with the G and D bands', *physica status solidi (b)*, vol. 247, no. 11–12, pp. 2980–2982, Dec. 2010, doi: 10.1002/pssb.201000247.
- [160] H. Liu, J. Wang, J. Wang, and S. Cui, 'Sulfonitric Treatment of Multiwalled Carbon Nanotubes and Their Dispersibility in Water', *Materials*, vol. 11, no. 12, p. 2442, Dec. 2018, doi: 10.3390/ma11122442.
- [161] G. Yu, S. Lu, H. Chen, and Z. Zhu, 'Oxidative Desulfurization of Diesel Fuels with Hydrogen Peroxide in the Presence of Activated Carbon and Formic Acid', *Energy & Fuels*, vol. 19, no. 2, pp. 447–452, Mar. 2005, doi: 10.1021/ef049760b.
- [162] Q. Wu *et al.*, 'Synthesis of Surface-Active Heteropolyacid-Based Ionic Liquids and Their Catalytic Performance for Desulfurization of Fuel Oils', *ACS Omega*, vol. 5, no. 48, pp. 31171–31179, Dec. 2020, doi: 10.1021/acsomega.0c04398.
- [163] Z. Ismagilov *et al.*, 'Oxidative desulfurization of hydrocarbon fuels', *Catal Rev Sci Eng*, vol. 53, no. 3, pp. 199–255, 2011, doi: 10.1080/01614940.2011.596426.
- [164] A. Haghghat Mamaghani, S. Fatemi, and M. Asgari, 'Investigation of influential parameters in deep oxidative desulfurization of dibenzothiophene with hydrogen peroxide and formic acid', *International Journal of Chemical Engineering*, 2013, doi: 10.1155/2013/951045.
- [165] A. Akopyan, E. Eseva, P. Polikarpova, A. Kedalo, A. Vutolkina, and A. Glotov, 'Deep oxidative desulfurization of fuels in the presence of Brønsted acidic polyoxometalate-based ionic liquids', *Molecules*, vol. 25, no. 3, Jan. 2020, doi: 10.3390/molecules25030536.
- [166] B. Tao, X. Li, M. Yan, and W. Luo, 'Solubility of dibenzothiophene in nine organic solvents: Experimental measurement and thermodynamic modelling', *J Chem Thermodyn*, vol. 129, pp. 73–82, Feb. 2019, doi: 10.1016/j.jct.2018.09.017.
- [167] M. ALI, A. ALMALKI, B. ELALI, G. MARTINIE, and M. SIDDIQUI, 'Deep desulphurization of gasoline and diesel fuels using non-hydrogen consuming techniques', *Fuel*, vol. 85, no. 10–11, pp. 1354–1363, Jul. 2006, doi: 10.1016/j.fuel.2005.12.006.